SURFACE-CATALYZED GROWTH OF pH-RESPONSIVE COPOLYMER THIN FILMS

By

Dongshun Bai

Dissertation

Submitted to the Faculty of the

Graduate School of Vanderbilt University

in partial fulfillment of the requirements

for the degree of

DOCTOR OF PHILOSOPHY

in

Chemical Engineering

May, 2007

Nashville, Tennessee

Approved:

Professor G. Kane Jennings

Professor Bridget R. Rogers

Professor M. Douglas LeVan

Professor Piotr Kaszynski

Professor Peter T. Cummings

To my amazing daughters, Jingyi and Jiayi,

and

To my beloved wife, Qing Pu.

ACKNOWLEDGMENTS

I would like to thank my advisor, Dr. Kane Jennings, who has led me in this research in the area of organic thin films. He has been very helpful and patient and has given me great encouragement throughout my research. His guidance has made my research more straightforward and full of joy. His passion in research and teaching has also inspired me. I am very lucky to have had Dr. Jennings as my Ph.D. advisor, and I appreciate everything he has done for me. I thank all my committee members, Dr. Douglas LeVan, Dr. Bridget Rogers, Dr. Peter Cummings, and Dr. Piotr Kaszynski for their direction and time. Their constructive suggestions have made this work more complete and meaningful.

I thank all the professors in the Department of Chemical Engineering. They not only taught me advanced engineering concepts but also provided helpful suggestions in my career development. I also thank Margarita Talavera, Mary Gilleran, and Mark Holmes. They always gave me warm greetings and made my life here easier. I will never forget the nice conversations we have had during my study.

I thank all the group members in Dr. Jennings's lab: Dr. Wengfeng Guo, Dr. Eric Brantley, Dr. Helen Kincaid, Mayker Bantz, Brad Berron, Angeline Cione, and Chris Faulkner for their constructive discussion and support of my research and their great help and friendship in my life. I thank Dr. Honggang Zhao and Dr. Lixin Sun for their support and encouragement during my job search. I also would like to thank all the undergraduates who worked with me during my study, including Brian Habersberger, Steven Elliott, Zulkifli Ibrahim, and Craig Hardwick. They are very bright and helpful

young men and have made great contributions toward this research. I thank all my friends at Olin Hall and Vanderbilt. They have made my life here very enjoyable and memorable. I wish them all the best.

I would like to acknowledge Dr. Bridget Rogers for use of her ellipsometer and XPS, Dr. Tomlinson Fort for use of the contact angle goniometer, and Dr. Wittig for use of the SEM.

I would like to give my great appreciation to my wife Qing Pu. She has given me endless love and support during my studies here. I could never finish my studies without her. She is such a great woman, and I am very lucky to have her as my wife. I thank my daughters Jingyi and Jiayi. They have brought a lot of fun into my life and often help me to remind myself to be a good father. I am also grateful for the love and support from other family members. Their support and high expectations of me always encourage me to be the best I can be.

Finally, I thank the financial support that made this research project possible, from the American Chemical Society Petroleum Research Fund (ACS-PRF #38553-AC5) and the National Science Foundation (CTS-0522937).

TABLE OF CONTENTS

LIST OF TABLES

LIST OF FIGURES

CHAPTER I

INTRODUCTION

pH-Responsive Polymer Thin Films

Polymer films that respond to pH by altering structure, barrier properties, and/or surface properties have broad applications in chemical sensors,[1-3] membrane separations,[4,5] responsive surfaces,[6] drug delivery and release,[7-10] and other biological applications.[11-15] In many types of chemical sensors and biosensors, pH-sensitive coatings are an integral part of the transduction mechanism to detect the release of H^+ ions by a chemically specific reaction between an immobilized moiety (e.g. enzyme) and an analyte compound.[16,17] In separations, pH-responsive polymers can extend/contract to close/open pores in the presence of target molecules and form the basis of smart membranes.[4] For responsive surfaces, the polymer films change their conformation and hydrophobicity with pH to change the surface wettablity. If rough substrates are used, reversible switching between superhydrophobicity and superhydrophilicity can be realized over a broad range of pH.[6] In biological applications, pH responsive polymers can rapidly release encapsulated materials at a targeted pH[7] or can be used in microarray to precisely pattern both peptides and proteins for various biological applications including medical sensors.[14] For successful utilization in many of these applications, a defect-free ultrathin film that exhibits a large, rapid, and reversible response must be prepared.

Current Approaches toward the Preparation of pH-Responsive Films

Polymer films that respond to pH are most commonly prepared as hydrogels[18] by mixing appropriate polymers[1,19] or synthesizing copolymers[20] that can be diluted in solvent and cast onto surfaces. The hydrogels contain carboxylic acids or other ionizable groups, and over a range of pH near the pK_a of the sensitive groups, the film becomes ionized and swells due to additional uptake of water and ions driven by differences in electrochemical potential.[21] The thicker hydrogel films exhibit rather slow response due to the increased lengths for diffusion, requiring several minutes to hours to completely change chemical states.[16,17] The concentration of hydrophilic, ionizable groups in these hydrogels is often high,[19,20] ensuring that water is present in the films at all pH ranges. Therefore, the ultimate response in aqueous-phase barrier properties for these films upon ionization is not expected to be large. Moreover, casting approaches are less effective for creating patterned films, controlling film thickness with nanometer-level precision, or coating irregular surfaces. Further, the precise engineering of pH-responsive sensitivity has not been reported to date through these approaches.

New Approach to pH-Responsive Polymer Thin Films

To overcome the inherent drawbacks of the hydrogels in pH-responsive film applications and to obtain a large, fast and reversible response, a polymer with a structure as shown in Figure 1.1 is proposed. This polymer film will have predominate hydrophobic part (A>>B) with a small percentage of ionizable carboxylic acid groups. On the basis of octanol-water partition coefficients,[22] the carboxylate group is ~10^4 times more hydrophilic than the protonated acid. This extreme difference in the affinity of

these groups toward water provides the basis for the work described herein. Briefly, polymer films that are predominately hydrophobic but contain a dilute fraction of carboxylic acid groups should exhibit a dramatic change in barrier properties when the pH is increased sufficiently to ionize the acid groups. At low pH, the polymers would be mostly dry, but upon ionization, the large difference in hydrophilicity of the carboxylate versus the acid should result in significant water and ion permeation. Such films may provide extremely pH-sensitive materials and could be useful in sensing and separations.

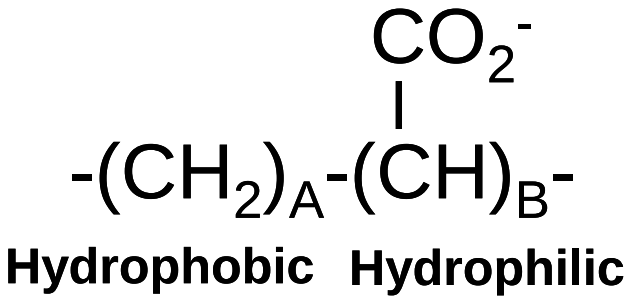

Figure 1.1 Proposed polymer structure to obtain large pH-Response.

The ability to grow these films directly from the electrode surface instead of physically casting them after liquid phase synthesis would be a great advantage. On one hand, the covalent linkage between the polymer film and the substrate will make the films more stable on the surface to provide a reversible response; on the other hand, the electrode can be directly used in analysis. Also, for the film to exhibit a very fast response, the film thickness must be as low as possible and preferably controllable at the

nanometer scale. The ability to control film thickness can also provide the opportunity to study the effect of film thickness on the rate of pH-response.

Based on these considerations, we have developed a new surface-catalyzed polymerization process to grow polymer thin films directly from the substrate surface. We have discovered that by simply exposing gold substrates to an ether solution containing both diazomethane (CH_2N_2; DM) and ethyl diazoacetate (EDA), a copolymer film containing polymethylene (PM) segments with randomly distributed ethyl ester side chains will be produced (Figure 1.2c). Figure 1.3 shows a scheme for preparing pH-responsive PM-CO2H films by surface-catalyzed growth and subsequent modification. This one step synthesis method can introduce functionalized groups into the polymer film

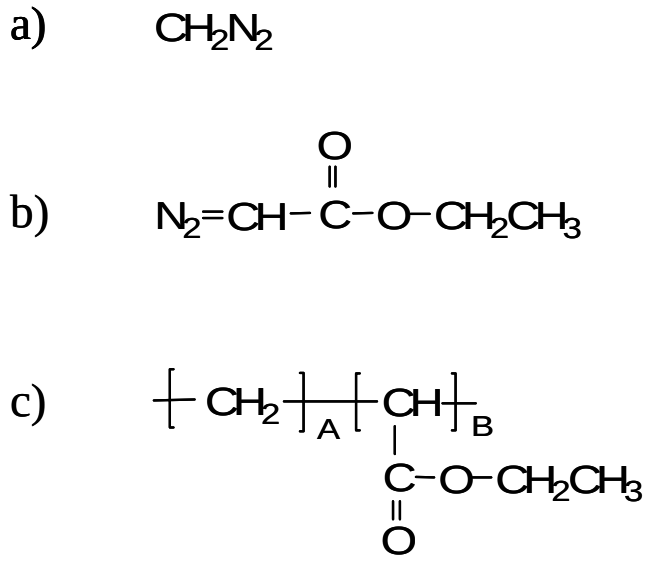

Figure 1.2. Chemical structures of a) DM and b) EDA. Structure c) represents the likely polymer formed when gold is exposed to a solution of DM and EDA.

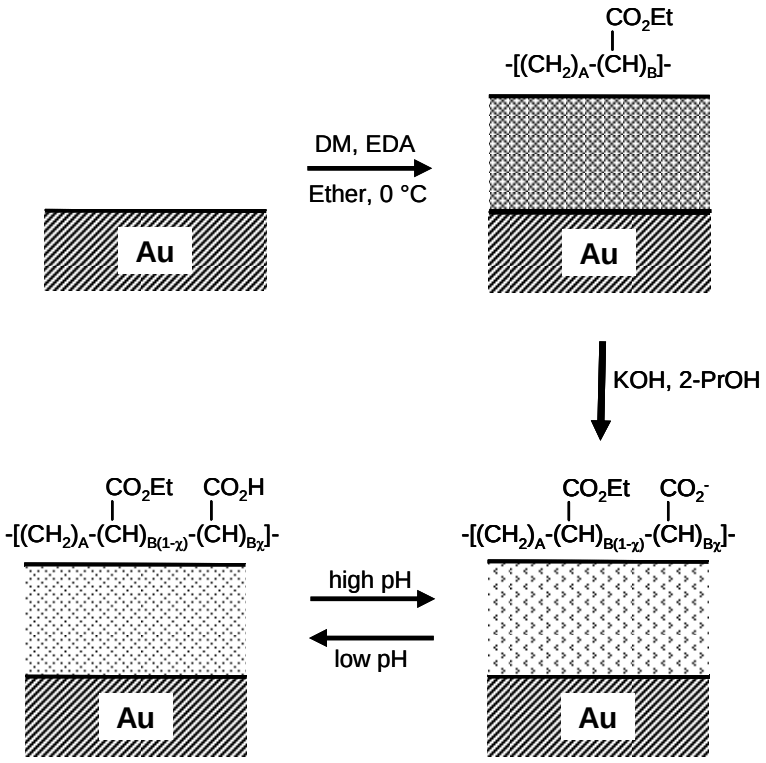

Figure 1.3. Schematic method for preparing pH-responsive PM-CO2H films by surface-catalyzed growth and subsequent modification. In these films, A >> B.

and tailor the film properties for specific applications. The side groups of poly(methylene-*co*-ethyl acetate) (Figure 1.2c) can be hydrolyzed to carboxylic acids (PM-CO2H) that are commonly used as the pH-sensitive moiety in responsive films.

This thesis addresses the creation of pH-responsive ultrathin polymer thin films through surface-catalyzed polymerization and post-polymerization reactions. It reports how the film composition and thickness affects the pH-responsive behavior of the film, with the ultimate goal being to prepare films that exhibit large, fast, and reversible pH-induced responses. This thesis will also show how a surface-catalyzed polymerization

can be used to fabricate pH-responsive composite membranes to control water and ion transport. To investigate how the polymer composition and charge affect its response, polymer films with basic side chains are also reported. Polyacids such as poly(acrylic acid) (PAAc), are protonated or uncharged at low pH and deprotonated or negatively charged at high pH, while polybases such as poly(N,N'-dimethyl aminoethyl methacrylate) are neutralized at high pH and positively charged at low pH.[23] This reverse response in pH could be useful for targeted, pH-specific swelling and transport, and in combination with PM-CO2H, could provide a broader range of pH sensitivity. Our ability to measure barrier properties of the films with different functional side groups may promote a fundamental understanding of the effect of film composition on response.

References

1. Richter, A.; Bund, A.; Keller, M.; Arndt, K. F. "Characterization of a Microgravimetric Sensor Based on pH Sensitive Hydrogels," *Sensors and Actuators B-Chemical* **2004**, *99*, 579-585.

2. Gerlach, G.; Guenther, M.; Suchaneck, G.; Sorber, J.; Arndt, K. F.; Richter, A. "Application of Sensitive Hydrogels in Chemical and pH Sensors," *Macromolecular Symposia* **2004**, *210*, 403-410.

3. Lakard, B.; Herlem, G.; de Labachelerie, M.; Daniau, W.; Martin, G.; Jeannot, J. C.; Robert, L.; Fahys, B. "Miniaturized pH Biosensors Based on Electrochemically Modified Electrodes with Biocompatible Polymers," *Biosensors & Bioelectronics* **2004**, *19*, 595-606.

4. Hester, J. F.; Olugebefola, S. C.; Mayes, A. M. "Preparation of pH-Responsive Polymer Membranes by Self-Organization," *Journal of Membrane Science* **2002**, *208*, 375-388.

5. Ito, Y.; Park, Y. S.; Imanishi, Y. "Nanometer-Sized Channel Gating by a Self-Assembled Polypeptide Brush," *Langmuir* **2000**, *16*, 5376-5381.

6. Xia, F.; Feng, L.; Wang, S. T.; Sun, T. L.; Song, W. L.; Jiang, W. H.; Jiang, L. "Dual-Responsive Surfaces That Switch Superhydrophilicity and Superhydrophobicity," *Advanced Materials* **2006**, *18*, 432-436.

7. Lynn, D. M.; Amiji, M. M.; Langer, R. "pH-Responsive Polymer Microspheres: Rapid Release of Encapsulated Material within the Range of Intracellular pH," *Angewandte Chemie-International Edition* **2001**, *40*, 1707-1710.

8. Lamprecht, A.; Yamamoto, H.; Takeuchi, H.; Kawashima, Y. "pH-Sensitive Microsphere Delivery Increases Oral Bioavailability of Calcitonin," *Journal of Controlled Release* **2004**, *98*, 1-9.

9. Murthy, N.; Robichaud, J. R.; Tirrell, D. A.; Stayton, P. S.; Hoffman, A. S. "The Design and Synthesis of Polymers for Eukaryotic Membrane Disruption," *Journal of Controlled Release* **1999**, *61*, 137-143.

10. Cheung, C. Y.; Murthy, N.; Stayton, P. S.; Hoffman, A. S. "A pH-Sensitive Polymer That Enhances Cationic Lipid-Mediated Gene Transfer," *Bioconjugate Chemistry* **2001**, *12*, 906-910.

11. Rehfeldt, F.; Steitz, R.; Armes, S. P.; Von Klitzing, R.; Gast, A. P.; Tanaka, M. "Reversible Activation of Diblock Copolymer Monolayers at the Interface by pH Modulation, 1: Lateral Chain Density and Conformation," *Journal of Physical Chemistry B* **2006**, *110*, 9171-9176.

12. Patton, J. N.; Palmer, A. F. “Physical Properties of Hemoglobin-Poly(acrylamide) Hydrogel-Based Oxygen Carriers: Effect of Reaction pH,” *Langmuir* **2006**, *22*, 2212-2221.

13. Roy, I.; Gupta, M. N. “pH-Responsive Polymer-Assisted Refolding of Urea- and Organic Solvent-Denatured Alpha-Chymotrypsin,” *Protein Engineering* **2003**, *16*, 1153-1157.

14. Christman, K. L.; Maynard, H. D. “Protein Micropatterns Using a pH-Responsive Polymer and Light,” *Langmuir* **2005**, *21*, 8389-8393.

15. Matsukuma, D.; Yamamoto, K.; Aoyagi, T. “Stimuli-Responsive Properties of *N*-Isopropylacrylamide-Based Ultrathin Hydrogel Films Prepared by Photo-Cross-Linking,” *Langmuir* **2006**, *22*, 5911-5915.

16. Cai, Q. Y.; Zeng, K. F.; Ruan, C. M.; Desai, T. A.; Grimes, C. A. “A Wireless, Remote Query Glucose Biosensor Based on a pH-Sensitive Polymer,” *Analytical Chemistry* **2004**, *76*, 4038-4043.

17. Marshall, A. J.; Young, D. S.; Blyth, J.; Kabilan, S.; Lowe, C. R. “Metabolite-Sensitive Holographic Biosensors,” *Analytical Chemistry* **2004**, *76*, 1518-1523.

18. Roy, I.; Gupta, M. N. “Smart Polymeric Materials: Emerging Biochemical Applications,” *Chemistry & Biology* **2003**, *10*, 1161-1171.

19. Jin, X.; Hsieh, Y. L. “pH-Responsive Swelling Behavior of Poly(vinyl alcohol)/Poly(acrylic acid) Bi-Component Fibrous Hydrogel Membranes,” *Polymer* **2005**, *46*, 5149-5160.

20. Cai, Q. Y.; Grimes, C. A. “A Remote Query Magnetoelastic pH Sensor,” *Sensors and Actuators B-Chemical* **2000**, *71*, 112-117.

21. Chiu, H. C.; Lin, Y. F.; Hung, S. H. “Equilibrium Swelling of Copolymerized Acrylic Acid- Methacrylated Dextran Networks: Effects of pH and Neutral Salt,” *Macromolecules* **2002**, *35*, 5235-5242.

22. Schwarzenbach, R.; Gschwend, P.; Imboden, D. *Environmental Organic Chemistry*; Wiley: New York, 1993.

23. Gil, E. S.; Hudson, S. A. “Stimuli-Responsive Polymers and Their Bioconjugates,” *Progress in Polymer Science* **2004**, *29*, 1173-1222.

CHAPTER II

BACKGROUND

Surface-Catalyzed Polymerizations

Within the past few years, a growing research effort has focused on extending the advances in solution-phase polymer chemistry to surfaces to enable the construction of polymer films by the continual addition of repeat units onto growing chains. This so-called surface-initiated polymerization strategy[1] offers several advantages over traditional methods for preparing polymer films and coatings, including (1) improved adhesion due to a chemical coupling of the initiator/polymer chain to the substrate, (2) the ability to prepare uniform, conformal coatings on objects of any shape,[2] (3) excellent control over film thickness, from a few nanometers up to the micron level[2] in some cases, (4) tunable grafting densities, based on the surface coverage of the initiator, (5) simplified separations issues, since the polymer is grown from a support, and (6) good control over depth-dependent composition by growing additional blocks to prepare copolymer films.[3-5] A drawback of these surface-initiated approaches is that the chemical attachment is often mediated through a functionalized organic monolayer, which may take a series of steps to prepare. In addition, for hydrophobic monomers that are useful in the preparation of barrier films, the polymerization reaction is often kinetically sluggish and may require several days at elevated temperatures to form highly uniform coatings.[6-9]

A unique class of surface-initiated polymerizations that overcomes these drawbacks is the surface-catalyzed approach where a monomer decomposes directly at a

metal surface to initiate a polymerization. These polymerizations tend to be kinetically rapid, can grow hydrophobic polymers, and do not require synthesis of initiator-terminated adsorbates.[10-14]

The concept of surface-catalyzed polymerizations was introduced by Leitch and Cambron[15] in 1948 when they discovered that copper powder catalyzed the decomposition of DM from solution to produce PM in high yields. In 1950, Buckley et al.[16] performed a systematic study in which they used various copper salts and powders to catalyze the decomposition of DM and higher diazoalkanes. They found that copper with less oxide was more effective in catalyzing the growth of a polymer with high molecular weight in good yield. In a later paper, Buckley and Ray[17] determined that trimethyl borate ($B(OCH_3)_3$) also served as an effective catalyst for the decomposition of diazoalkanes. By mixing DM with higher diazoalkanes in the presence of trimethyl borate, they generated polymers with varying degrees of crystallinity that depended on the solution ratio of DM to the higher diazoalkane. In the early work, the mechanism of the polymerization was proposed to be either living insertion,[18] cationic,[19] or a combination of the two,[20] depending on the catalyst. More recently, Shea and co-workers[21,22] have shown that dimethyl sulfoxonium methylide, a molecule similar to DM, does indeed undergo an insertion reaction with an alkyl borane in solution to produce PM. This insertion reaction enables subsequent addition of methylene groups between the borane and PM chain with minimal terminations to produce chains with low polydispersity (1.01-1.17).

From 1997 to 2000, Allara, Tao, and co-workers recognized that the chemistry described by Buckley et al. to produce bulk polymers could be used to generate ultrathin

films of PM on gold surfaces.[10,13,14] They formed ultrathin PM films and clusters on gold surfaces by simply immersing the substrate in an ethereal solution containing DM. DM decomposes at the catalytic gold surface to produce an adsorbed methylidene species that initiates a free radical polymerization. This straightforward processing strategy is particularly useful since many polyolefins, most notably polyethylene, suffer from poor processibility and cannot be solution-cast or spin-coated.[13] They determined that the polymerization reaction initiates at lower-coordination defect sites on the gold surface that provide stronger interactions with the adsorbed methylidene species than do higher-coordination terrace sites.[13] They proposed a free-radical mechanism for the polymerization where DM decomposes to yield an adsorbed methylidene species, which can subsequently react with other methylidenes to create a propagating biradical species.[13] Since free radical polymerizations are prone to terminations, the growing chains eventually die and film growth ceases. By using rough, sputter-deposited gold, Allara and co-workers showed that a higher concentration of high-coordination gold defect sites enhances the binding of methylidenes to enable the initiation of thicker, more uniform polymer films.[14] These results suggest that methods for modifying the surface of gold to provide stronger bonding with methylidene species could yield PM films with a greater degree of uniformity that are more suitable for many applications.

The drawbacks of this initial work by Allara, Tao, and co-workers include (1) the lack of diversity in both polymer film and metal surface since only PM on gold has been studied, (2) the inability to prepare films thicker than ~100 nm due to chain terminations, and (3) the lack of control over film properties required to enable directed growth.

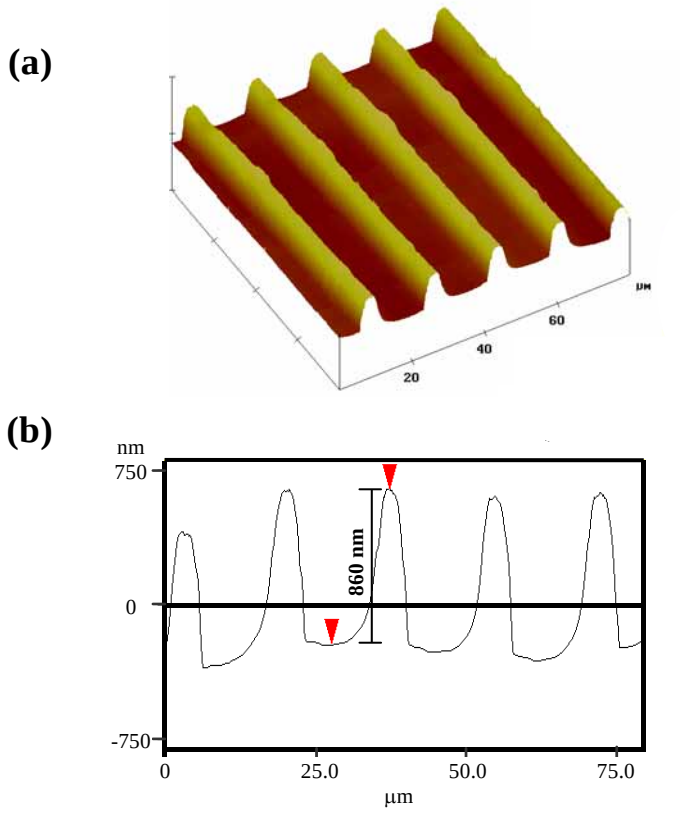

Figure 2.1. Tapping mode AFM image (a) and section analysis (b) of a patterned PM film grown from a surface containing lines of Cu(upd)/Au and adjacent lines of Ag(upd)/Au.[24]

Our group has reported that atomic-scale modification of gold surfaces with underpotentially deposited (upd) metal (sub)monolayers greatly alters the catalytic properties of the metal surface, thereby affecting the surface-initiated decomposition of DM and providing a methodology for controlling the properties of the resulting PM films.[23] By tuning the coverage and composition of the upd adlayer on gold, one can

greatly enhance (using copper) or inhibit (using silver) the polymerization in order to direct the growth of highly insulating PM films into micron-scale patterns (Figure 2.1).[24]

Although the chemical inertness of PM is useful in many processes, it prevents straightforward functionalization, which could promote interactions with other materials and expand the applications of these surface-catalyzed films. Common methods to modify the surfaces of PM or PE include bromination[25] or oxygenation[26] with UV irradiation or treatment with strong acids[27] or oxygen plasma,[28] each of these occurring under harsh conditions that may be incompatible with other materials present on a particular surface. Synthetic methods, such as polyhomologation, have been pioneered by Shea and co-workers[21,22,29-32] to create uniquely end-functionalized PM, but this remarkable chemistry has not been extended into thin film processing. In general, well-controlled methods for preparing PM films with functionalized side chains could be useful in interfacing these cost-efficient and widely utilized materials with other components or in tuning their physical properties.

If this innovative processing is to become more useful in a broader sense, methods to generate a greater range of polymer films, and methods to direct the polymerization in order to form microstructures will be important. In addition, a fundamental understanding of the relevant properties—both of the metal surface and of the initiating molecule—that govern the efficiency of the surface-catalyzed polymerization must be developed.

pH-Responsive Films

Films that respond to pH have been prepared using a variety of techniques (self-assembled monolayers (SAMs), Langmuir-Blodgett (LB) films, cast films, surface-initiated films) and used to study adhesion,[33] chemical detection,[34] membrane separations,[35,36] and other applications already discussed in Chapter I. Leckband and co-workers[33] prepared LB films from a hydrophobically modified N-isopropylacrylamide-glycinylacrylamide copolymer and used a surface forces apparatus to study adhesional forces within the film at different pH values. They concluded that the ionization of the film at higher pH causes swelling and polyelectrolyte behavior whereas neutralization results in H-bond-mediated adhesion and reduced thicknesses to greatly alter interfacial properties. Martin and co-workers[35] and Stroeve and co-workers[36-38] have modified the gold-coated pores of membranes with SAMs terminated in ionizable groups. These membranes provide pH- and charge-dependent transport to demonstrate the modification of pore charge to influence separations. Mayes and co-workers[39] cast blends of poly(vinylidene fluoride) and poly(methacrylic acid) to produce membranes with open pores at pH 2 and blocked pores at pH 8 where the film becomes charged and swells. Combined these very distinct approaches demonstrate the ability to dramatically alter surface and barrier properties of materials by merely changing pH of the contacting solution.

In many types of chemical sensors and biosensors, pH-sensitive coatings are an integral part of the transduction mechanism as local pH is altered by a chemically specific reaction between an immobilized moiety (e.g. enzyme) and an analyte compound.[40-43] As local pH is perturbed, the pH-sensitive film becomes charged and swells to alter the

potential of an electrode or field effect transistor (FET) or the resonant frequency of a piezoelectric crystal. The pH-sensitive films are most often composed of hydrogels that contain a high fraction of poly(acrylic acid).[34,40] As a recent example, Cai et al.[40] attached glucose oxidase to the surface of a 1-μm thick poly(acrylic acid-isooctylacrylate) hydrogel atop a wireless, mass-sensitive transducer. The sensor tracked glucose concentration from 1 – 15 mM, but the response time was ~1 h at the highest concentrations. Since the response time of the hydrogel is dependent on diffusion, thinner films are likely to respond more rapidly, as demonstrated by Richter and co-workers[34] who cast ~400 nm films of a PAA hydrogel and observed a more rapid response than that measured by Cai et al. In cases where ultra thin (70 nm), pH-sensitive inorganic films have been used instead of hydrogels, the response time is much faster, but the sensitivity is poor.[43] While these approaches demonstrate the concept of pH-sensitive coatings, current drawbacks include insufficient sensitivity due to the small magnitude of the film response, and slow response, most often due to excessively high film thickness that enhances the time for water and ion permeation. Films that exhibit large changes in properties upon exposure to a pH stimulus and can be prepared as defect-free, thin films have the potential to revolutionize sensor design and manufacture.

Herein, we utilize surface-catalyzed polymerization[13,23,24] to engineer a new class of pH-responsive copolymer films. As shown in Figure 1.3, we have discovered that the side groups of poly(methylene-*co*-ethyl acetate) (Figure 1.2c) can be hydrolyzed to carboxylic acids (PM-CO2H) to provide pH responsiveness. The proposed strategy toward pH-responsive films has several advantages over other approaches. (1) Surface-catalyzed polymerizations offer the ability to rapidly grow films with controlled

thicknesses; film thickness increases linearly with time.[44] (2) Film growth is selective in that polymerization occurs on gold but not on most other materials (silicon, silver, aluminum, plastics, etc.), enabling straightforward patterning of films by directed growth.[24] (3) An initiator is not required as the film growth propagates directly from the metal surface. (4) Film composition can easily be tuned to affect the film response without requiring a completely new macromolecular synthesis. Using this surface-catalyzed approach, a careful control over film composition and thickness can be employed to tailor the onset, magnitude, and rate of the response in barrier properties. This research focuses on films with well-controlled and reproducible thicknesses and uses Electrochemical Impedance Spectroscopy (EIS) method to monitor film response.

Specific Focus of Dissertation

I. Investigate the preparation of PM-rich copolymer films with randomly distributed ester side chains by surface-catalyzed polymerizations. Investigate the kinetics of film growth and the effect of monomer concentration on polymer growth and thickness.

II. Prepare pH-responsive films by modifying the ester side chains of the PM–rich copolymer films to carboxylic acid groups. Investigate the effect of fractional carboxylic acid concentration on the pH-responsive barrier properties of the polymer films.

III. Investigate kinetics of response for pH-active copolymer films. Determine optimal film thickness and functional group concentration to maximize the pH-induced response.

IV. Incorporate pH-responsive thin films within membrane supports to create smart nano-gates to control water and ion transport.

V. Broaden the pH-response range by designing pH-responsive films with amine side chains and study the dependence of side chain hydrophilicity on pH responsive behavior

References

1. Jennings, G. K.; Brantley, E. L. “Physicochemical Properties of Surface-Initiated Polymer Films in the Modification and Processing of Materials,” *Advanced Materials* **2004**, *16*, 1983-1994.

2. Rutenberg, I. M.; Scherman, O. A.; Grubbs, R. H.; Jiang, W. R.; Garfunkel, E.; Bao, Z. “Synthesis of Polymer Dielectric Layers for Organic Thin Film Transistors via Surface-Initiated Ring-Opening Metathesis Polymerization,” *Journal of the American Chemical Society* **2004**, *126*, 4062-4063.

3. Matyjaszewski, K.; Miller, P. J.; Shukla, N.; Immaraporn, B.; Gelman, A.; Luokala, B. B.; Siclovan, T. M.; Kickelbick, G.; Vallant, T.; Hoffmann, H.; Pakula, T. “Polymers at Interfaces: Using Atom Transfer Radical Polymerization in the Controlled Growth of Homopolymers and Block Copolymers from Silicon Surfaces in the Absence of Untethered Sacrificial Initiator,” *Macromolecules* **1999**, *32*, 8716-8724.

4. Boyes, S. G.; Brittain, W. J.; Weng, X.; Cheng, S. Z. D. “Synthesis, Characterization, and Properties of ABA Type Triblock Copolymer Brushes of Styrene and Methyl Acrylate Prepared by Atom Transfer Radical Polymerization,” *Macromolecules* **2002**, *35*, 4960-4967.

5. Kim, J. B.; Huang, W. X.; Bruening, M. L.; Baker, G. L. “Synthesis of Triblock Copolymer Brushes by Surface-Initiated Atom Transfer Radical Polymerization,” *Macromolecules* **2002**, *35*, 5410-5416.

6. Huang, X. Y.; Wirth, M. J. “Surface-Initiated Radical Polymerization on Porous Silica,” *Analytical Chemistry* **1997**, *69*, 4577-4580.

7. Husseman, M.; Malmstrom, E. E.; McNamara, M.; Mate, M.; Mecerreyes, D.; Benoit, D. G.; Hedrick, J. L.; Mansky, P.; Huang, E.; Russell, T. P.; Hawker, C. J. “Controlled Synthesis of Polymer Brushes by "Living" Free Radical Polymerization Techniques,” *Macromolecules* **1999**, *32*, 1424-1431.

8. Jordan, R.; Ulman, A. “Surface Initiated Living Cationic Polymerization of 2-Oxazolines,” *Journal of the American Chemical Society* **1998**, *120*, 243-247.

9. Prucker, O.; Ruhe, J. “Polymer Layers through Self-Assembled Monolayers of Initiators,” *Langmuir* **1998**, *14*, 6893-6898.

10. Tao, Y. T.; Pandian, K.; Lee, W. C. “Microfabrication of Interdigitated Polyaniline/Polymethylene Patterns on a Gold Surface,” *Langmuir* **1998**, *14*, 6158-6166.

11. Zhang, X.; Bell, J. P. “The in-Situ Synthesis of Protective Coatings on Steel through a Surface Spontaneous Polymerization Process,” *Journal of Applied Polymer Science* **1997**, *66*, 1667-1680.

12. Agarwal, R.; Bell, J. P. “Protective Coatings on Aluminum by Spontaneous Polymerization,” *Polymer Engineering and Science* **1998**, *38*, 299-310.

13. Seshadri, K.; Atre, S. V.; Tao, Y. T.; Lee, M. T.; Allara, D. L. “Synthesis of Crystalline, Nanometer-Scale, -$(CH_2)_x$- Clusters and Films on Gold Surfaces,” *Journal of the American Chemical Society* **1997**, *119*, 4698-4711.

14. Seshadri, K.; Wilson, A. M.; Guiseppi-Elie, A.; Allara, D. L. “Toward Controlled Area Electrode Assemblies: Selective Blocking of Gold Electrode Defects with Polymethylene Nanocrystals,” *Langmuir* **1999**, *15*, 742-749.

15. Leitch, J.; Cambron, R.; "Improved Yields of Polymethylene by Decomposition of Diazomethane;" National Research Council of Canada Review **1948**, 94-98.

16. Buckley, G. D.; Cross, L. H.; Ray, N. H.; "The Copper-Catalyzed Decomposition of Aliphatic Diazo-Compounds: The Formation of Paraffins of High Molecular Weight;" Journal of the Chemical Society **1950**, 2714-2718.

17. Buckley, G. D.; Ray, N. H.; "The Decomposition of Aliphatic Diazo-Compounds by Trimethyl Borate: The Percipitation of Branched-Chain Paraffins of High Molecular Weight;" Journal of the Chemical Society **1952**, 3701-3704.

18. Bawn, C. E. H.; Ledwith, A.; Matthies, P. “The Mechanism of the Polymerization of Diazoalkanes Catalyzed by Boron Compounds,” *Journal of Polymer Science* **1959**, *84*, 93-108.

19. Davies, A. G.; Hare, D. G.; Khan, O. R.; Sikora, J. “Monomethylation and Polymethylenation by Diazomethane in the Presence of Boron Compounds,” *Journal of the Chemical Society* **1963**, 4461-4471.

20. Mucha, M.; Wunderlich, B. “Crystallization during Polymerization of Diazomethane. I. The Boron Trifluride Catalyzed Reaction,” *Journal of Polymer Science* **1974**, *12*, 1993-2018.

21. Shea, K. J.; Walker, J. W.; Zhu, H.; Paz, M.; Greaves, J. “Polyhomologation. A Living Polymethylene Synthesis,” *Journal of the American Chemical Society* **1997**, *119*, 9049-9050.

22. Shea, K. J.; Staiger, C. L.; Lee, S. Y. “Synthesis of Polymethylene Block Copolymers by the Polyhomologation of Organoboranes,” *Macromolecules* **1999**, *32*, 3157-3158.

23. Guo, W. F.; Jennings, G. K. “Use of Underpotentially Deposited Metals on Gold to Affect the Surface-Catalyzed Formation of Polymethylene Films,” *Langmuir* **2002**, *18*, 3123-3126.

24. Guo, W. F.; Jennings, G. K. “Directed Growth of Polymethylene Films on Atomically Modified Gold Surfaces,” *Advanced Materials* **2003**, *15*, 588-591.

25. Chanunpanich, N.; Ulman, A.; Malagon, A.; Strzhemechny, Y. M.; Schwarz, S. A.; Janke, A.; Kratzmueller, T.; Braun, H. G. “Surface Modification of Polyethylene Films via Bromination: Reactions of Brominated Polyethylene with Aromatic Thiolate Compounds,” *Langmuir* **2000**, *16*, 3557-3560.

26. Wu, S. S.; Xu, X. “Effect of the Reaction Atmosphere on High-Density Polyethylene Functionalized by Ultraviolet Irradiation,” *Journal of Applied Polymer Science* **2004**, *91*, 2326-2329.

27. Bergbreiter, D. E.; Franchina, J. G.; Kabza, K. “Hyperbranched Grafting on Oxidized Polyethylene Surfaces,” *Macromolecules* **1999**, *32*, 4993-4998.

28. Zheng, Z.; Tang, X. Z.; Shi, M. W.; Zhou, G. T. “Surface Modification of Ultrahigh-Molecular-Weight Polyethylene Fibers,” *Journal of Polymer Science Part B-Polymer Physics* **2004**, *42*, 463-472.

29. Shea, K. J. “Polyhomologation: The Living Polymerization of Ylides,” *Chemistry-A European Journal* **2000**, *6*, 1113-1119.

30. Shea, K. J.; Busch, B. B.; Paz, M. M. “Polyhomologation: Synthesis of Novel Polymethylene Architectures by a Living Polymerization of Dimethylsulfoxonium Methylide,” *Angewandte Chemie-International Edition* **1998**, *37*, 1391-1393.

31. Busch, B. B.; Paz, M. M.; Shea, K. J.; Staiger, C. L.; Stoddard, J. M.; Walker, J. R.; Zhou, X. Z.; Zhu, H. D. “The Boron-Catalyzed Polymerization of Dimethylsulfoxonium Methylide. A Living Polymethylene Synthesis,” *Journal of the American Chemical Society* **2002**, *124*, 3636-3646.

32. Busch, B. B.; Staiger, C. L.; Stoddard, J. M.; Shea, K. J. “Living Polymerization of Sulfur Ylides. Synthesis of Terminally Functionalized and Telechelic Polymethylene,” *Macromolecules* **2002**, *35*, 8330-8337.

33. Zhu, X.; DeGraaf, J.; Winnik, F. M.; Leckband, D. “Tuning the Interfacial Properties of Grafted Chains with a pH Switch,” *Langmuir* **2004**, *20*, 1459-1465.

34. Richter, A.; Bund, A.; Keller, M.; Arndt, K. F. “Characterization of a Microgravimetric Sensor Based on pH Sensitive Hydrogels,” *Sensors and Actuators B-Chemical* **2004**, *99*, 579-585.

35. Lee, S. B.; Martin, C. R. “pH-Switchable, Ion-Permselective Gold Nanotubule Membrane Based on Chemisorbed Cysteine,” *Analytical Chemistry* **2001**, *73*, 768-775.

36. Hou, Z. Z.; Abbott, N. L.; Stroeve, P. “Self-Assembled Monolayers on Electroless Gold Impart pH-Responsive Transport of Ions in Porous Membranes,” *Langmuir* **2000**, *16*, 2401-2404.

37. Chun, K. Y.; Stroeve, P. “External Control of Ion Transport in Nanoporous Membranes with Surfaces Modified with Self-Assembled Monolayers,” *Langmuir* **2001**, *17*, 5271-5275.

38. Chun, K. Y.; Stroeve, P. “Protein Transport in Nanoporous Membranes Modified with Self-Assembled Monolayers of Functionalized Thiols,” *Langmuir* **2002**, *18*, 4653-4658.

39. Hester, J. F.; Olugebefola, S. C.; Mayes, A. M. “Preparation of pH-Responsive Polymer Membranes by Self-Organization,” *Journal of Membrane Science* **2002**, *208*, 375-388.

40. Cai, Q. Y.; Zeng, K. F.; Ruan, C. M.; Desai, T. A.; Grimes, C. A. “A Wireless, Remote Query Glucose Biosensor Based on a pH-Sensitive Polymer,” *Analytical Chemistry* **2004**, *76*, 4038-4043.

41. Korpan, Y. I.; Volotovsky, V. V.; Martelet, C.; Jaffrezic-Renault, N.; Nazarenko, E. A.; El'skaya, A. V.; Soldatkin, A. P. “A Novel Enzyme Biosensor for Steroidal Glycoalkaloids Detection Based on pH-Sensitive Field Effect Transistors,” *Bioelectrochemistry* **2002**, *55*, 9-11.

42. Schoning, M. J.; Arzdorf, M.; Mulchandani, P.; Chen, W.; Mulchandani, A. “Towards a Capacitive Enzyme Sensor for Direct Determination of Organophosphorus Pesticides: Fundamental Studies and Aspects of Development,” *Sensors* **2003**, *3*, 119-127.

43. Keusgen, M.; Kloock, J. P.; Knobbe, D. T.; Junger, M.; Krest, I.; Goldbach, M.; Klein, W.; Schoning, M. J. “Direct Determination of Cyanides by Potentiometric Biosensors,” *Sensors and Actuators B-Chemical* **2004**, *103*, 380-385.

44. Bai, D.; Jennings, G. K. “Surface-Catalyzed Growth of Polymethylene-Rich Copolymer Films on Gold,” *Journal of the American Chemical Society* **2005**, *127*, 3048-3056.

CHAPTER III

EXPERIMENTAL PROCEDURES AND CHARACTERIZATION METHODS

Experimental Procedures

Materials

Potassium hydroxide, Diazald (N-methyl-N-nitroso-P-toluenesulfonamide), ethyl diazoacetate (EDA), n-butyl amine, N,N-dimethyethylenediamine (DMEDA), thionyl chloride, and poly(ethylene-co-ethylacrylate) (PEEA) were used as received from Aldrich (Milwaukee, WI). Benzoic acid, 2-propanol, sodium bicarbonate, sodium carbonate, potassium hydrogen phthalate, sodium phosphate monobasic, and acetone were used as received from Fisher (Fair Lawn, NJ). Hydrochloric acid and sodium hydroxide were used as received from EM Science (Gibbstown, NJ). Ethyl ether anhydrous was obtained from EMD Chemicals (Gibbstown, NJ). Gold shot (99.99%) and chromium-coated tungsten filaments were obtained from J&J Materials (Neptune City, NJ) and R.D. Mathis (Signal Hill, CA), respectively. Silicon (100) wafers (Montco Silicon; Spring City, PA) were rinsed with ethanol and deionized water and dried with nitrogen. Ethanol (absolute) was used as received from AAPER (Shelbyville, KY). Nitrogen gas was obtained from J&M Cylinder Gas, Inc (Decatur, AL). Deionized water (16.7 MΩ·cm) was purified with a Modu-Pure system (Continental Water Systems Corporation; San Antonio, TX) and used for rinsing.

All pH buffer solutions were prepared according to a literature procedure[1] except that we used NaH_2PO_4 instead of KH_2PO_4 and the pH 9 solution was prepared by mixing appropriate volumes of 0.1 M Na_2CO_3 with 0.1 M $NaHCO_3$. In a typical preparation procedure, specified volumes[1] of 0.1 M HCl (pH 4) or 0.1 M NaOH (pH 5 – 8, 10 – 11) were added to 50 mL of a solution containing 0.1 M potassium hydrogen phthalate (pH 4 - 5), 0.1 M NaH_2PO_4 (pH 6 – 8), or 0.05 M $NaHCO_3$ (pH 10 – 11) and the solution volume was diluted to 100 mL using deionized water. The pH was then measured using a Corning 430 pH meter with 3-in-1 combination electrode and adjusted by addition of HCl, NaOH, or appropriate salt.

Preparation of Gold Substrates

Gold substrates were prepared by evaporating chromium (100 Å) and gold (1250 Å) in sequence onto silicon (100) wafers at rates of 1-2 Å s^{-1} in a diffusion-pumped chamber with a base pressure of 4 x 10^{-6} torr. After removal from the evaporation chamber, the wafers were cut into 1.2 cm x 4 cm pieces, rinsed with ethanol, and dried in a stream of N_2 gas.

Preparation of Diazomethane

DM was carefully prepared according to a literature procedure[2] and diluted with ether at 0 °C to prepare solutions of different concentration. CAUTION: Diazomethane is toxic and potentially explosive and should be handled carefully![2] The concentration of DM was determined by titration with benzoic acid.[3]

Preparation of Copolymer Films

Typically, polymer films were prepared by exposure of gold-coated silicon substrates to ether solutions containing desired concentrations of DM or DM and EDA at 0 °C for various times. Film growth was carried out in capped 20 mL vials, and only one substrate was placed in each vial. Upon removal, the samples were rinsed with ether and ethanol and dried in a stream of nitrogen.

Characterization Methods

Reflectance Absorption Infrared Spectroscopy

Reflectance absorption infrared spectroscopy (RAIRS) is a non-destructive, vibrational spectroscopic method used to determine film composition and to derive structural information from the polymer films. Vibrational spectra are used as characteristic fingerprints for adsorbate molecules, adsorption configurations and structures. Substrates can be metallic or non metallic and should not produce absorption bands in the spectral range of interest.[4] RAIRS involves a single external reflection of an IR beam at a reflective substrate that is coated by an organic film. The reflected light creates an electric field normal to the substrate.

Although several types of IR spectroscopy exist, RAIRS specifically has the ability to aid in determination of structural information of films. The observed peak intensity for a given stretching or bending mode from RAIRS is proportional to the square of the component of its dynamic dipole moment normal to the surface, as indicated by the following proportionality:[5]

$$I \propto cos^2 \theta_{mz} \tag{3-1}$$

where I represents the spectral intensity and θ_{mz} is the average angle between the transition dipole moment (m) for a particular band and the surface normal (z). This dependence arises because, for radiation polarized parallel to the plane of incidence (substrate), the resulting electric field vector is mostly perpendicular to the substrate.[6,7] Thus, during absorbance of IR radiation, band intensity will be highest when the transition dipole moment is most closely aligned normal to the surface ($\theta_{mz} \rightarrow 0°$), and transition dipole moments that lie nearly parallel to the surface normal ($\theta_{mz} \rightarrow 90°$) will have much less spectral intensity.

Peak positions and intensities in the RAIRS spectrum can provide compositional and structural information on the polymer films. Molecular groups within the polymer film absorb the IR radiation to yield absorbance peaks in the spectrum with intensities that depend on the concentration of those groups within the films and the orientation of their transition dipole moments relative to the electric field.[5] Table 3.1 lists the peak positions and chemical group assignments for IR peaks commonly encountered in the polymer films in this study. More detailed discussion of specific IR peaks will be addressed as necessary.

RAIRS was performed using a Varian 3100 FT-IR spectrometer. The p-polarized light was incident at 80° from the surface normal. The instrument was run in single reflection mode and equipped with a Universal sampling accessory. A liquid nitrogen-cooled, narrow-band MCT detector was used to detect reflected light. Spectral resolution

was 2 cm^{-1} after triangular apodization. Each spectrum was accumulated over 1000 scans with a deuterated octadecanethiol-d_{37} self-assembled monolayer on gold as the background.

Table 3.1. Important IR vibrational mode peak positions for characterization of polymer films in this study. The chemical group assignment and a brief description of the relevance of the peaks to this study are listed. Unless noted, all peaks represent stretching vibrational modes.

Absorbance (cm^{-1})	Assignment	Comment
1000-1300	C-O	Multiple bands of varying intensity
1100-1400	C-F	Multiple strong bands, especially for long chains; ratio of certain of these peaks leads to structural information for fluorocarbon chains in bulk
1400-1500	C-H (bending)	Moderate bands
1400-1500	C⋯O	Weak bands; from Carboxylate ion symmetrical stretching
1500-1600	C⋯O	Strong bands; from Carboxylate ion asymmetrical stretching
1500-1600	Amide II	Strong bands; from N-H bending
1600-1700	Amide I	Strong bands; from C=O stretching
1700-1800	C=O	Strong bands; C=O stretching bond from ester or carboxylic acid
1800-1900	C=O	Strong Bonds, C=O stretching from acid chloride
2800-2950	C-H	Various moderate bands; CH_2 peak positions contain crystallinity/structuring information

Ellipsometry

Ellipsometry allows measurement of thickness and refractive index of single films, layer stacks, and substrate materials with very high sensitivity.[8] Film thickness between 0.1 nm and 100 μm can be measured, depending on the spectral range used and the homogeneity of the thicker films. Thickness < 1 μm can be determined with a sensitivity better than 0.01 nm.[8] Linear polarized light in a specified wavelength range is reflected from a sample surface and changed into elliptically polarized light. Both the phase (Δ) and amplitude (Ψ) of the reflected light are collected by a detector. Information about the properties of the sample are contained in the complex ratio, ρ of the Fresnel coefficient of reflection of the parallel (r_p) and perpendicular (r_s) incident plane polarized electrical field vector

$$\rho = \frac{r_P}{r_s} \tag{3-2}$$

The fundamental equation of ellipsometry

$$\rho = \tan\psi e^{i}\Delta \tag{3-3}$$

describes the connection between the measured quantities Ψ and Δ and the sample properties contained in the coefficient of reflection ρ.[8] Model layers representing the film on the surface can be created to fit theory to the measured data. Typically for polymer films, a generic two-term Cauchy layer model is used for this purpose.

$$n = A_n + \frac{B_n}{\lambda^2} \tag{3-4}$$

where n is the film refractive index, A_n and B_n are model fit parameters, and λ is the wavelength of incident light. Since both the film refractive index, n, and thickness are usually not known, this model allows both of these physical film parameters to be determined by fitting experimental data with the model and minimizing the mean square error between the two.[9]

Ellipsometry measurements were obtained on a J.A. Woollam Co. M-2000DI variable angle spectroscopic ellipsometer with WVASE32 software for modeling. Measurements at three spots per sample were taken with light incident at a 75° angle from the surface normal using wavelengths from 250 to 1000 nm. Optical constants for a bare gold substrate, cut from the same wafer as the samples to be characterized, were measured by ellipsometry and used as the baseline for all polymer film samples. Film thickness of the polymer layer on samples was determined using a Cauchy layer model. Since the copolymer films are PM rich (ester content < 5%), the refractive index for the film was set to 1.5, consistent with the ranges measured for polyethylene.[10]

Electrochemical Impedance Spectroscopy

Impedance is a measure of the ability of a circuit to resist the flow of electrical current. The technique where the impedance of a cell or electrode impedance is determined as a function of frequency is called electrochemical impedance spectroscopy.[11] In the imdepance study, when a sinusoidal potential of small magnitude is

applied to the cell, the excitation signal, expressed as a function of time, can be expressed as[12]

$$E(t) = E_0 \cos(\omega t) \tag{3-5}$$

where E(t) is the potential at time t, E_0 is the amplitude of the signal, and ω is the radial frequency, given as

$$\omega = 2\pi f \tag{3-6}$$

where f is the frequency. In a linear system, the response signal, I(t) is shifted in phase angle ϕ and has an amplitude I_0

$$I(t) = I_0 \cos(\omega t - \phi) \tag{3-7}$$

Thus, the impedance of the system can be expressed in terms of a magnitude, Z_0 and a phase shift ϕ as

$$Z = \frac{E(t)}{I(t)} = \frac{E_0 \cos(\omega t)}{I_0 \cos(\omega t - \phi)} = Z_0 \frac{\cos(\omega t)}{\cos(\omega t - \phi)} \tag{3-8}$$

Using Euler's relationship,

$$\exp(j\phi) = \cos(\phi) + j\sin(\phi) \tag{3-9}$$

It is possible to express the impedance as a complex function,[12] where the potential is given as

$$E(t) = E_0 \exp(j\omega t) \tag{3-10}$$

and the current response as,

$$I(t) = I_0 \exp(j\omega t - \phi) \tag{3-11}$$

The impedance is then represented as a complex number.

$$Z = \frac{E(t)}{I(t)} = \frac{E_0 \exp(j\omega t)}{I_0 \exp(j\omega t - j\phi)} = Z_0 \exp(j\phi) = Z_0(\cos\phi + j\sin\phi) \tag{3-12}$$

Since an electrochemical cell is used, the results can be modeled using an equivalent electrical circuit consisting of resistors and capacitors. Thus, the magnitude of Z written as $|Z|$, is given by[13]

$$|Z|^2 = (Z_R)^2 + (Z_I)^2 \tag{3-13}$$

$$Z_R = R \tag{3-14}$$

$$Z_I = 1/j\omega C \tag{3-15}$$

where Z_R and Z_I are the real (resistance) and imaginary (capacitance) components of the impedance. The phase angle, ϕ, is given by

$$\tan\phi = Z_I/Z_R = 1/\omega RC \tag{3-16}$$

The phase angle ϕ expresses the balance between the real and imaginary components in the circuit. For a pure resistance, ϕ= 0˚, for a pure capacitance, ϕ= -90˚, and for a mixture, intermediate phase angles are observed.

The impedance data can be fitted by an equivalent circuit model to quantitatively determine physical film properties (resistance and capacitance). Depending on the film, various circuit models may fit the impedance data. By obtaining the component values under different experimental conditions such as different pH, we can quantify film property changes upon stimuli.

For time-dependent impedance studies, ω is a constant (100 Hz in this study). By monitoring the changes of Z_R, Z_I, and ϕ as a function of time when we switch the contacting solution pH from one value to the other, we can obtain useful information of the rate of the film response.

EIS was performed with a Gamry Instruments CMS300 impedance system interfaced to a personal computer. A Flat Cell (EG&G Instruments) was used to expose only 1 cm^2 of each sample to a pH buffer solution while preventing sample edges from being exposed. The electrochemical cell consisted of a pH buffer solution prepared as described above with an Ag/AgCl/saturated KCl reference electrode, a gold substrate counter electrode, and a gold substrate containing the film to be studied as the working electrode. In a typical study, the measurements were made at the open circuit potential with a 5 mV ac perturbation that was controlled between 0.05 Hz and 20 kHz. All data were collected in the range from 10^4 to 10^{-1} Hz using 10 points per decade and were fit with an appropriate equivalent circuit model to determine resistance and capacitance values. At each pH value, sufficient time was allowed to make sure that the film reached a stable state as evidenced by the accumulation of repeated spectra that did not change with time. Reported values and ranges for resistance and capacitance represent the average and standard deviation of values obtained from at least three independent sample preparations.

Contact Angle Goniometry

Contact angles are straightforward measurements that can provide much information on surface composition and properties. When a drop of liquid is placed on solid surface, it may remain as a drop of finite area, or it may spread across the surface. When a liquid is in contact with a solid surface in static equilibrium with its vapor, the contact angle θ is related to the interfacial tensions of the solid-vapor (γ_{SV}), solid-liquid (γ_{SL}), and liquid-vapor (γ_{LV}) interfaces through Young's Equation:[14]

$$\cos\theta = \frac{\gamma_{SV} - \gamma_{SL}}{\gamma_{LV}} \tag{3-17}$$

Eq. (3-17) is geometrical relation. If we consider the solid surface roughness (r), we will obtain the apparent contact angle as shown in eq. (3-18)[14]

$$\cos\theta' = r\frac{\gamma_{SV} - \gamma_{SL}}{\gamma_{LV}} = r\cos\theta \tag{3-18}$$

where θ' is the apparent contact angle, θ is the real contact angle in eq. (3-17) and r is the surface roughness which equals the real surface area over the plane geometrical area. Thus, increasing surface roughness enhances contact angles (θ) that are greater than 90° while reducing contact angles that are less than 90°.

Contact angles are sensitive to the outer half nanometer of film composition/structure to enable a semiquantitative assessment of surface properties of films. Water (H_2O) and hexadecane (HD) are generally used as contacting liquids to indicate the relative hydrophilicity/hydrophobicity and oleophilicity/oleophobicity of a surface. H_2O will exhibit high contact angles if any hydrophobic material is present at the surface whereas HD has a greater sensitivity to specific chemical groups, especially in distinguishing hydrocarbon groups from fluorocarbon groups.[15]

The contact angle hysteresis (H), which is a quantity that provides additional information about a film surface, is defined as:[16]

$$H = \theta_A - \theta_R \tag{3-19}$$

where θ_A, the advancing contact angle, is measured after liquid has been added to the drop, causing it to slowly advance across the surface, and θ_R, the receding contact angle, is measured after liquid has been removed from the drop, causing it to slowly recede across the surface. Hysteresis scales with surface roughness and chemical heterogeneity.

The contact angle is also very useful to assess the surface chemical heterogeneity via the Cassie equation[16]

$$\cos\theta = f_1 \cos\theta_1 + f_2 \cos\theta_2 \tag{3-20}$$

where f_1 and f_2 are the area fractions of the surface having inherent contact angles θ_1 and θ_2. Theoretically, if the inherent contact angles of a test liquid on the homogeneous surface are known, then the composition of a composite surface can be estimated from a simple contact angle measurement.

A Rame-Hart goniometer with a microliter syringe was used to measure advancing contact angles on static drops of water on the modified substrates. The needle tip of the syringe remained inside the liquid drop while measurements were taken on both sides of ~5 mL drops. Reported values and ranges represent the average and standard deviations of three drops per sample with both edges measured per drop.

Scanning Electron Microscopy

Scanning Electron Microscopy was used to obtain the surface images of the membrane skins. All images were obtained using a Hitachi S4200 high-resolution scanning electron microscope equipped with a cold field emission electron gun at an accelerating voltage of 5 kV.

Scanning electron microscopy is a powerful technique to yield topology, morphology, composition, and crystallographic information. In the SEM, an electron stream is produced by the electron gun and focused (in vacuum) into a fine probe that is rastered over the surface of the specimen. The primary electrons impinging on a surface will have an energy of a few hundred eV up to 30 keV. After the beam interacts with the sample, the emission of electrons or photons from (or through) the surface will be collected by appropriate detectors, and the output can be used to modulate the brightness of a cathode ray tube (CRT) whose x and y-inputs are driven in synchronism with the x-y voltage rastering the electron beam. In this way, an image is produced on the CRT. Every point that the beam strikes on the sample is mapped directly onto the corresponding point on the screen. Three types of images can be produced in the SEM: secondary electron images, backscattered electron images, and elemental X-ray maps. Secondary electrons with energy lower than 50 eV are produced within the first few nm of the surface. An image of the sample surface can thus be constructed by measuring secondary electron intensity as a function of the position of the scanning primary electron beam.[17]

If the sample is vacuum compatible, the use of SEM requires very little in regard to sample preparation. For the conductive samples, the major limitation is whether the

sample will fit onto the stage. If the sample is an insulator, a thinner layer of conductive material (10 nm) can be coated atop the sample before SEM analysis. Uncoated insulating samples also can be studied by using low primary beam voltage (<2.0 keV), but the image resolution will be compromised.[17]

References

1. Bates, R. G.; Bower, V. E. The Measurement of pH. In *Handbook of Analytical Chemistry;* Meites, L. Ed.; Mcgraw-Hill: New York, 1963.

2. Diazald, MNNG, and Diazomethane Generators, Aldrich Technical Information Bulletin Number Al-180, 1993.

3. Arndt, F. *Organic Synthesis*; Wiley: New York, 1943; Collect. Vol. IV, 165-167.

4. Hinrichs, K. Reflection Absorption IR Spectroscopy (RAIRS). In *Surface and Thin Film Analysis; Bubert*, H; Jenett, H., Ed.; Wiley-VCH: Weinheim, 2002.

5. Nuzzo, R. G.; Dubois, L. H.; Allara, D. L. "Fundamental-Studies of Microscopic Wetting on Organic-Surfaces. 1. Formation and Structural Characterization of a Self-Consistent Series of Polyfunctional Organic Monolayers," *Journal of the American Chemical Society* **1990**, *112*, 558-569.

6. Greenler, R. G. "Infrared Study of Adsorbed Molecules on Metal Surfaces by Reflection Techniques," *Journal of Chemical Physics* **1966**, *44*, 310-314.

7. Parikh, A. N.; Allara, D. L. "Quantitative-Determination of Molecular-Structure in Multilayered Thin-Films of Biaxial and Lower Symmetry from Photon Spectroscopies. I. Reflection Infrared Vibrational Spectroscopy," *Journal of Chemical Physics* **1992**, *96*, 927-945.

8. Gruska, B.; Roseler, A. UV-Vis-IR Ellipsometery (ELL). In *Surface and Thin Film Analysis;* Bubert, H.; Jenett, H., Ed.; Wiley-VCH: Weinheim, 2002.

9. Woollam, J. A.; Bungay, C.; Hilfiker, J.; Tiwald, T. "VUV and IR Spectroellipsometric Studies of Polymer Surfaces," *Nuclear Instruments & Methods in Physics Research Section B: Beam Interactions with Materials and Atoms* **2003**, *208*, 35-39.

10. Seferis, J. C. Refractive Indices of Polymers. In *Polymer Handbook*; Brandrup, J.; Immergut, E. H.; Grulke, E. A. Eds.; John Wiley & Sons: New York, 1999.

11. Bard, A. And Faulkner, L. *Electrochemical Methods Fundamentals and Applications;* John Wiley & Sons: New York, 2000.

12. Gamry Instrument, Inc. "Gamry Instruments Software Tutorials and Primers"; Warminster, PA, 2003.

13. Bard, A.; Faulkner, L. *Electrochemical Methods Fundamentals and Applications;* John Wiley & Sons: New York, 2000.

14. Zisman, W. A. *Contact Angle, Wettability, and Adhesion*; American Chemical Society: Washington, D.C., 1964; Vol. 43.

15. Bantz, M. R.; Brantley, E. L.; Weinstein, R. D.; Moriarty, J.; Jennings, G. K. "Effect of Fractional Fluorination on the Properties of ATRP Surface-Initiated Poly(hydroxyethyl methacrylate) Films," *Journal of Physical Chemistry B* **2004**, *108*, 9787-9794.

16. Myers, D. *Surfaces, Interfaces, and Colloids: Principles and Applications*; 2nd Ed. John Wiley & Sons: New York, 1999.

17. Bindell, J. B. Scanning Electron Microscopy. In *Encyclopedia of Materials Characterization: Surface, Interfaces, Thin Films;* Brundle, C. R.; Evans, C. A. Jr.; Wilson, S., Ed.; Butterworth-Heinemann: Boston, 1999.

CHAPTER IV

SURFACE-CATALYZED GROWTH OF POLYMETHYLENE-RICH COPOLYMER FILMS ON GOLD

Introduction

While polyethylene is produced abundantly and has many desirable properties, its use in thin films and coatings for advanced materials processing has been limited by its poor solubility,[1] which precludes spin coating and solution casting the polymer into films, and its chemical stability, which creates challenges in surface functionalization.[2] The former problem could be greatly alleviated by recent solution-phase methods to grow polymethylene (PM) from metal surfaces[3-7] based on decomposition of diazomethane (DM) and subsequent polymerization. However, common methods to modify the surfaces of PM or PE such as bromination[8] or oxygenation[9] with UV irradiation or treatment with strong acids[2] or oxygen plasma,[10] occur under harsh conditions that may be incompatible with other materials present on a particular surface. Synthetic methods, such as polyhomologation, have been pioneered by Shea and co-workers[11-16] to create uniquely end-functionalized PM, but this remarkable chemistry has not been extended into thin film processing.

Here, we report a new approach to create functionalized PM thin films. We simply expose gold substrates to an ether solution containing both DM and ethyl diazoacetate (EDA) to produce a copolymer film containing PM segments with randomly distributed ethyl ester side groups (Figure 1.3). We demonstrate that these ester side groups can be hydrolyzed to produce pH-responsive carboxylic acid groups that are

potentially useful for further film modification. We have varied the compositional ratio of DM to EDA to effect film composition and growth rates, as determined by reflectance-absorption infrared spectroscopy (RAIRS) and spectroscopic ellipsometry, respectively. We have also used ellipsometry and RAIRS to characterize the kinetics of film growth and track the film composition during growth. We have combined these tools with surface-sensitive wetting measurements to gain a greater understanding of the nature of copolymer film propagation. In particular, our results provide information on the location of the propagation site and on distinct mechanistic pathways for PM homopolymerization versus copolymerization.

Cationic,[17,18] free-radical,[3,19] and insertion[18,20] mechanisms have been proposed to describe the decomposition of DM to form PM in the presence of various catalysts. Seshadri et al.[3] proposed a free-radical mechanism to describe the heterogeneous propagation of PM on gold from ethereal DM solutions. Early results on homogeneous PM formation in the presence of a BF_3 catalyst have led researchers to propose an insertion mechanism where methylene adsorbs to the boron center and inserts into a B-halide or B-alkyl bond to increase the polymethylene chain length by one unit.[20] A similar insertion mechanism has been confirmed by Shea and coworkers[11] for the preparation of end-functionalized polymethylene using dimethylsulfoxonium methylide, a methylene producing precursor similar to DM, in the presence of alkyl boranes. An insertion mechanism has also been proposed for the photochemical polymerization of DM on hydrogen-terminated silicon[21] and for the propagation of alkyl chains on copper using methylene iodide at low pressures.[22] These insertion routes allow for the continual

creation of carbon-carbon bonds at an appropriate catalytic surface and may enable the controlled preparation of polymer films with novel compositions.

This study reports a unique type of polymerization and heterogeneous catalysis at evaporated gold surfaces to produce a new class of polymer films. We exploit the combination of two precursors in the polymerization to glean mechanistic insight into the catalyzed mechanism that is often not possible for homopolymerizations. The surface-initiated nature of this polymerization minimizes steric effects to enable nanometer-scale control over film thickness, is compatible with bottom-up processing to enable the directed growth of the films, and could be extended in a straightforward manner to surfaces of various geometries.

Experimental Procedures

Preparation of Polymer Films

Polymer films were formed by exposure of gold-coated silicon substrates (ca. 4 cm x 1 cm) to ether solutions containing desired concentrations of DM or DM and EDA at 0 °C from a few minutes to several hours. Film growth was carried out in capped 20 ml vials and only one substrate was placed in each vial. Upon removal, the samples were rinsed with ether and dried in a stream of nitrogen.

Air Exposure and Solvent Switch Experiments

Gold-coated silicon substrates were immersed into a solution containing 4 mM DM and 40 mM EDA in ether at 0 °C for 1 h, and then removed, rinsed with ether, and

placed into either 4 mM DM in ether, 40 mM EDA in ether, or the original solution for 8 h. After the 8-h exposure, the substrates were removed, rinsed with ether, and dried in a stream of N_2. The total time for air exposure and rinsing was ~15 s. Control samples that were exposed only to the original solution for 1 h and 9 h or to the latter solution for 8 h were also prepared to compare film properties.

In a separate experiment, a gold-coated silicon substrate was placed into a solution containing 4 mM DM and 40 mM EDA in ether at 0 °C for 18 h and then, was removed, rinsed with ether, and placed it into a different solution containing 1 mM DM and 80 mM EDA in ether at 0 °C for 6 h. Upon removal, the samples were rinsed with ether and dried in a stream of nitrogen. Control samples that were exposed only to the original solution for 18 h or to the latter solution for 6 h were also prepared to compare film properties.

Experiments with Additives

Hydroquinone, 4-*tert*-butylcatechol, styrene, isobutyl vinyl ether, or benzylamine was added to a solution containing 4 mM DM and 40 mM EDA in ether at 0 °C, such that the concentration of the additive was 20 mM. The gold-coated silicon substrates were then immersed into the solution for 24 h. Upon removal, the samples were rinsed with ether and dried in a stream of nitrogen. Control samples were also prepared by exposing gold substrates to a solution of 4 mM DM and 40 mM EDA without additives for 24 h.

Hydrolysis of Copolymer Films

Hydrolysis of the copolymer films was carried out in a solution of 0.5 M KOH in ethanol at reflux for 4 h. The hydrolyzed samples were rinsed with ethanol and DI water and dried in a N_2 stream.

Results

Film Composition

To assess whether homopolymer and copolymer films could be grown from gold surfaces, we immersed gold-coated silicon substrates in solutions containing either 4 mM DM, 40 mM EDA, or 4 mM DM and 40 mM EDA in ether at 0 °C for 24 h and then obtained reflectance-absorption IR spectra (Figure 4.1). For the gold substrate exposed to EDA, no peaks appear in the spectrum, indicating that EDA alone does not yield a polymer film on gold.[23] In contrast, gold exposed to DM results in a polymethylene (PM) film, as evidenced by the appearance of bands for CH_2 stretching (2800-3000 cm^{-1}) and CH_2 bending (1460-1475 cm^{-1}). The positions of the symmetric and asymmetric CH_2 stretching vibrational modes at 2851 and ~2921 cm^{-1}, respectively, suggest that the PM film is polycrystalline.[24] The absence of peaks at ~2960 cm^{-1} and 2880 cm^{-1} indicates that the polymer does not contain a detectable amount of methyl groups ($-CH_3$), which could be introduced through branching or terminations.

When gold substrates are exposed to a mixture of DM and EDA in ether, the IR spectrum shows the additional appearance of C=O stretching at 1735 cm^{-1}, C-O stretching from 1000-1300 cm^{-1}, CH_3 bending at 1375 cm^{-1}, and CH_3 stretching around

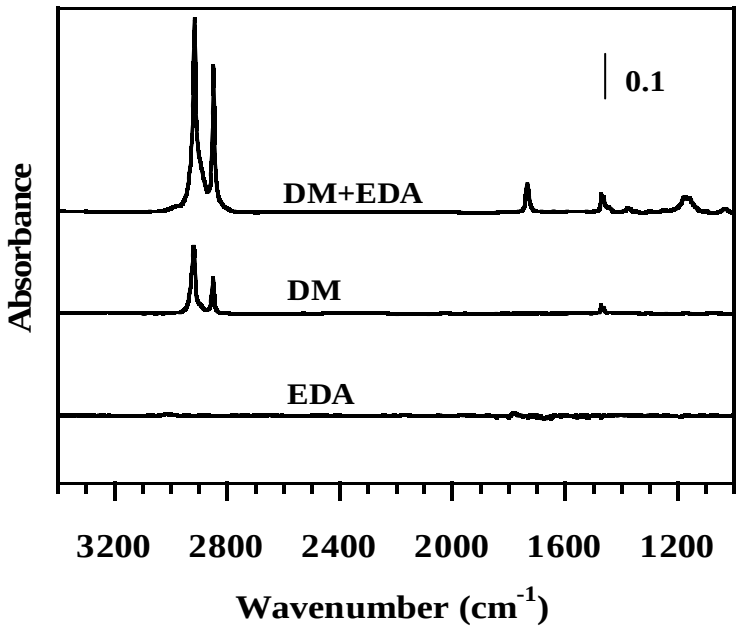

Figure 4.1. Reflectance-absorption infrared spectra for gold surfaces after exposure to 4 mM DM, 40 mM EDA or 4 mM DM and 40 mM EDA in ether at 0 °C for 24 h. There are several key regions of interest when evaluating the polymer film growth: C-H stretching, 2800-3000 cm^{-1}; C-H bending, 1460-1475 $cm^{-1;}$ C=O stretching, 1730-1740 cm^{-1}; and C-O stretching, 1000-1300 cm^{-1}.

2960 cm^{-1}.[25] These IR results, combined with the lack of polymerization for EDA alone, are consistent with a random copolymer, poly(methylene-*co*-ethyl acetate), with the structure shown in Figure 1.2c. An important phenomenon observed during the copolymer growth is that the presence of EDA results in dramatically enhanced C-H absorbance bands, consistent with a much thicker film than PM. For the same DM concentration after 24 h of growth, the CH_2 stretching peaks of the copolymer film are nearly three times more intense than those of PM alone. This enhancement in C-H stretching cannot be accounted for based on the addition of ethyl ester side chains to the

film since the C=O stretching and C-O bending peaks for the copolymer are very weak compared to the total C-H stretching peaks.

To estimate the molar ester content within the surface-catalyzed copolymer films, we cast a commercially available random copolymer (poly(ethylene-co-ethyl acrylate) (PEEA)) as a control film. The purchased PEEA has a known 18 wt% ethyl acrylate content and a chemical structure that is very similar to the studied copolymer. Based on the integrated ratio of CH_2 and C=O peak areas in the IR spectrum for the cast PEEA film, we have estimated that the ratio of methylene to ethyl ester units within the copolymer film of Figure 4.1 is ~110 to 1 (molar ester content = 0.9%). The enhancement in growth, therefore, is not due to a stoichiometric complex derived from EDA and DM, but likely due to either faster or additional modes of utilizing DM in the film growth when EDA or an adsorbed intermediate is present.

Growth Kinetics

To investigate the kinetics of copolymerization, we have obtained thicknesses and IR spectra for gold substrates exposed to 4 mM DM and 40 mM EDA in ether at 0 °C for various times (Figure 4.2a). Based on thickness measurements, the copolymerization results in pronounced growth during the first ~3 min (see inset) and a constant rate of growth thereafter for the entire 24 h. Since the rate of film growth should scale with the concentration of actively propagating chains, the initially decaying growth rate suggests a termination of polymer chains whereas the constant rate of growth over 24 h is consistent with a controlled polymerization in which the rate of chain termination is extremely slow.[26] We have previously shown that the PM homopolymer on gold exhibits a very

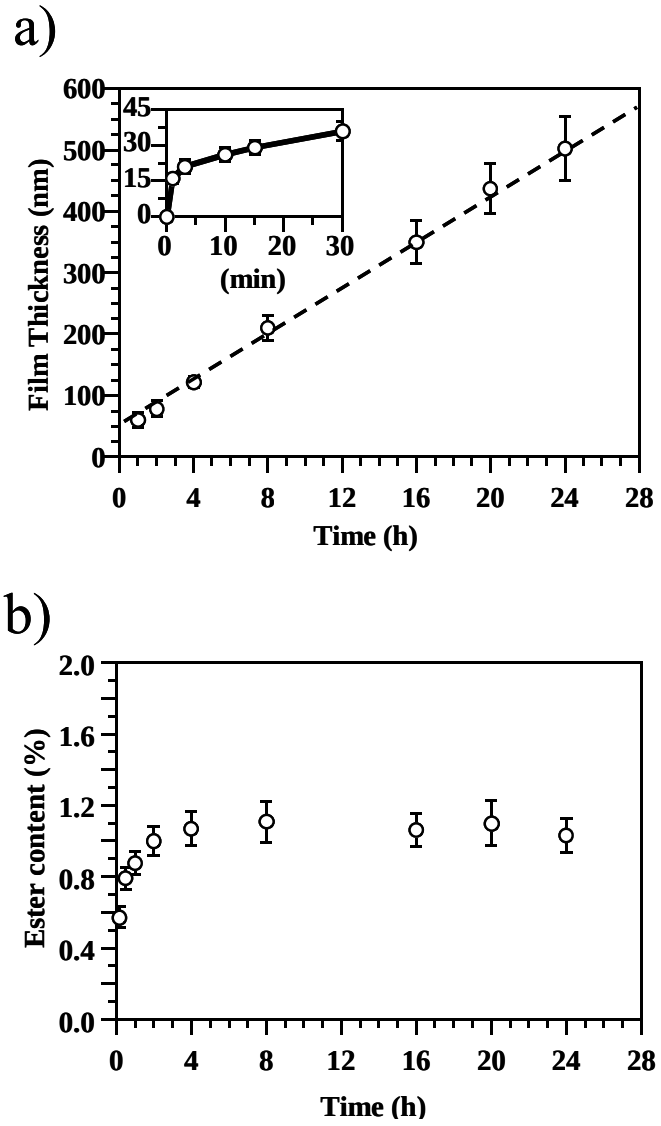

Figure 4.2. Time dependence of a) copolymer film thickness and b) ester content upon exposure of gold substrates to 4 mM DM and 40 mM EDA in ether at 0 ºC. The inset in a) shows the time-dependence of film thickness during the first 30 min of exposure. The data points and error bars represent the averages and standard deviations, respectively, of measurements obtained on at least three samples prepared independently. The dashed line serves as a guide to the eye.

rapid growth in the first few minutes but barely grows at all during longer exposures.[6]

For comparison with the copolymer growth kinetics shown here, we also obtained

thickness measurements for gold exposed to 4 mM DM in ether (not shown). While the PM thickness (~45 nm) is similar to that of the copolymer (~60 nm) after 1 h of film growth, the homopolymer film does not continue to show such rapid growth, exhibiting a thickness of only 97 nm after 24 h (as compared to ~500 nm for the copolymer film). These results suggest that the initial, rapid growth in Figure 4.2a (inset) may be due to a PM homopolymerization that coexists with the copolymerization but becomes much less active at longer times.

To demonstrate the cooperation of both DM and EDA to form the copolymer, we have also plotted the time-dependence of the molar ester content (Figure 4.2b) as derived from IR spectra. We attribute the increase in ester content from 0.6% to 1.1% at early times to the steady growth of copolymer combined with the decay in PM homopolymer growth, consistent with the early exponential growth of film thickness in Figure 4.2a. The relatively constant ester content at long times reveals the dominance of the copolymerization and indicates that both DM and EDA (or their intermediates) continue to contribute to the copolymer growth at a constant ratio as film thickness increases. During film growth, the position of the asymmetric methylene band shifts from 2921 cm^{-1} (1 h) to 2916 cm^{-1} (24 h), consistent with an improved chain crystallinity as film thickness is increased.[27]

Effect of Precursor Concentration

To study the effect of EDA concentration on copolymer growth, we fixed the DM concentration at 4 mM and varied EDA concentration from 10 – 80 mM. Figures 4.3a and 4.3b show the film thickness and molar ester content as a function of EDA

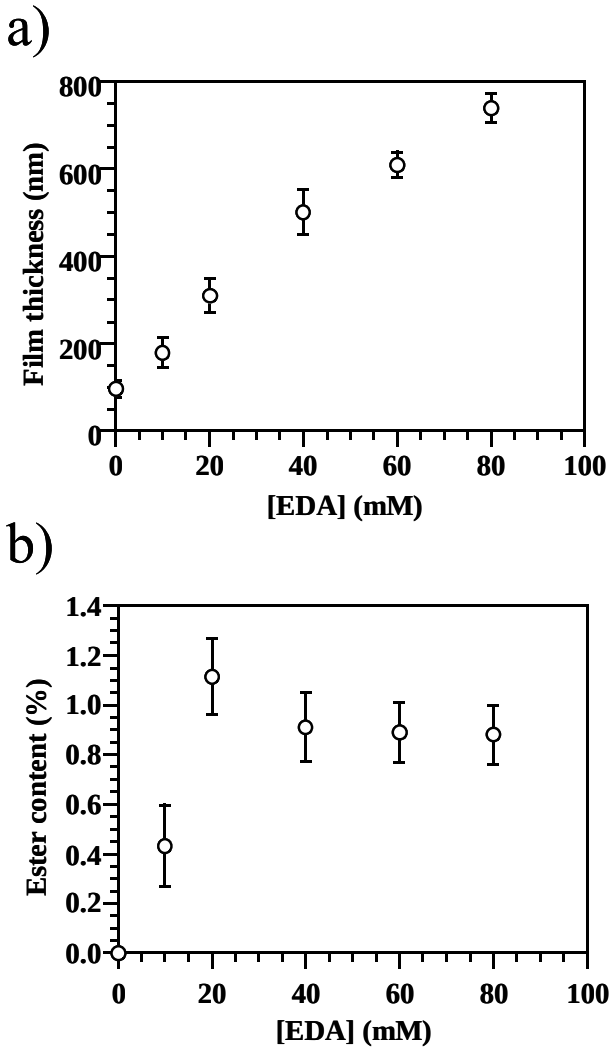

Figure 4.3. Effect of EDA concentration on a) film thickness and b) ester content. The films were prepared by placing gold-coated substrates into an ether solution at 0 ºC for 24 h with DM concentration fixed at 4 mM and EDA concentration varied from 0 to 80 mM. The data points and error bars represent the averages and standard deviations, respectively, of measurements obtained on at least three samples prepared independently.

concentration after 24 h of film growth in ether at 0 °C. The case of 0 mM EDA provides a measure of the contribution of the PM homopolymer in the overall film growth (~ 100 nm). The presence of EDA dramatically enhances PM growth, and the film thickness is directly proportional to the EDA concentration from 0 – 40 mM but becomes less

sensitive as concentration is further increased. This linear behavior is suggestive of a first-order concentration after 24 h of film growth in ether at 0 °C. The case of 0 mM EDA provides a measure of the contribution of the PM homopolymer in the overall film

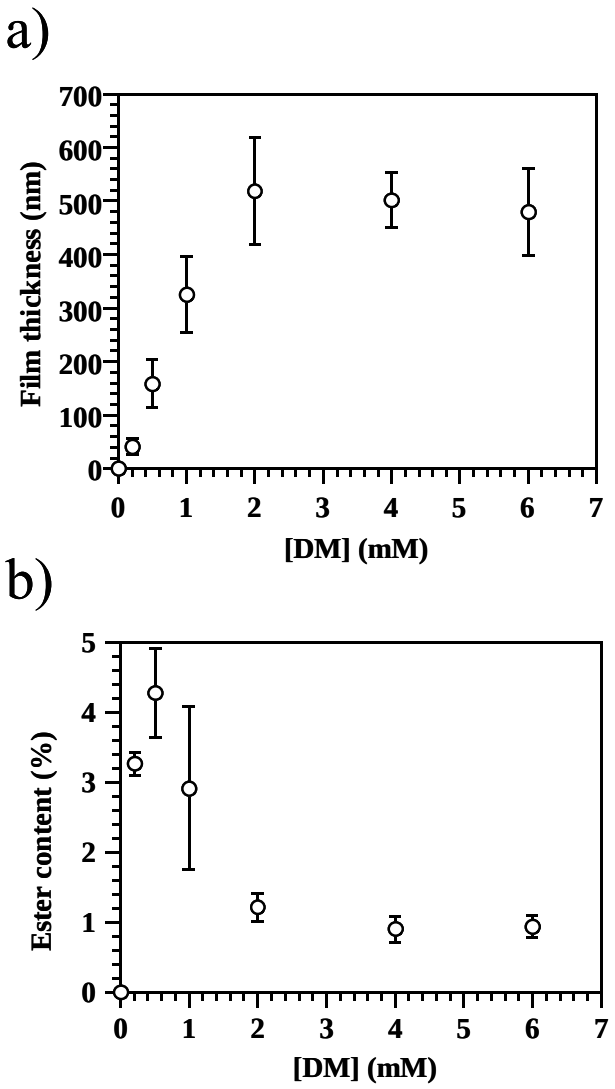

Figure 4.4. Effect of DM concentration on a) film thickness and b) ester content. The films were prepared by placing gold-coated substrates into an ether solution at 0 ºC for 24 h with EDA concentration fixed at 40 mM and DM concentration varied from 0 to 6 mM. The data points and error bars represent the averages and standard deviations, respectively, of measurements obtained on at least three samples prepared independently.

growth (~ 100 nm). The presence of EDA dramatically enhances PM growth, and the film thickness is directly proportional to the EDA concentration from 0 – 40 mM but becomes less sensitive as dependence of film growth rate on EDA concentration. The molar ester content increases sharply from 0.4 to 1.1 % with EDA concentration from 10 to 20 mM, but is constant from 40 to 80 mM. Therefore, the ester content in the copolymer does not scale in a general manner with the EDA to DM concentration ratio.

To study the effect of DM concentration on copolymer growth, we fixed the EDA concentration at 40 mM and varied DM concentration from 0 to 6 mM. Figures 4.4a and 4.4b show the film thickness and the molar ester content of the copolymer film as a function of DM concentration. Consistent with Figure 4.1, when no DM is present, the polymerization does not occur. Film thickness increases nearly linearly with DM concentration from 0 to 2 mM whereas the molar ester content is reduced from ~4% to ~1%, consistent with a competition between DM and EDA at the propagating site. Upon increasing DM concentration from 2 to 6 mM, film thickness and ester content do not respond, remaining at ~500 nm and 1%, respectively. This insensitivity in film thickness and composition at high DM concentration is consistent with surface saturation effects, where the rate-limiting step may be incorporation of an adsorbed intermediate into a propagating chain. Interestingly, for a DM concentration of 4 mM (in reference to Figure 4.3), an increase in EDA concentration from 40 to 60 or 80 mM would increase film thickness but would not alter the ester content. The insensitivity of film thickness to further DM addition coupled with the measurable change in film thickness upon further EDA addition suggests that an EDA-derived species can promote additional chain growth that utilizes methylene species to offset surface saturation effects. The results in Figures

4.3 and 4.4 provide clues as to the roles of DM and EDA in the copolymerization and demonstrate that, with judicious selection of DM and EDA concentrations, the ester content of the polymer can be varied from < 1 to ~4%, enabling incremental control over film composition and properties.

Probing the Nature of the Copolymerization

Copolymers derived from exposure of gold surfaces to DM and EDA exhibit a strong linear growth with time after an early exponential stage, suggesting that a significant concentration of chains remain active or exhibit "living" character. If the

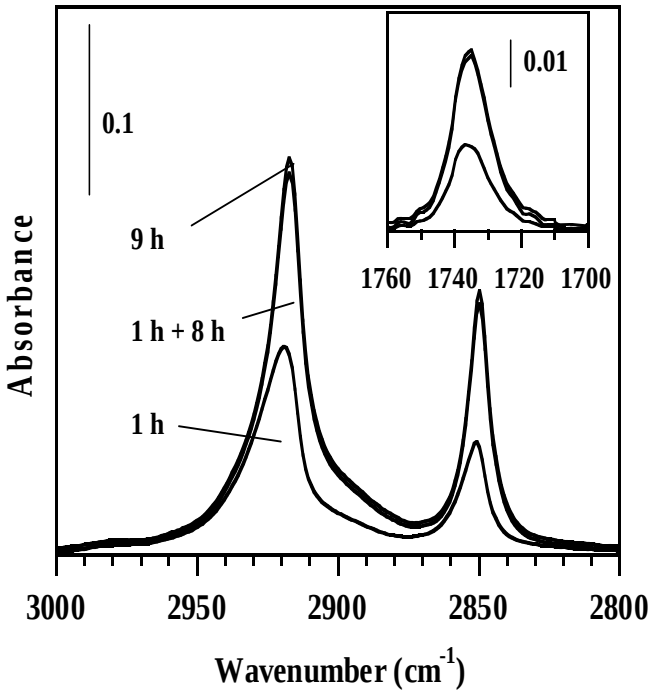

Figure 4.5. The C-H and C=O (inset) stretching regions of IR spectra for copolymer samples exposed to 4 mM DM and 40 mM EDA solution for 1 h, 1 h followed by rinsing and replacement in the same solution for another 8 h, and 9 h. The least intense spectrum in the inset also corresponds to the 1 h control.

chains are truly living, then the film could be removed from solution, exposed to air, and replaced in solution without terminating chain growth. To obtain more insight into the mechanism of copolymer formation on gold, we have run carefully controlled experiments where growing chains were removed from solution and placed in other solutions. We have also spiked additives such as quenchers into the ethereal DM and EDA solution to investigate the effects on the growing chains and help elucidate mechanistic aspects of chain propagation.

To test the effect of air exposure during copolymer formation, we have removed the samples from the DM and EDA solutions, rinsed them with ether, and then placed them back into the same solution for further film growth. This rinse procedure exposes the sample to air for ~15 s. We have observed that the film continues to grow after the rinsing and air exposure process. Figure 4.5 shows the C-H and C=O stretching regions of the IR spectra for copolymer samples exposed to 4 mM DM and 40 mM EDA in ether at 0 °C for 1 h (control), 1 h, followed by rinsing, and replacement in the same solution for another 8 h (denoted as 1 h + 8 h), and 9 h (control). In comparing the spectrum for the rinsed sample with those for the two controls, the results indicate that the copolymer continues to grow after the rinsing and air exposure and that the ester content is the same as for the 9 h control. Ellipsometric measurements show that the thickness of the films are 62 (1 h), 206 (1 h + 8 h) and 230 (9 h) nm respectively, which are consistent with IR intensities. In comparison with the 9 h control, the rinsed and air exposed sample nearly achieves the same level of growth. This slight loss in thickness could be attributed to either a loss of some active chains or a depletion of DM and EDA concentration within the film upon air exposure.

We also performed an experiment to determine the function of DM or EDA in copolymer growth. After exposure of samples to a solution containing 4 mM DM + 40 mM EDA for 1 h and subsequent rinsing, we immediately placed the samples in either 4 mM DM or 40 mM EDA solutions for another 8 h. The sample placed into the EDA solution stopped growing while the sample placed in the DM solution grew slightly from 62 nm to 90 nm, although this sample was much thinner than the 9 h control (230 nm) continually exposed to 4 mM DM + 40 mM EDA. This experiment confirms that DM and EDA must both be present to propagate film growth at the normal rate observed during copolymerization.

A very important mechanistic consideration in a surface-initiated polymerization is whether the copolymer propagates from the chain ends at the metal surface or those near the film/solution interface. To address the site of propagation, we have used highly surface-sensitive contact angle measurements to determine if film surface composition is altered upon a step change in DM and EDA concentrations. As a basis for this experiment, copolymer films with different ester contents yield different water contact angles. For example, a copolymer film prepared from 1 mM DM and 80 mM EDA exhibits an ester content of 3.0 % and an advancing contact angle of 90º, whereas a copolymer film prepared from 4 mM DM and 40 mM EDA exhibits a lower ester content (0.9 %) and a higher contact angle 117º,[28] consistent with fewer oxygen-rich ester groups at the outer surface. To test whether the propagation site is at the outer film surface, we first placed a gold substrate into an ether solution containing 4 mM DM and 40 mM EDA for 18 h and then removed it, rinsed with ether, and placed it into an ether solution containing 1 mM DM and 80 mM EDA for another 6 h. Comparison with a control

sample exposed only to the original solution for 18 h revealed that the film grew an additional 35 nm during the latter 6 h exposure and that the overall ester content of the film was measurably higher. However, the advancing contact angle of the film after the latter exposure was 117º, identical to that of the control film that did not undergo the latter 6 h exposure. Since water contact angles are sensitive to the outer half nanometer of film composition,[29] the latter 35 nm of film growth did not occur at the outer film/solution interface and most likely occurred at the gold/polymer interface where catalyzed intermediates are present to push the chains and film farther away from the metal surface.

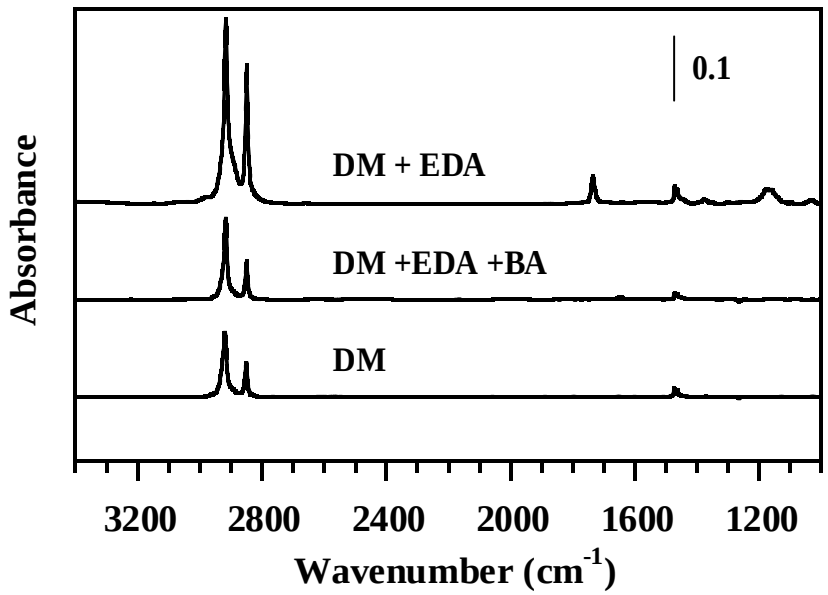

Figure 4.6. Reflectance-absorption IR spectra for gold surfaces after exposure to 4 mM DM, 4 mM DM + 40 mM EDA + 20 mM BA, or 4 mM DM + 40 mM EDA in ether at 0°C for 24 h.

To obtain additional information on the chemical nature of the active chains, we have added specific molecules that are known to either quench certain classes of propagating chains or become incorporated into the active chain. Both hydroquinone and 4-*tert*-butylcatechol are known to quench radical polymerizations,[17] but neither affected homopolymer or copolymer film growth on gold. Likewise, styrene and isobutyl vinyl ether are known to react and copolymerize with radicals and cationic chains,[30] respectively, but no inhibition of film growth was observed upon addition of these species and neither was detected in the films by RAIRS. These results suggest that the dominant mode of chain growth is not by radical or cationic propagation. However, primary amines such as benzylamine (BA) and alkyl amines do inhibit copolymer growth. Figure 4.6 shows IR spectra of films formed upon exposure to 4 mM DM and 40 mM EDA (with and without 20 mM BA) or 4 mM DM. The presence of BA prevents copolymer growth, as evidenced by the weaker C-H stretching intensities and the absence of C=O stretching in the IR spectra. The ability of BA to prevent copolymerization, combined with the observation that copolymerization occurs from the metal surface, suggests an interaction between the nucleophilic amine and the propagating site at the metal surface. In contrast to the quenching behavior of BA for the copolymerization, it appears to slightly enhance PM homopolymer growth based on the ~5 % increase in methylene stretching intensities as compared with those from the DM control. These results provide further evidence that two types of chain propagation routes exist—one for copolymerization and one for homopolymerization of PM.

Carboxylate-Functionalization of Copolymer Films

An important advantage of the studied copolymer films is that the ester groups can be chemically modified to produce functionalized PM-rich films directly on gold. For example, the esters can be converted to carboxylate groups by hydrolysis in a basic solution. These carboxylate groups in the copolymer are sensitive to pH, remaining ionized at high pH and becoming protonated at low pH, and can alter both the surface and barrier properties of the film. Figure 4.7 shows the IR spectra of the copolymer before and after the hydrolysis process in a refluxed solution of 0.5 M KOH in ethanol. In this study, we have adjusted the DM:EDA concentration ratio to 0.5 mM to 80 mM to

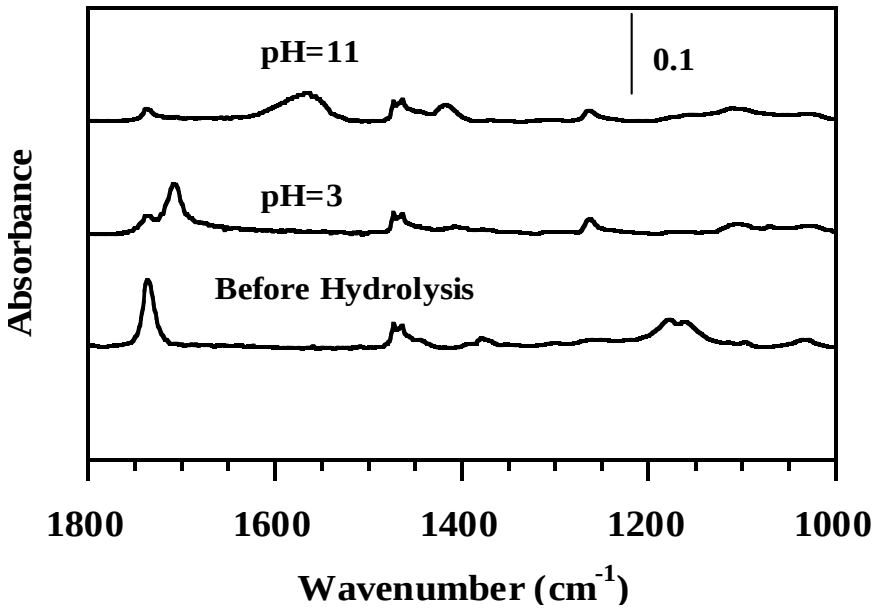

Figure 4.7. Reflectance-absorption IR spectra of copolymer films (3% ester content) before hydrolysis and after hydrolysis (4 h, 0.5 M KOH, ethanol, reflux) upon exposure to aqueous solutions at pH 3 and 11 for 30 min.

emphasize the copolymer structural changes from IR spectra. After 24 h of growth, the ester content within the copolymer film is 3.2%. During the 4 h hydrolysis, ~80% of the ester groups are converted to carboxylates.[31] For hydrolyzed films exposed to a solution at pH 11, Figure 4.7 (top) shows diminution of the C=O stretching peak at 1735 cm^{-1} and the CH_3 bending peak ~1370 cm^{-1}, and the appearance of peaks at 1560 and 1420 cm^{-1}, which are characteristic of carboxylate ions within the polymer. If this hydrolyzed film is exposed to a pH 3 solution for 10 min, the carboxylate side groups are protonated to carboxylic acids, as evidenced by the disappearance of peaks at 1560 and 1420 cm^{-1} and appearance of a peak at 1710 cm^{-1} in Figure 4.7 (middle), consistent with the carbonyl stretching mode of an acid.

Table 4.1. Effect of pH on advancing and receding contact angles of water on a 320 nm copolymer film (3% ester content).

Film State	pH	Contact Angle	
		$\theta_{A,water}$	$\theta_{R,water}$
Before hydrolysis	3	85±2	60±3
	11	85±2	60±4
After hydrolysis	3	84±2	50±3
	11	55±3	33±4

This reversible protonation/deprotonation of side groups also affects the surface properties of the copolymer films (Table 4.1). After the hydrolysis process, the advancing and receding contact angles were measured by placing the samples in a chamber saturated with deionized water. Using a water drop at pH 3, the advancing water contact angle (84°) on the hydrolyzed film is nearly identical to that of the copolymer before hydrolysis (85°), but if using a drop at pH 11, the contact angle drops by ~30° due to the greater hydrophilicity of the charged carboxylate groups that are distributed along the surface. Therefore, the hydrolyzed copolymer film is sensitive to pH and exhibits outstanding potential for preparing surface-initiated, smart polymeric materials.

Discussion

PM Growth on Gold

Exposure of gold surfaces to DM in ether yields a PM film with a growth rate that slows with time.[6] Seshadri et al. have studied the decomposition of DM on both smooth[3] and rough[5] gold surfaces to form PM films and clusters. They used AFM to show that PM growth initiates at or near gold defect sites that likely provide enhanced stabilization for adsorbed methylidene species.[3] They postulated a free radical mechanism to describe the growth of PM on gold.[3] In principle, a free-radical mechanism agrees with our previously reported kinetics for PM growth on gold where the growth rate slows with time,[6] consistent with chain terminations that limit the final thickness of the film.

However, we have not been able to definitively prove the mechanism of chain propagation since the film growth is insensitive to the presence of various quenchers.

When the surface of gold is modified by a submonolayer of copper before exposure to DM, the kinetics of PM film growth is dramatically altered and much thicker PM films are formed, as we have recently demonstrated.[6,7] The growth rate for PM on Cu-modified gold is nearly constant with time,[6] exhibiting similar behavior to that observed for the copolymerization in this study. Another important commonality between PM homopolymer growth on Cu-modified gold and the copolymer growth on gold reported here is that primary amines quench both polymerizations. Since Cu adatoms have a partially positive charge,[32,33] we hypothesize that the nucleophilic amines adsorb and shut down propagation at these metallic sites. The altered growth in the presence of the copper monolayer illustrates the extreme sensitivity of surface charge and composition on surface-catalyzed polymerizations.

Copolymer Growth

Exposure of gold surfaces to ether containing both DM and EDA results in the growth of a copolymer film that contains a predominate methylene repeat structure with random ethyl ester side chains. The growth rate of this film, initially rapid, decays sharply in the first ~5 min and ultimately becomes constant over many hours. These two distinct regimes of film growth suggest that two types of active chains contribute toward film growth. One chain appears to be a PM homopolymer and exhibits the characteristic decaying rate of film growth while the other chain is largely immune to terminations and is a copolymer, containing both methylene and ester components. This two-chain model

is supported by the fact that primary amines quench the copolymerization but not the homopolymerization of PM. These differences and the results described herein provide several clues regarding the mechanism of the copolymer chain growth. In the remainder of this section, we focus on the copolymerization, summarizing key results and offering interpretation as to the nature of film growth.

Chain propagation for the copolymer occurs at the metal surface and not at the solution/polymer interface. This observation implies that chain propagation is not due to common radical, cationic, or anionic growth where the active propagation site is at the outer chain terminus. Rather, the gold surface appears to catalyze carbon-carbon bond formation to push the outer chain termini further away from the metal-polymer interface, consistent with an insertion-type chain growth.[18,20-22]

DM must be present to propagate the copolymerization, as no polymer was observed in the absence of DM and the copolymerization ceased when the film was transferred to a solution containing only EDA. This observation is consistent with a steric hindrance in the propagation reaction at the gold surface that prevents EDA-derived species from occupying consecutive links in the polymer chain. DM is also a more active participant in copolymer chain propagation, and a competition exists between DM and EDA at the propagating site. The more active participation of DM could be due to its enhanced reactivity[34] as compared with the larger and perhaps sterically hindered intermediate from EDA.

The presence of EDA with DM results in a greatly enhanced rate of overall film growth on the gold surface and produces linear increases of film thickness with time. Based on the growth enhancement and the low ester contents in the film, one might

assume that an adsorbed intermediate of EDA functions to initiate an alternative chain growth and occasionally participates in the propagation. However, since transfer of a growing film to a solution without EDA dramatically slows polymerization, the role of EDA is far more significant than merely initiating the growth of a copolymer chain or occupying a small fraction of the film. Moreover, the presence of EDA is required to maintain the growth, even long times after the polymerization has begun. The required presence of EDA suggests that the adsorbed ester intermediate has a prominent role in the propagation as a co-catalyst even though it is only a minor component in the copolymer.

Further insight into the roles of DM and EDA in the copolymerization is obtained by examining the concentration dependence of film growth in Figures 4.3 and 4.4. Increasing EDA concentration at constant DM results in nearly linear increases in film thickness without affecting the ester content within the film. This linear dependence of thickness on EDA concentration suggests that the growth rate of the film is directly influenced by the concentration of adsorbed ester intermediates. Also revealing is the fact that increasing DM concentration above 2 mM (at 40 mM EDA) does not affect film thickness whereas increasing EDA concentration to 60 or 80 mM (at 4 mM DM) does indeed increase film thickness. These results imply a surface saturation of adsorbed methylene and a film growth that is limited by the propagation reaction. Thus, addition of DM in solution cannot increase the concentration of adsorbed methylene due to saturation effects so that the propagation rate remains constant. On the other hand, addition of EDA results in a higher concentration of active chains that can utilize the adsorbed methylene. These findings, combined with the requirement that EDA be

present to promote the propagation, provide further evidence that an adsorbed intermediate of EDA functions as a cocatalyst in this copolymerization process.

While the exact mechanistic nature of the copolymerization, especially the initiation, is unclear at this time, we propose a candidate mechanism for chain propagation (Figure 4.8) that is consistent with recent literature[11,14,21] and the results

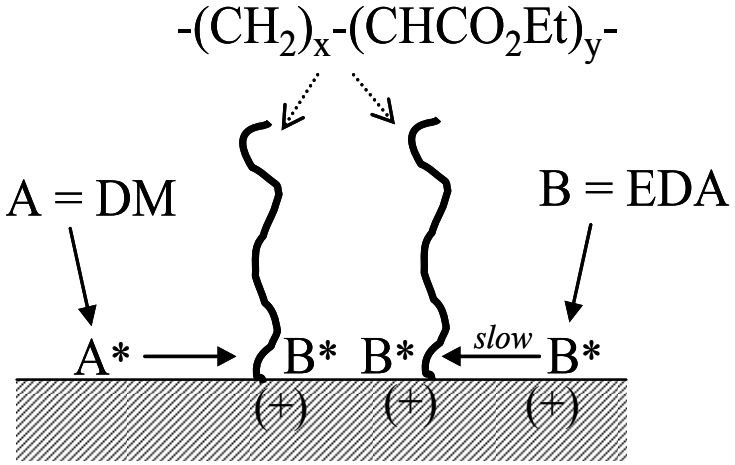

Figure 4.8. Proposed mechanism of copolymer growth on a gold surface. A* represents adsorbed methylene (Au=CH_2) and B* represents an adsorbed ethyl ester carbene (Au=$CHCO_2Et$). To grow copolymer, both types of carbenes may participate in an insertion reaction at the metal surface. The adsorbed ethyl ester carbene species pulls electron density away from the gold surface atoms toward the electronegative ester oxygens to create a partial positive charge across the metal surface and thereby alter the surface potential. These electron-deficient gold atoms may serve as the reactive center for an insertion chain growth polymerization.

obtained in this work. Based on other reports, we assume that both EDA[35-37] and DM[3,38,39] adsorb onto gold with loss of nitrogen to form carbene species. Once adsorbed,

methylidenes may collide to form a biradical species, as proposed by Seshadri et al.,[3] to initiate the growth of a PM homopolymer. To grow copolymer, both types of carbenes may participate in a propagation reaction at the metal surface. We propose that the adsorbed ethyl ester carbene species pulls electron density away from the gold surface atoms toward the electronegative ester oxygens to create a partial positive charge across the metal surface and thereby alter the surface potential. Consistent with the behavior of copper adatoms on gold (vide supra), these electron-deficient gold atoms may serve as the reactive center for an insertion chain growth polymerization. Methylene and ethyl ester carbenes can then insert into a gold-carbon bond to propagate the chain by one unit and push the outer chain terminus away from the metal surface. Thus, we propose that two types of polymer chains exist on the surface—PM homopolymer chains, which participate in film growth at early times but eventually terminate, and copolymer chains that resist termination due to the controlled nature of the insertion reaction. Functioning as a co-catalyst, the ethyl ester carbene must be adsorbed on the metal surface to create a reactive center and influence the propagation (Figure 4.8). The proposed mechanism is consistent with the fact that this type of polymerization cannot continue in the absence of EDA. If adsorbed ethyl ester carbenes are lost, the electron-deficient gold surface atoms revert to their neutral state and are no longer catalytic toward the insertion reaction. That this propagation is terminated upon exposure to nucleophilic amines is consistent with direct adsorption and deactivation at the electrophilic metal surface sites.

Carbenes of both EDA and DM are known to insert into metal-carbon bonds although, to our knowledge, EDA has not been used in heterogeneous catalysis. In studying homogeneous catalysis with Pt(II) complexes, Bergamini et al.[35] observed that

the carbene intermediate of EDA inserts into Pt-CH_3 bonds through an alkyl to carbene migration and have proposed a cationic intermediate. A carbene intermediate of EDA is also known to insert into C-H bonds of alkanes, ethers, and various other hydrocarbons.[36,37] Across these studies, the metallocarbene intermediate is viewed as electrophilic, supported by its tendency of to insert into electron-rich bonds. As for DM, McCrindle et al.[39] have shown that its addition to a solution containing a Pt complex resulted in continual insertion of methylene into the alkyl-Pt bond and have also proposed a cationic intermediate. This mechanism for homogeneous catalysis with DM is similar to that reported for the heterogeneous insertion of adsorbed methylene into Cu (100)-alkyl bonds for chain propagation in vacuum.[22]

The constant rate of copolymer film growth, as shown in Figure 4.2, in conjunction with propagation at the metal/polymer interface, implies that the propagation is limited by reaction rather than diffusion. If the process were limited by diffusion, the growing film would be expected to slow diffusion of DM or EDA to the metal surface, and the rate would decrease with increasing film thickness. Based on the growth rate of 20 nm per hour from Figure 4.2, we have performed calculations that indicate a diffusion-limited propagation is unlikely when film thicknesses are in the sub-micron regime.[40] Based on a reaction-limited propagation from the gold surface, the constant rate of film growth further implies that the adsorbed polymer chains do not block access by adsorbed intermediates to active surface sites.

To our knowledge, the use of EDA in catalysis at gold surfaces has not been reported. In general, 2-D gold surfaces are typically thought to be poor catalysts, but a growing body of literature supports the fact that nanoscale gold particles, especially those

on TiO_2 supports,[41,42] are effective catalysts for CO oxidation. Seshadri et al.,[3] who studied the decomposition of DM on 2-D gold to form PM films and clusters, have speculated that the favorable catalytic properties of gold in this reaction stem from its relatively weak interaction with adsorbed methylene that enables facile surface diffusion. In the present work, the addition of an EDA co-catalyst appears to enhance the catalytic properties of the gold surface and promote a unique heterogeneous polymer chemistry.

Conclusions

We have developed a novel approach to prepare ester-modified polymethylene films on gold surfaces by exposure to a solution containing DM and EDA. This methodology enables a high level of control over film properties. The film thickness can be controlled by time or by increasing EDA concentration. The molar ester content can be tuned between 0 and 5% by using appropriate solution ratios of EDA to DM, and this content is nearly constant throughout the depths of the film. Finally, the film can be further modified by hydrolysis to prepare carboxylate-modified PM that exhibits pH-responsive properties.

The results suggest that the films propagate from the metal-polymer interface and that an adsorbed intermediate of EDA functions as a co-catalyst. The most likely mode of propagation is an insertion mechanism, in which adsorbed methylene and/or ethyl ester groups insert into a Au-C bond to push the chain away from the metal surface. That this unique film growth occurs directly from a gold surface, combined with the precise control over film properties and the ability to generate pH-responsive films by

straightforward modification, implies that such an approach could be broadly applied to modify materials properties with well-defined, smart coatings.

References

1. Bloch, D. R. Solvents and Non Solvents for Polymers. In *Polymer Handbook*; Brandrup, J.; Immergut, E. H.; Grulke, E. A., Ed.; Wiley: New York, 1998.

2. Bergbreiter, D. E.; Franchina, J. G.; Kabza, K. "Hyperbranched Grafting on Oxidized Polyethylene Surfaces," *Macromolecules* **1999**, *32*, 4993-4998.

3. Seshadri, K.; Atre, S. V.; Tao, Y.-T.; Lee, M.-T.; Allara, D. L. "Synthesis of Crystalline, Nanometer-Scale Polymethylene Clusters and Films on Gold Surfaces," *Journal of the American Chemical Society* **1997**, *119*, 4698-4711.

4. Tao, Y.-T.; Pandian, K.; Lee, W.-C. "Microfabrication of Interdigitated Polyaniline/Polymethylene Patterns on a Gold Surface," *Langmuir* **1998**, *14*, 6158-6166.

5. Seshadri, K.; Wilson, A. M.; Guiseppi-Elie, A.; Allara, D. L. "Toward Controlled Area Electrode Assemblies: Selecitve Blocking of Gold Electrode Defects with Polymethylene Nanocrystals," *Langmuir* **1999**, *15*, 742-749.

6. Guo, W.; Jennings, G. K. "Use of Underpotentially Deposited Metals on Gold to Affect the Surface-Catalyzed Formation of Polymethylene Films," *Langmuir* **2002**, *18*, 3123-3126.

7. Guo, W.; Jennings, G. K. "Directed Growth of Polymethylene Films on Atomically Modified Gold Surfaces," *Advanced Materials* **2003**, *15*, 588-591.

8. Chanunpanich, N.; Ulman, A.; Malagon, A.; Strzhemechny, Y. M.; Schwarz, S. A.; Janke, A.; Kratzmueller, T.; Braun, H. G. "Surface Modification of Polyethylene Films via Bromination: Reactions of Brominated Polyethylene with Aromatic Thiolate Compounds," *Langmuir* **2000**, *16*, 3557-3560.

9. Wu, S. S.; Xu, X. "Effect of the Reaction Atmosphere on High-Density Polyethylene Functionalized by Ultraviolet Irradiation," *Journal of Applied Polymer Science* **2004**, *91*, 2326-2329.

10. Zheng, Z.; Tang, X. Z.; Shi, M. W.; Zhou, G. T. "Surface Modification of Ultrahigh-Molecular-Weight Polyethylene Fibers," *Journal of Polymer Science Part B-Polymer Physics* **2004**, *42*, 463-472.

11. Shea, K. J.; Walker, J. W.; Zhu, H.; Paz, M.; Greaves, J. "Polyhomologation. A Living Polymethylene Synthesis," *Journal of the American Chemical Society* **1997**, *119*, 9049-9050.

12. Shea, K. J.; Busch, B. B.; Paz, M. M. "Polyhomologation: Synthesis of Novel Polymethylene Architectures by a Living Polymerization of

Dimethylsulfoxonium Methylide," *Angewandte Chemie-International Edition* **1998**, *37*, 1391-1393.

13. Shea, K. J.; Staiger, C. L.; Lee, S. Y. "Synthesis of Polymethylene Block Copolymers by the Polyhomologation of Organoboranes," *Macromolecules* **1999**, *32*, 3157-3158.

14. Shea, K. J. "Polyhomologation: The Living Polymerization of Ylides," *Chemistry-a European Journal* **2000**, *6*, 1113-1119.

15. Busch, B. B.; Staiger, C. L.; Stoddard, J. M.; Shea, K. J. "Living Polymerization of Sulfur Ylides. Synthesis of Terminally Functionalized and Telechelic Polymethylene," *Macromolecules* **2002**, *35*, 8330-8337.

16. Busch, B. B.; Paz, M. M.; Shea, K. J.; Staiger, C. L.; Stoddard, J. M.; Walker, J. R.; Zhou, X. Z.; Zhu, H. D. "The Boron-Catalyzed Polymerization of Dimethylsulfoxonium Methylide. A Living Polymethylene Synthesis," *Journal of the American Chemical Society* **2002**, *124*, 3636-3646.

17. Davies, A. G.; Hare, D. G.; Khan, O. R.; Sikora, J. "Monomethylation of Polymethylenation by Diazomethane in the Presence of Boron Compounds," *Journal of the American Chemical Society* **1963**, 4461-4471.

18. Mucha, M.; Wunderlich, B. "Crystallization during Polymerization of Diazomethane. I. The Boron Trifluride Catalyzed Reaction," *Journal of Polymer Science* **1974**, *12*, 1993-2018.

19. Nasini, A. G.; Saini G.; Trossarelli, L. "Polymers Obtained by Catalytic Decomposition of Diazoalkanes in Hetergeneous Systems," *Pure & Applied Chemistry* **1962**, *4*, 255-271.

20. Bawn, C. E. H.; Ledwith, A.; Matthies, P. "The Mechanism of the Polymerization of Diazoalkanes Catalyzed by Boron Compounds," *Journal of Polymer Science* **1959**, *84*, 93-108.

21. Lie, L. H.; Patole, S. N.; Hart, E. R.; Houlton, A.; Horrocks, B. R. "Photochemical Reaction of Diazomethane with Hydrogen-Terminated Silicon Surfaces," *Journal of Physical Chemistry B* **2002**, *106*, 113-120.

22. Lin, J. L.; Chiang, C. M.; Jenks, C. J.; Yang, M. X.; Wentzlaff, T. H.; Bent, B. E. "Alkyl Chain Propagation by Methylene Insertion on Cu(100)," *Journal of Catalysis* **1994**, *147*, 250-263.

23. To verify that the absence of polymer film upon exposure to EDA is not related to solvent, other solvents such as toluene and iso-octane were used, but no polymer was formed on the gold surface by EDA alone. However, copolymer films were

formed in toluene and iso-octane solvents upon exposure of gold to DM and EDA. In toluene, we obtained a film with nearly the same composition and thickness as that grown in ether, but in iso-octane, the contribution of EDA toward the copolymerization is higher and the DM contribution is lower than that observed for the film grown in ether. PM films also formed on gold surface by DM in both toluene and isooctane solvent, no difference was observed among PM films from ether, toluene and isooctane by IR analysis. A more detailed analysis of this solvent dependence will be discussed in a later manuscript.

24. Snyder, R. G. "Vibrational Spectra of Crystalline *n*-Paraffins," *Journal of Molecular Spectroscopy* **1961**, *7*, 116-144.

25. Silverstein, R. M.; Webster F. X.; Kiemle D. J. *Spectrometric Identification of Organic Compounds*, 6th ed.; John Wiley & Sons: New York, 1998.

26. Jones, D. M.; Huck, W. T. S. "Controlled Surface-Initiated Polymerizations in Aqueous Media," *Advanced Materials* **2001**, *13*, 1256-1259.

27. Hagemann, H.; Strauss, H. L.; Snyder, R. G. "Structure and Crystallization of Normal-$C_{21}H_{44}$, Normal-$C_{36}H_{74}$, and Low-Molecular-Weight Polyethylene Glasses," *Macromolecules* **1987**, *20*, 2810-2816.

28. For comparison, the advancing contact angle of water on the PM homopolymer is 125°. This high value is likely due to surface roughness as the contact angle hysteresis for the homopolymer is 55°.

29. Laibinis, P. E.; Bain, C. D.; Nuzzo, R. G.; Whitesides, G. M. "Structure and Wetting Properties of *ω*-Alkoxy-*n*-Alkanethiolate Monolayers on Gold and Silver," *Journal of Physical Chemistry* **1995**, *99*, 7663-7676.

30. Kennedy, J. P.; Marechal, E. *Carbocationic Polymerization*; John Wiley & Sons: New York, 1982.

31. The complete hydrolysis can occur but is slow and often causes damage to the film.

32. Mishra, A. K. "Electronic Structure of a Chemisorbed Layer at Electrochemical Interface: Copper Layer on Gold Electrode," *Journal of Physical Chemistry B* **1999**, *103*, 1484-1498.

33. Tadjeddine, A.; Guay, D.; Ladouceur, M.; Tourillon, G. "Electronic and Structural Characterization of Underpotentially Deposited Submonolayers and Monolayer of Copper on Gold (111) Studied by Insitu X-Ray-Absorption Spectroscopy," *Physical Review Letters* **1991**, *66*, 2235-2238.

34. McAllister, M. A.; Tidwells, T. T. "Substituent Effects on Diazomethanes and Diazirines by ab initio Molecular Orbital Calculations," *Journal of the American Chemical Society* **1992**, *114*, 6553-6555.

35. Bergamini, P.; Costa, E.; Orpen, A. G.; Pringle, P. G.; Smith, M. B. "Reactions of Diazo Carbonyls with $PtX(CH_3)$(Chiral Diphosphine) (X=Cl, Br, I) - Chemoselectivity and Diastereoselectivity of Pt-C and Pt-X Carbene Insertion," *Organometallics* **1995**, *14*, 3178-3187.

36. Morilla, M. E.; Molina, M. J.; Diaz-Requejo, M. M.; Belderrain, T. R.; Nicasio, M. C.; Trofimenko, S.; Perez, P. J. "Copper-Catalyzed Carbene Insertion into O-H Bonds: High Selective Conversion of Alcohols into Ethers," *Organometallics* **2003**, *22*, 2914-2918.

37. Caballero, A.; Diaz-Requejo, M. M.; Belderrain, T. R.; Nicasio, M. C.; Trofimenko, S.; Perez, P. J. "Functionalization of Carbon-Hydrogen Bonds of Hydrocarbons and Ethers via Carbene Insertion with Copper(I)-Homoscorpionate Catalysts," *Organometallics* **2003**, *22*, 4145-4150.

38. Mango, F. D.; Dvoretzk.I. "Introduction of Methylene into an Iridium Complex," *Journal of the American Chemical Society* **1966**, *88*, 1654-1657.

39. McCrindle, R.; Arsenault, G. J.; Farwaha, R.; Hampdensmith, M. J.; McAlees, A. J. "A Model for the Polymerization of Diazomethane by Transition-Metal Complexes," *Journal of the Chemical Society-Chemical Communications* **1986**, 943-944.

40. Based on the experimental conditions and results of Figure 3a (DM concentration (C) = 4 x 10^{-6} mol/cm^3; growth rate (η) = 20 nm/h or 5.56 x 10^{-10} cm/s) and estimating film density (ρ) as 0.95 g/cm^3 (same as that for HDPE) and diffusivity (D) of DM through the film as 1 x 10^{-8} cm^2/s (based on values obtained for molecules of similar molecular weight (M) through HDPE), the film thickness (d) at which the growth becomes diffusion-limited is estimated as ~30 μm via $d=DCM/(\eta\rho)$. This analysis equates the known flux of the growing film (obtained from Figure 3a) to the diffusive flux of DM (the dominant contributor toward film growth) through the film. Since the typical film thicknesses in this study range from 100 – 500 nm (orders of magnitude below the critical thickness (d)), the film growth can be viewed as reaction-limited.

41. Valden, M.; Pak, S.; Lai, X.; Goodman, D. W. "Structure Sensitivity of CO Oxidation over Model Au/TiO2 Catalysts," *Catalysis Letters* **1998**, *56*, 7-10.

42. Bond, G. C.; Thompson, D. T. "Catalysis by Gold," *Catalysis Reviews-Science and Engineering* **1999**, *41*, 319-388.

CHAPTER V

pH-RESPONSIVE COPOLYMER FILMS BY SURFACE-CATALYZED GROWTH

Introduction

Carboxylic acid groups are commonly used as the pH-sensitive moiety in responsive films as the acid is deprotonated to a carboxylate ion as pH is increased above a certain value. On the basis of octanol-water partition coefficients,[1] the carboxylate group is ~10^4 times more hydrophilic than the protonated acid. This extreme difference in the affinity of these groups toward water provides the basis for the work described herein. Briefly, polymer films that are predominately hydrophobic but contain a dilute fraction of carboxylic acid groups should exhibit a huge change in barrier properties when the pH is increased sufficiently to ionize the acid groups. At low pH, the polymers would be mostly dry, but upon ionization, the large difference in hydrophilicity of the carboxylate versus the acid should result in significant water and ion permeation. Such films may provide extremely pH-sensitive materials and could be useful in sensing and separations.

Here, we report a unique approach known as surface-catalyzed polymerization to engineer new classes of pH-responsive copolymer films. The films are prepared by exploiting a selective catalysis at gold surfaces that enables nanometer-level control over film thickness. Briefly, we have recently reported that exposure of gold substrates to a dilute solution containing diazomethane (DM) and ethyl diazoacetate (EDA) (Figure 1.2) results in a controlled copolymerization of a film containing linear polymethylene (PM)

with randomly distributed ethyl ester side groups (denoted as PM-CO2Et).[2] These films exhibit tunable thicknesses up to several hundred nanometers based on polymerization times and concentrations and controllable film composition based on the solution ratio of the DM and EDA precursors. In the current work, we demonstrate that the hydrolysis of the ester side groups to carboxylic acids with fractional conversion χ provides a film we denote as PM-CO2H that exhibits unusually large changes in barrier properties when the pH of the contacting solution is altered beyond a film-specific, critical pH range. When the acid groups become deprotonated or charged, the water solubility of the acid functional groups increases markedly to dramatically alter the film properties.[1] We have designed PM-CO2H films to consist predominately (>95%) of polymethylene (PM) so that the film is hydrophobic in the uncharged state, and thereby exhibits an extremely large pH-induced response in barrier properties once pH is increased sufficiently to charge the film.

This surface-catalyzed strategy toward pH-responsive films has several advantages over other approaches. (1) Surface-catalyzed polymerizations[3-5] offer the ability to rapidly grow films with controlled thicknesses up to the micron level. In fact, film thicknesses for PM-CO2Et increase linearly with time.[2] (2) The film growth is selective in that polymerization occurs on gold but not on most other materials (silicon, silver, aluminum, plastics, etc.), enabling the patterning of films by directed growth and straightforward integration into bottom-up processing schemes.[5] (3) In contrast to depositing pre-grown polymer onto a surface, the chain growth propagates directly from the metal surface and thereby, enables modification of surfaces of any geometry with a pH-responsive film. (4) Film composition can be tailored to affect the onset and

magnitude of the film response without requiring a completely new macromolecular synthesis.

Hydrophobic polymer films that contain carboxylic acid groups have been prepared by surface functionalization of polyethylene.[6,7] Holmes-Farley et al.[7] exposed bulk polyethylene films to chromic acid/sulfuric acid to produce an acid-rich surface. They used contact angle measurements to determine that the initial ionization of the carboxylic acids occurs at a solution pH of ~6 and that the pKa(1/2) is ~7.5 and unaffected by salt concentration. The elevation of pKa(1/2) over the pKa value for acetic acid (4.7), a simple monobasic acid, has been reported by others[7-10] for acid-containing films and is likely affected by hydrogen bonding between nearby acid groups at a surface[9,10] or the heterogeneous environment of the acids in a predominately hydrophobic medium.[7] The ability to prepare polymer films with dilute and well-defined fractions of carboxylic acid groups could provide additional insight on the pH-responsive behavior of these films.

In this chapter, we examine the effect of fractional acid content (1 – 4%) on the ionization and barrier properties of PM-CO2H films. An important goal of this work is to engineer the fractional acid content to investigate and perhaps tailor the onset and magnitude of the response in barrier properties. We use reflectance-absorption infrared spectroscopy (RAIRS) to investigate the effect of solution pH on the ionization of the carboxylic acid groups. The fractional ionization greatly affects the barrier properties of the film, which we examine with electrochemical impedance spectroscopy (EIS) to quantify film resistance and capacitance. Since such films have broad applications in amperometric sensors and as membrane skins, the use of EIS enables pertinent insight on

how solution pH can affect the resistance of the film against ion diffusion and the capacitive current measured at the electrode surface. Through EIS measurements, we are able to quantify the effect of dilute acid content on the performance and responsiveness of the film.

Experimental Procedures

Hydrolysis of Polymer Film

Hydrolysis of the copolymer films was carried out in capped 20 mL vials of 0.2 M KOH in 2-propanol at 75 °C for 1, 2, 3.5 and 24 h to obtain copolymer films with 1%, 2%, 3%, and 4% acid contents, respectively. Only one substrate was placed in each vial. The hydrolyzed samples were rinsed with ethanol and DI water and dried in a N_2 stream.

Effect of pH on Film Composition

PM-CO2H films with different acid content were immersed in a pH buffer solution in a 20 mL capped vial for times ranging from 1 h (not in critical pH range) to 12 h (near critical pH range) and then dried with N_2. After IR analysis, the sample was rinsed with DI water and dried with N_2 and then placed into a buffer solution in which pH was one unit higher or lower. Reported peak area ratios for carboxylate (1560 cm^{-1}) to methylene (asymmetric (2919 cm^{-1}) plus symmetric (2851 cm^{-1})) are based on average peak areas obtained at each pH value upon first decreasing pH from 11 to 4 and then increasing pH from 4 to 11.

Results and Discussion

Film Hydrolysis

We exposed 75 nm PM-CO_2Et films (4.2% molar ester content) to a 2-propanol solution of 0.2 M KOH at 75 ºC for 24 h and verified that the ester groups can be hydrolyzed to carboxylates (CO_2^-) with high conversions (~95%). The use of 2-propanol

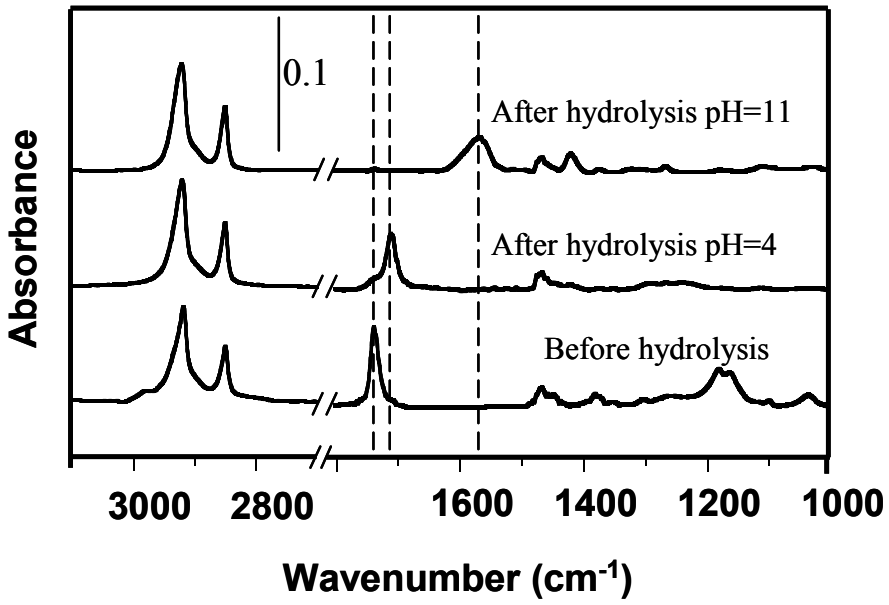

Figure 5.1. Reflectance-absorption IR spectra of copolymer films (4.2% ester content, 75 nm) before hydrolysis and after hydrolysis (24 h, 0.2 M KOH, 2-propanol, 75 ºC) and subsequent exposure to aqueous buffer solutions at pH 4 and 11 for 1 h.

rather than ethanol, used in our previous study,[2] affords higher conversion without adversely affecting film quality. Figure 5.1 shows reflectance-absorption infrared (RAIR) spectra for the film before hydrolysis and after hydrolysis upon exposure to pH 4 or pH 11 buffer solutions. The ester carbonyl group, represented by a peak at 1735 cm^{-1}

in the spectrum for the pre-hydrolysis film, is greatly diminished after hydrolysis, and new peaks appear corresponding to the carbonyl stretching vibration in CO_2H (1710 cm^{-1}; pH 4) or CO_2^- (1560 and 1420 cm^{-1}; pH 11).[11] The hydrolysis and subsequent exposure to buffer solutions does not affect the structure of the film based on the similar peak positions (2919 cm^{-1}) and intensities for CH_2 stretching in the three spectra. The films can be converted between charged (deprotonated) and uncharged (protonated) states repeatedly and reversibly by exposure to the respective buffer solutions.

One approach toward tailoring the acid content of the film is to control the extent of the hydrolysis reaction by controlling the time in which the film is exposed to the KOH solution. To determine the feasibility of such control over acid content, we investigated the kinetics of the hydrolysis reaction. In this study, we used 75 nm copolymer films with an ester content of 4.2% before hydrolysis and exposed them to a solution of 0.2 M KOH in 2-propanol at 75 ºC. Figure 5.2 shows that 70% of the ester groups are converted to acids in the first 3 h, and a nearly linear relationship exists between the conversion and time. For conversion > 70%, hydrolysis occurs more gradually, and a full 24 h is required to achieve 95% conversion. The remaining 5% of the conversion is extremely slow, even for such a thin film.

To obtain quantitative kinetics information for hydrolysis of the copolymer film, the conversion data in Figure 5.2 were fit with a simplest-case, reaction-limited model, which assumes that the rate of hydrolysis is proportional to the concentrations of KOH in solution (C) and accessible ester groups within the film:[12]

$$\frac{d\chi}{dt} = kC(\chi_f - \chi) \tag{5-1}$$

or, upon integration,

$$\chi = \chi_f (1 - e^{-kCt}) \tag{5-2}$$

where t is time, χ is conversion and χ_f is the limiting conversion (0.95 after 24 h). Use of eq. 5-2 provides a good fit to the transient conversion data in Figure 5.2 (correlation coefficient = R^2 = 0.99) and enables an estimate of kC as 1.17×10^{-4} s^{-1}. The long time scale for the hydrolysis of a 75 nm film combined with the good fit of the reaction-limited model to the data suggests that the hydrolysis process is not limited by diffusion.

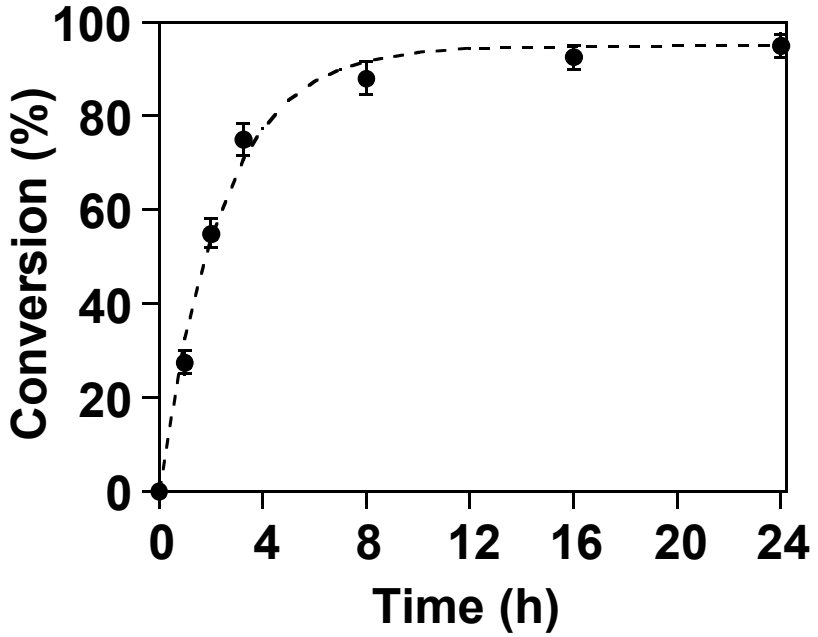

Figure 5.2. Time dependence of the conversion of ester to acid for a 75 nm PM-CO2Et (4.2% ester) film upon exposure to 0.2 M KOH in 2-propanol solution at 75 ºC. The dashed curve is a fit of the data based on Eq. 5-2, where kC is estimated from the fit as 1.17×10^{-4} s^{-1}. The correlation coefficient (R^2) for the fit is 0.99.

To provide additional evidence that the hydrolysis process is reaction-limited instead of diffusion-limited, the advancing contact angles for droplets of pH 4 or pH 11 buffer solution on the films with different acid contents are listed in Table 1 (0% represents PM-CO2Et). All the films show pH-responsive wettability with the carboxylic acid surfaces exhibiting ~20° higher contact angles than the carboxylate surfaces. Water contact angles are sensitive to the outer half nanometer of film composition.[13] In a diffusion-limited process, the hydrolysis reaction occurs rapidly at the outer surface and the reaction front gradually penetrates into the bulk film. If this hydrolysis were a diffusion-limited process, we would expect all the films to exhibit similar contact angles

Table 5.1. Advancing contact angles on PM-CO2H films with different acid contents at pH 4 and pH 11.

Acid Content	Advancing Contact Angle θ_A	
	pH4	pH11
0%	101±3	101±2
1%	92±3	72±2
2%	87±3	65±2
3%	82±3	60±1
4%	73±2	54±2

since their outermost surface would have approximately the same composition. The only difference would be the depth of penetration of the diffusing front. However, the measured contact angles decrease as the acid content of the film increases (Table 1), indicating that surface composition changes with the extent of hydrolysis. Therefore, the

good fit of the kinetics data in Figure 5.2 to a reaction-limited model and the compositionally dependent wettability in Table 1 are both consistent with a reaction-limited hydrolysis process rather than a diffusion-limited one.

In our recent work, we demonstrated that the ester content within the copolymer film could be controlled between ~1 and 5% by varying monomer concentration ratio. Here, we demonstrate that the ester conversion to acid can be controlled through the hydrolysis time. Combining these two factors, the final acid content within the copolymer film can be controlled over the range of 1 to 5%. All the PM-CO2H films reported in this manuscript were prepared by controlling the time of hydrolysis for 75 nm PM-CO2Et films with 4.2% ester content.

pH-Dependence of Film Composition

To obtain an improved understanding of the pH-responsive behaviors of the

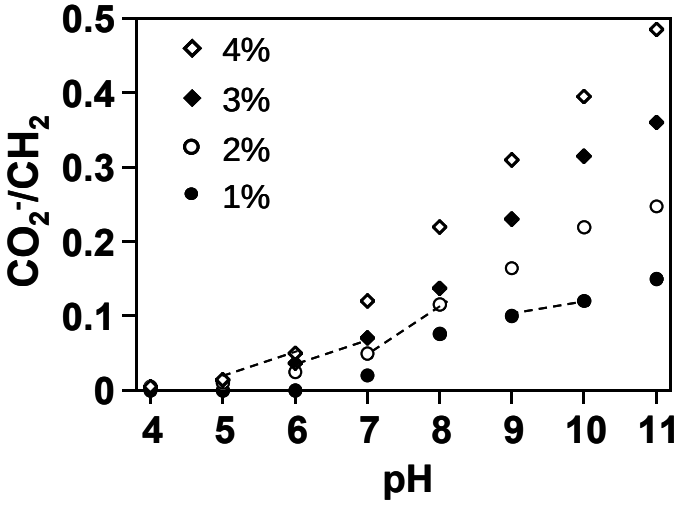

Figure 5.3. The peak area ratio of the carboxylate stretching band at 1560 cm^{-1} to the sum of the asymmetric (2919 cm^{-1}) and symmetric (2851 cm^{-1}) methylene stretching bands as a function of pH for 75 nm films with acid content ranging from 1% to 4%. The dashed lines in the figure represent the critical pH region (vide infra).

studied films, we have investigated how the film composition changes after contacting solutions of different pH. We performed RAIRS analysis on 75 nm copolymer films with 1% to 4% acid content at each pH increment between 4 and 11; Figure 5.3 shows the CO_2^- to CH_2 (both asymmetric and symmetric) stretching peak ratio within the films as a function of pH. Since all films have approximately the same CH_2 stretching peak area, the ratios here reflect the relative concentration of carboxylate within the film. For all films at pH 4 and 5, very weak, if any, CO_2^- stretching was observed by IR, indicating that the films are predominately in the acid state. At pH 6, carboxylate began to form in films with 2%, 3%, and 4% acid content. From pH 7 to 11, the carboxylate concentration increased almost linearly at each pH step for each film. No large jumps in the carboxylate concentration were observed, indicating that the films are gradually ionized over a broad range of pH.

pH-Responsive Barrier Properties

We have used EIS to measure the effect of pH on the barrier properties of PM-CO2H films using pH buffer solutions without redox probes. Figure 5.4 shows the equivalent circuits used to model impedance spectra for polymer films on gold. The following terms are used to denote various film and solution characteristics: solution resistance, R_s; interfacial capacitance, C_i; interfacial resistance, R_i; film capacitance, C_f; film resistance, R_f; and Warburg impedance, Z_w. Figure 5.4a shows a model that is commonly used for polymer-coated metals,[14] which contains two time constants, one due to the polymer film and one due to the polymer-metal interface. Figures 5.4b and 5.4c show models with a single time constant that represent two simplifications of the overall

model in Figure 5.4a. Figure 5.4b is used when the impedance due to the polymer film R_f is much smaller than the combined impedance of R_i and C_i in parallel, so only the time constant due to the polymer-metal interface is observed in the impedance spectrum. The equivalent circuit simplifies to R_i and C_i in parallel with one another but in series with R_s. The model in Figure 5.4c is used when R_f is much greater than the combined impedance of R_i and C_i in parallel, so only the time constant due to the polymer is observed in the impedance spectrum. In Figures 5.4a and 5.4c, Z_w represents a Warburg impedance that is occasionally observed and is related to ion transport through the film.[15]

To demonstrate the effect of pH on film barrier properties, Figure 5.5 shows EIS spectra in the form of Bode plots for a 75 nm PM-CO2H film on gold with 1% molar acid content. Solid curves in the plot represent best fits of the data with appropriate equivalent circuit models (Figure 5.4) to provide quantitative information on the effect of pH on film capacitance and resistance (Figures 5.6a and 5.6b). For comparison, the spectrum for bare gold exposed to pH 11 buffer solution is also shown and fit with the model in Figure 5.4b. Since no redox probes are in solution, the spectrum for bare gold is dominated by a double-layer capacitance of ~10^{-5} F/cm^2, similar to the value provided by Loveday and Peterson.[16] Changing solution pH had negligible effect on the spectrum for bare gold. As a second comparison, the spectrum for an unhydrolyzed PM-CO2Et copolymer film on gold at pH 4 is also shown. Changing solution pH from 4 to 11 had negligible effect on the spectrum for PM-CO2Et. The unhydrolyzed polymer film exhibits a straight line of slope -1 with high impedance (>10^7 Ω cm^2) at low frequency, indicating a strong barrier against ion penetration.[16-19]

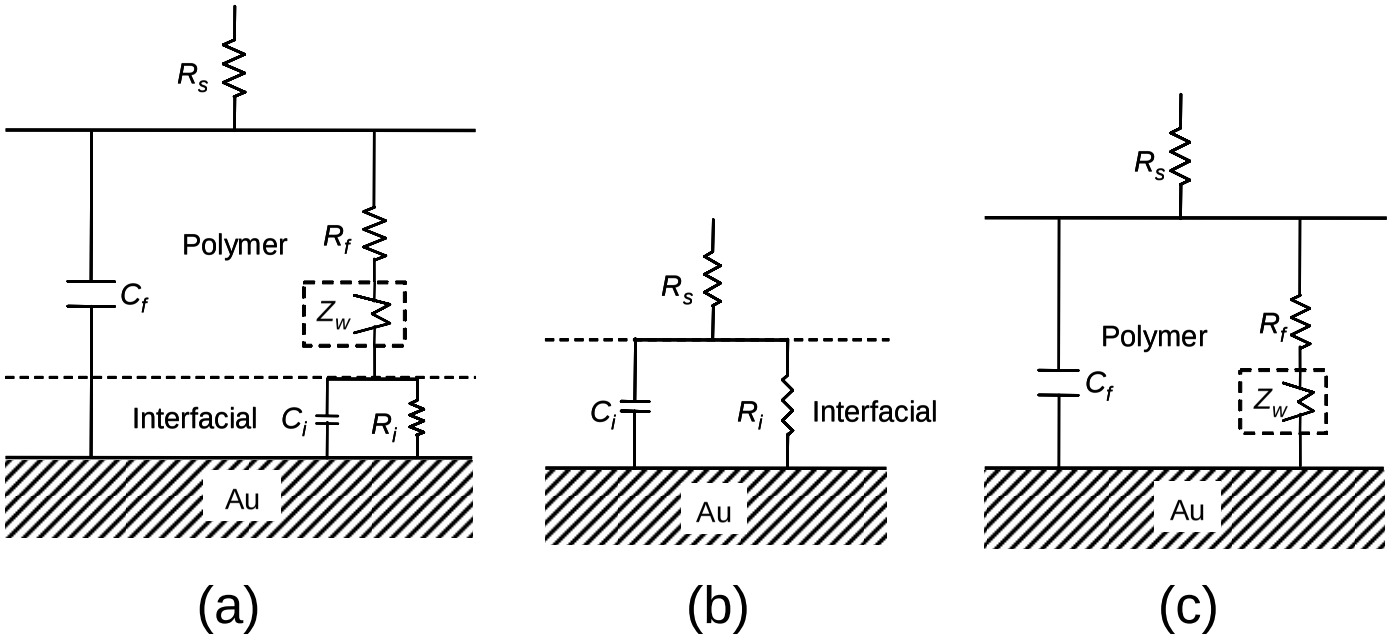

Figure 5.4. Equivalent circuits used to model impedance spectra for polymer films on gold: (a) model commonly used for polymer/metal interfaces; (b) model used when interfacial components dominate the impedance; (c) model used when the film dominates the impedance spectrum.

Upon hydrolysis, the impedance spectrum of the PM-CO2H film changes in a pH-dependent manner. The hydrolyzed film exhibits spectra very similar to that of the unhydrolyzed film from pH 4 to 9, indicating the impedance due to the film dominates the entire frequency region. The slight decrease in the magnitude of the film impedance with increasing pH is consistent with the gradual deprotonation of the carboxylic acid side chains (Figure 5.3), which increases the hydrophilicity of the film and the effective film capacitance due to aqueous ion penetration (Figure 5.6a). Water has a higher dielectric constant (~80) than that of the PM-rich film (~2 to 3),[20] so the capacitance of the coating with water and ion penetration is higher than that of the unhydrolyzed film. As pH is increased from 9 to 10, the impedance spectrum is greatly affected. The increasing charge of the film with pH results in markedly reduced film resistance such that two time constants appear in the impedance spectrum, and the spectrum is fit by the more complex model shown in Figure 5.4a. The time constant at lower frequencies is from the interface and the one at higher frequencies is from the polymer film and corresponds to the combined capacitance and resistance of the polymer film (see Figure 5.4a).[17,21,22] This latter time constant provides a measure of the time required for ionic permeation through the film, in this case ~0.003 s. As pH is increased from 10 to 11, the film resistance decreases further and the time required for ions to reach the interfacial region becomes even shorter. This spectrum is dominated by the interfacial capacitance. The spectra for pH 10 and 11 are offset at low frequency to represent an interfacial capacitance that increases with pH as the gold/polymer interface presumably becomes more concentrated with water and ions.

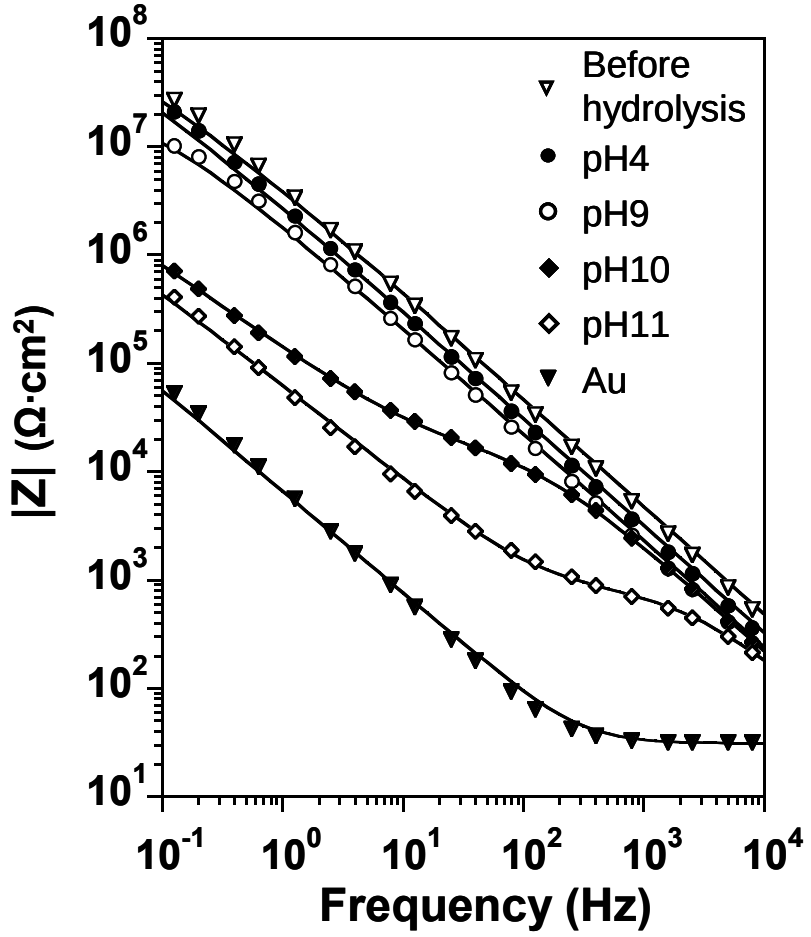

Figure 5.5. Electrochemical impedance spectra in the form of a Bode plot as a function of pH for a 75 nm copolymer film with 1% acid content on gold. Spectra for uncoated gold and an unhydrolyzed PM-CO2Et film are shown for comparison.

From pH 9 to pH 11, we did not observe a large increase in the carboxylate composition of the film (refer to Figure 5.3), but the small amount of carboxylate increase has a profound influence on film resistance, which decreases from ~10^8 Ω·cm^2 at pH 9 to ~10^4 Ω·cm^2 at pH 10 and ~10^3 Ω·cm^2 at pH 11 (Figure 5.6b). At pH 11, the film resistance is still evident, suggesting a small but measurable barrier to ion transfer. This ~5 order of magnitude drop in resistance over a narrow pH range is much larger than an

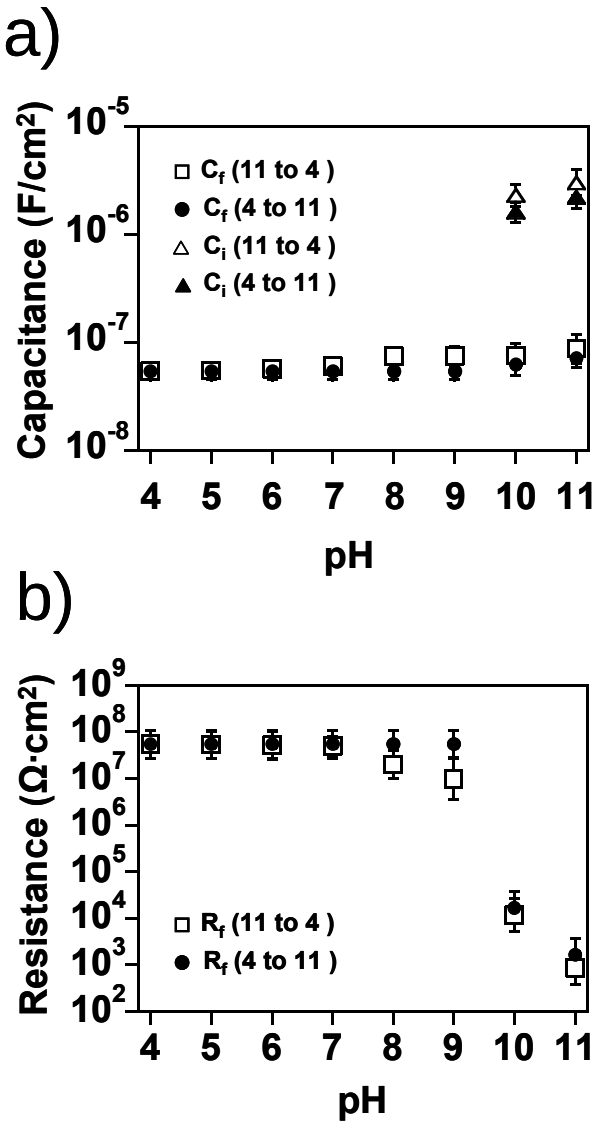

Figure 5.6. pH-Dependent (a) capacitance and (b) resistance for a 75 nm film with 1% acid content. Open squares represent C_f or R_f and open triangles represent C_i when pH was incrementally decreased from 11 to 4. Solid circles represent C_f and R_f and solid triangles represent C_i when pH was incrementally increased from 4 to 11.

order of magnitude decrease reported for poly(acrylic acid) thin films[23] and could be powerful in applications such as pH-responsive membranes. In contrast, film capacitance is much less sensitive to pH, remaining < 10^{-7} F/cm^2 for the entire pH range (Figure

5.6a). This lack of sensitivity in capacitance is due to the predominately hydrophobic nature of the 1% acid film and the high frequency measurement of film capacitance, which does not allow sufficient time for ions to penetrate the film.

Figures 5.6a and b show resistance and capacitance values respectively, obtained upon first decreasing pH incrementally from 11 to 4 and then upon increasing pH incrementally from 4 back to 11. In general, the closeness of the values, as evidenced by the overlap of error bars at each pH value, combined with the large change in film resistance near the critical pH range suggests a (statistically) reversible pH-induced response of the polymer film. We have also cycled the films ~20 times between buffer solutions at pH 4 and pH 11 and measured impedance modulus at a constant frequency (100 Hz) (not shown). For each cycle, the measured impedance values increase upon exposure to pH 4 buffer and decrease upon exposure to pH 11 buffer. For all the cycles, the steady-state impedance values at pH 4 are within ~3% of each other and those at pH 11 are within ~7% of each other, demonstrating good reversibility.

For comparison with the film containing 1% acid, we also show impedance spectra at different pH values for a 75 nm film with 3% acid content in Figure 5.7 with fitted capacitance and resistance values shown in Figure 5.8. From pH 4 to 6, only one time constant appears in the spectra, and these can be fitted by the model in Figure 5.4c. Similar to the more hydrophobic 1% acid film at low pH values, the film impedance dominates the entire frequency range. However, these curves are not straight lines but indicate a film resistance at the lowest frequencies. The 3% acid film is therefore less blocking against ion transfer as compared to the 1% acid film. At pH 7, two time constants appear in the spectrum for the 3% acid film, similar to the 1% acid film at pH

10. Again, the high frequency time constant is attributed to the polymer film and the low frequency time constant is due to the polymer/metal interface. With the increasing deprotonation of the carboxylic acid groups, aqueous ions can more easily penetrate the film to reach the gold surface, but the film still provides a quantifiable resistance against ion transfer. As shown in Figure 5.8b, the film resistance drops dramatically from ~ 10^7

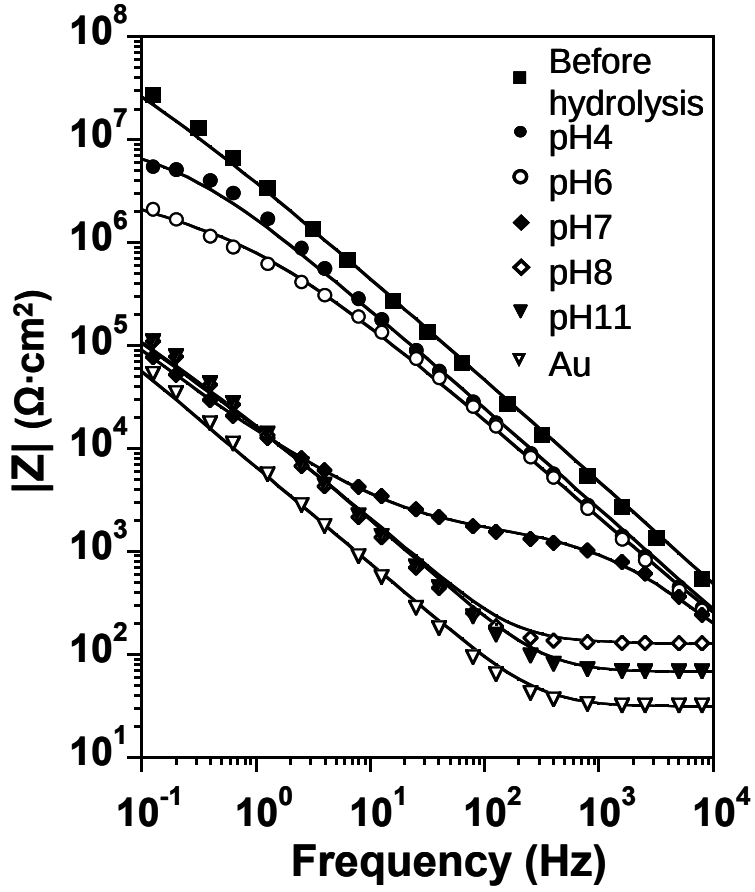

Figure 5.7. Electrochemical impedance spectra in Bode plot form as a function of pH for a 75 nm copolymer film with 3 % acid content on gold. Spectra for uncoated gold and an unhydrolyzed PM-CO2Et film are shown for comparison.

$\Omega \cdot cm^2$ at pH 4 to 5 to ~ 10^5 $\Omega \cdot cm^2$ at pH 6 to ~ 10^3 $\Omega \cdot cm^2$ at pH 7 due to the enhanced hydrophilicity of the increasingly charged film. The film capacitance is essentially constant over this same range.

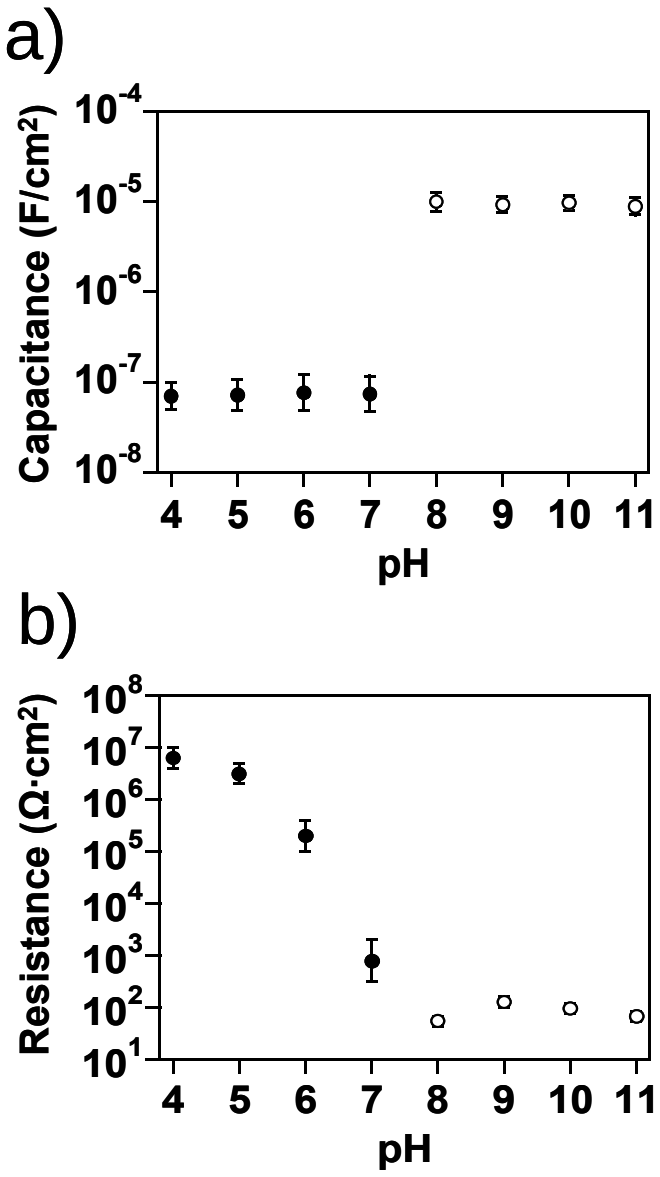

Figure 5.8. pH-Dependent (a) capacitance and (b) resistance for a 75 nm film with 3% acid content. Solid circles represent C_f or R_f; empty circles represents the C_i or R_s.

From pH 8 to pH 11, only one time constant due to the polymer/metal interface appears, and the spectra are fit with the model in Figure 5.4b. At these pH values, the film is not providing any measurable resistance against ion transport, so only R_s values are shown in Figure 5.8b and C_i values are shown in Figure 5.8a. Spectra at these pH values approach convergence at low to moderate frequencies due to similar C_i but are distinct at high frequency, where R_s varies due to slight differences in ion concentration and different compositions in the buffer solutions (Figure 5.8b).[15]

Compared with the film containing 1% acid at the same thickness of 75 nm, the 3% film exhibits lower resistances and higher capacitances at the same pH values from 4 to 7. In addition, comparison of Figures 5.6b and 5.8b reveals that the 3% film exhibits a ~5 order of magnitude decrease in resistance over a pH range of 5 – 8 whereas the transition range for the 1% film is from pH 9 – 11. These differences imply that the response of the film is extremely sensitive to the acid content or hydrophilicity within the film.

To further explore the effect of acid content within the films, we have also investigated the pH-responsive barrier properties for 75 nm films with 2% and 4% acid contents. The R_f, C_f, and C_i values for the films with 1% through 4% carboxylic acid content are listed in Table 5.2. All these films have the same composition before hydrolysis and the only difference among them is the hydrolysis time applied. From Table 5.2, film resistances decrease and film capacitances increase as acid content is increased. In addition, the pH where film properties become immeasurable shifts to lower pH as acid content is increased. From these results, we can extract the critical pH range, the pH increment over which the largest change in R_f occurs. This critical pH

Table 5.2. Effect of acid content and pH on the barrier properties of PM-CO2H copolymer films when pH was incrementally decreased from 11 to 4

	1%			2%			3%			4%		
pH	$\log R_f$ ($\Omega \cdot cm^2$)	C_f (nF/cm^2)	C_i (nF/cm^2)	$\log R_f$ ($\Omega \cdot cm^2$)	C_f (nF/cm^2)	C_i (nF/cm^2)	$\log R_f$ ($\Omega \cdot cm^2$)	C_f (nF/cm^2)	C_i (nF/cm^2)	$\log R_f$ ($\Omega \cdot cm^2$)	C_f (nF/cm^2)	C_i (nF/cm^2)
4	7.7±0.3	55±5	-	7.4±0.2	69±6	-	6.8±0.2	71±10	-	6.6±0.2	130±9	-
5	7.7±0.3	55±4	-	7.3±0.4	69±6	-	6.5±0.2	72±12	-	6.4±0.2	110±11	-
6	7.7±0.3	58±4	-	7.1±0.3	71±8	-	5.3±0.3	76±15	-	4.0±0.3	155±19	-
7	7.7±0.2	60±4	-	6.8±0.3	74±8	-	2.9±0.5	74±15	10200±900	-	-	11000±100
8	7.3±0.3	74±5	-	4.5±0.6	79±8	7200±700	-	-	10000±1000	-	-	12000±110
9	7.0±0.5	78±7	-	3.3±0.5	83±10	6600±800	-	-	9800±700	-	-	11000±130
10	4.1±0.3	78±9	2300±300	-	-	6500±600	-	-	9300±900	-	-	12000±100
11	2.8±0.4	87±11	3000±400	-	-	6200±600	-	-	8900±800	-	-	13000±130

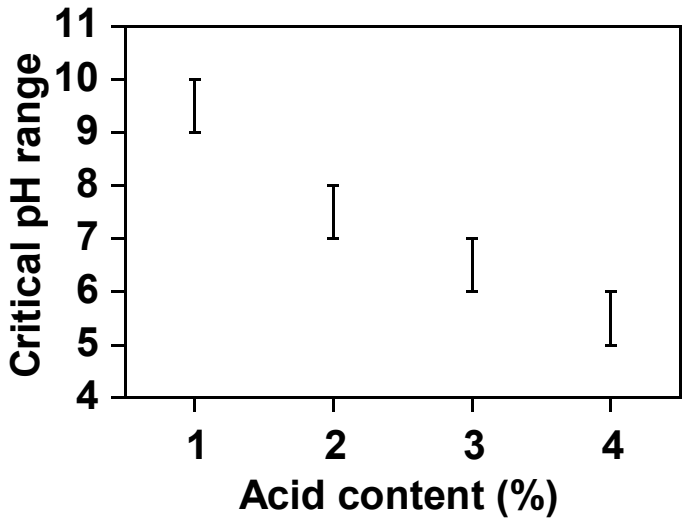

Figure 5.9. Effect of acid content of PM-CO2H films on the critical pH, defined as the pH increment over which the largest change in R_f occurs.

region shifts downward as acid content is increased (Figure 5.9), demonstrating a tunability over the critical pH by careful control over film composition. Interestingly, the pH ranges that result in these dramatic drops in R_f do not yield large increases in carboxylate content, as shown in the compositional results of Figure 5.3. Upon highlighting these critical pH ranges on Figure 5.3, we observe that all the dramatic changes in film barrier properties occur between the CO_2^-:CH_2 peak ratios of 0.03 to 0.12. Films with lower acid content require higher carboxylate contents for their film resistances to break down. This effect is attributed to film hydrophobicity; since the total acid content is reduced (4% down to 1%), a higher fractional deprotonation of the more hydrophobic films is required to produced the same level of ion diffusion pathways and the similar break down in film resistance. That the large change in film resistance occurs

over a pH range where carboxylate concentration changes gradually suggests that a critical film hydrophilicity is required to generate these coherent ion pathways.

An important finding of this work is that the critical pH range can be tailored by varying the acid content within the film. This result suggests that PM-CO2H films can be engineered to open/close at any pH in the range of 5 to 10 to respond in a versatile manner with specific requirements in separations or sensing. The ~5 order of magnitude drop in film resistance should provide high signal-to-noise in sensing and large pH-induced modulation of transport rates in separations.

Conclusions

We have prepared pH-responsive carboxyl-modified polymethylene films by a surface-catalyzed polymerization and subsequent hydrolysis. The films are uncharged and hydrophobic at low pH but become charged at moderate to high pH to facilitate ion transfer. Film resistances decrease by up to ~5 orders of magnitude over the critical pH range, demonstrating the effect of pH and charge on film hydrophobicity. This critical range can be tuned from pH 5 to 10 by varying the acid content within the film. The surface-catalyzed preparation of these films enables selective growth on gold surfaces of any shape, provides a precise control over film thickness, and offers the ability to tune the concentration of the pH-sensitive groups within the film.

References

1. Schwarzenbach, R.; Gschwend, P.; Imboden, D. *Environmental Organic Chemistry*; Wiley: New York, 1993.

2. Bai, D.; Jennings, G. K. "Surface-Catalyzed Growth of Polymethylene-Rich Copolymer Films on Gold," *Journal of the American Chemical Society* **2005**, *127*, 3048-3056.

3. Seshadri, K.; Atre, S. V.; Tao, Y. T.; Lee, M. T.; Allara, D. L. "Synthesis of Crystalline, Nanometer-Scale, $-(CH_2)_x-$ Clusters and Films on Gold Surfaces," *Journal of the American Chemical Society* **1997**, *119*, 4698-4711.

4. Guo, W. F.; Jennings, G. K. "Use of Underpotentially Deposited Metals on Gold to Affect the Surface-Catalyzed Formation of Polymethylene Films," *Langmuir* **2002**, *18*, 3123-3126.

5. Guo, W. F.; Jennings, G. K. "Directed Growth of Polymethylene Films on Atomically Modified Gold Surfaces," *Advanced Materials* **2003**, *15*, 588-591.

6. Wilson, M. D.; Whitesides, G. M. "The Anthranilate Amide of Polyethylene Carboxylic-Acid Shows an Exceptionally Large Change with pH in Its Wettability by Water," *Journal of the American Chemical Society* **1988**, *110*, 8718-8719.

7. Holmes-Farley, S. R.; Reamey, R. H.; McCarthy, T. J.; Deutch, J.; Whitesides, G. M. "Acid-Base Behavior of Carboxylic-Acid Groups Covalently Attached at the Surface of Polyethylene - the Usefulness of Contact-Angle in Following the Ionization of Surface Functionality," *Langmuir* **1985**, *1*, 725-740.

8. Bain, C. D.; Whitesides, G. M. "A Study by Contact-Angle of the Acid-Base Behavior of Monolayers Containing ω-Mercaptocarboxylic Acids Adsorbed on Gold - an Example of Reactive Spreading," *Langmuir* **1989**, *5*, 1370-1378.

9. Lee, T. R.; Carey, R. I.; Biebuyck, H. A.; Whitesides, G. M. "The Wetting of Monolayer Films Exposing Ionizable Acids and Bases," *Langmuir* **1994**, *10*, 741-749.

10. Hu, K.; Bard, A. J. "Use of Atomic Force Microscopy for the Study of Surface Acid-Base Properties of Carboxylic Acid-Terminated Self-Assembled Monolayers," *Langmuir* **1997**, *13*, 5114-5119.

11. Silverstein, R. M.; Webster, F. X. *Spectrometric Identification of Organic Compounds*; John Wiley & Sons: New York, 1998.

12. Bantz, M. R.; Brantley, E. L.; Weinstein, R. D.; Moriarty, J.; Jennings, G. K. "Effect of Fractional Fluorination on the Properties of ATRP Surface-Initiated Poly(hydroxyethyl methacrylate) Films," *Journal of Physical Chemistry B* **2004**, *108*, 9787-9794.

13. Laibinis, P. E.; Bain, C. D.; Nuzzo, R. G.; Whitesides, G. M. "Structure and Wetting Properties of *ω*-Alkoxy-*n*-Alkanethiolate Monolayers on Gold and Silver," *Journal of Physical Chemistry* **1995**, *99*, 7663-7676.

14. Brantley, E. L.; Holmes, T. C.; Jennings, G. K. "Modification of ATRP Surface-Initiated Poly(hydroxyethyl methacrylate) Films with Hydrocarbon Side Chains," *Journal of Physical Chemistry B* **2004**, *108*, 16077-16084.

15. Bard, A.; Faulkner, L. *Electrochemical Methods Fundamentals and Applications;* John Wiley & Sons: New York, 2000.

16. Loveday, D.; Peterson, P.; Rodgers, B. "Evaluation of Organic Coatings with Electrochemical Impedance Spectroscopy. Part 1: Fundamentals of Electrochemical Impedance Spectroscopy," *JCT Coatings Technology* August **2004**, 46-52.

17. Loveday, D.; Peterson, P.; Rodgers, B. "Evaluation of Organic Coatings with Electrochemical Impedance Spectroscopy. Part 2: Application of EIS to Coatings," *JCT Coatings Technology* October **2004**, 88-93.

18. Park, S. M.; Yoo, J. S. "Electrochemical Impedance Spectroscopy for Better Electrochemical Measurements," *Analytical Chemistry* **2003**, *75*, 455A-461A.

19. Rammelt, U.; Reinhard, G. "Application of Electrochemical Impedance Spectroscopy (EIS) for Characterizing the Corrosion-Protective Performance of Organic Coatings on Metals," *Progress in Organic Coatings* **1992**, *21*, 205-226.

20. Zhu, L.; Chiu, F.; Fu, Q.; Quirk, R.; Cheng, S. Physical Constants of Poly(ethylene). In *Polymer Handbook*; Brandrup, J., Immergut, E. H., Grulke, E. A., Eds.; John Wiley & Sons: New York, 1999.

21. Murray, J. N. "Electrochemical Test Methods for Evaluating Organic Coatings on Metals: An Update. Part III: Multiple Test Parameter Measurements," *Progress in Organic Coatings* **1997**, *31*, 375-391.

22. Bellucci F.; Kloppers M.; Latanision R. M. "Protective Properties of Polyimide (PMDA-ODA) on Aluminum Metallic Substrate," *Journal of the Electrochemical Society* **1991**, 138, 40-48.

23. Zhao, M.; Bruening, M. L.; Zhou, Y.; Bergbreiter, D. E.; Crooks, R. M. "Effect of pH, Fluorination, and Number of Layers on the Inhibition of Electrochemical

Reactions by Grafted, Hyperbranched Poly(acrylic acid) Films," *Israel Journal of Chemistry* **1997**, 37, 277-286.

CHAPTER VI

KINETICS OF pH-RESPONSE FOR POLYMETHYLENE-RICH COPOLYMER FILMS

Introduction

For successful utilization in sensing and separations, the pH-responsive film must exhibit a large, rapid, and reversible response and should be straightforward to process on appropriate substrates. In chapter V, we reported the design and performance of a new class of pH-responsive copolymer films on gold surfaces. These films were prepared by a controlled, surface-catalyzed polymerization in the presence of diazomethane (DM) and ethyl diazoacetate (EDA) to produce a copolymer film consistent with poly(methylene-*co*-ethyl acetate) and subsequently hydrolyzing the ester side chains to varying extents to yield carboxylic acids (denoted as PM-CO2H).[1] These films are predominately hydrophobic but contain a controlled, dilute fraction (1-4%) of carboxylic acid groups to exhibit a remarkable change in barrier properties when the pH is increased sufficiently to ionize the acid groups. We have shown that at a 1% - 4% molar acid content, the copolymer film exhibits a five order of magnitude change in its resistance to ion transport over 2 – 3 pH units.[1] The onset pH at which this response initiates can be tailored from pH 5 to 10 by decreasing the acid content in the film from 4% to 1%.

The ability to precisely control the acid content within the film and tailor the thickness of these surface-catalyzed polymer films from a few to several hundred nm enables a thorough assessment of film composition and thickness on response rate. While film response should be more rapid for thinner films, the film must be sufficiently

uniform to function as a defect-free barrier in the uncharged state. To examine the rate of film response, we measured film impedance at a fixed frequency during a step change in pH, a technique that our group has previously used to measure the kinetics of self-assembled monolayer formation.[2] We compared the kinetic rates for the step up in pH with those for the step down to determine if the hydrophobic nature of the uncharged films provides a diffusive barrier for aqueous ions. We expect that protonation of the films will be slower than ionization because, for the former case, water and ions have to penetrate a neutralized region of hydrophobic film formed during the protonation. Through this study, we seek to identify optimal film composition and thicknesses that enable uniform permeation but enhance the rates of response.

Experimental Procedures

Preparation of Polymer Films

Polymer films were prepared by exposure of gold-coated silicon substrates to ether solutions containing 0.3 mM DM and 40 mM EDA (to obtain 50 nm films) or 0.3 mM DM and 80 mM EDA (to obtain 95 nm films) at 0 °C for 16 h. Film growth was carried out in capped 20 mL vials, and only one substrate was placed in each vial. Upon removal, the samples were rinsed with ether and ethanol and dried in a stream of nitrogen. The resulting PM-CO2Et film contained 3.6% and 4.2% (molar) of the ethyl ester group for 50 nm and 95 nm films, respectively.

Hydrolysis of Polymer Films

Hydrolysis of the copolymer films was carried out in capped 20 mL vials of 0.2 M KOH in 2-propanol at 75 °C for 40, 80 and 180 min to obtain copolymer films with 1%, 2%, and 3% acid contents for 50 nm films, and 1, 2, and 3.5 h to obtain copolymer films with 1%, 2%, and 3% acid contents for 95 nm films. Only one substrate was placed in each vial. The hydrolyzed samples were rinsed with ethanol and DI water and dried in a N_2 stream.

Ellipsometry

A Simple Liquid Cell with the M-2000DI system is used to perform ellipsometric measurements on samples immersed in a pH buffer solution. Before sample measurement, the liquid cell was calibrated with a 50 mm silicon wafer with a ~250 Å thermally grown SiO_2 film to insure that the effects of window birefringence are minimized. After the sample is mounted and the cell is aligned, a single data scan is acquired to provide a baseline measurement prior to the injection of the solution into the cell. After the pH solution was added to the cell, the alignment was checked again, and then single data sets are acquired. A top layer with the optical constants for the pH solutions was added to the Cauchy layer model to determine the film thicknesses in the pH solutions.

Impedance Study at Single Frequency

Impedance measurements were obtained at 100 Hz. The cell initially contained 6 mL of pH 11/pH 4 buffer solution. After a stable impedance was obtained, the pH

solution was removed from the cell and 6 mL of pH 4/pH 11 buffer solution were added immediately. Impedance and phase angle readings were recorded every 3 s. Reported values for t_{95}, the time required for the impedance to exhibit 95% of the pH-induced response represent the average and standard deviation of values obtained from at least three measurements.

Results and Discussion

Motivation for Single Frequency Measurements

Figure 6.1 shows electrochemical impedance spectra in the form of Bode plots for a 95 nm PM-CO2H film with 1% acid content on gold at pH 4 and pH 11. The spectra

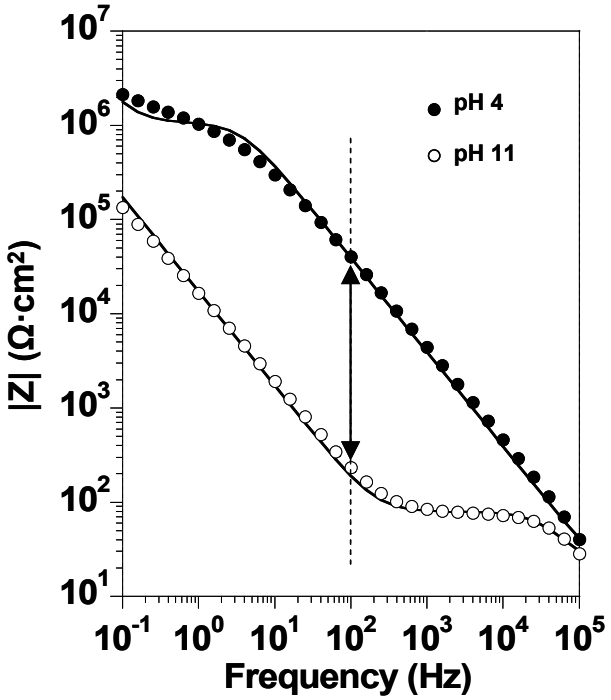

Figure 6.1. Electrochemical impedance spectra in the form of Bode plots for a 95 nm PM-CO2H film with 1% acid content at pH 4 and pH 11 on gold.

can be fitted with a model commonly used for polymer-coated metals[3] as shown in Figure 5.4a. This model contains two time constants, one due to the polymer film and one due to the polymer-metal interface. The following terms are used to denote various film and solution characteristics: solution resistance, R_s; interfacial capacitance, C_i; interfacial resistance, R_i; film capacitance, C_f; film resistance, R_f; and Warburg impedance, Z_w. One simplification to the circuit in Figure 5.4a for the present study is that R_i is effectively infinite since no redox probes are present to transfer charge at the electrode; thus, we do not expect to observe a resistance due to the polymer/metal interface in the spectra.

At pH 4, the side chains of PM-CO2H are in the uncharged state (-CO2H), and the film is hydrophobic. The film impedance dominates most of the frequency region (from 2×10^1 to 10^5 Hz), and R_f is much greater than the combined impedance of R_i and C_i in parallel. At low frequencies, a Warburg component appears which is due to mass-transfer limited ion diffusion. At pH 11, the deprotonation of the carboxylic acid side chains increases the hydrophilicity of the film. The increasing charge of the film with pH results in markedly reduced film resistance such that two time constants appear in the impedance spectrum. The time constant at lower frequencies is from the polymer/metal interface, and the one at higher frequencies is from the polymer film and corresponds to the combined capacitance and resistance of the polymer film. At pH 11, the film resistance is still evident from 1 – 40 kHz, representing a small but measurable barrier to ion transfer.

While EIS can provide a way to evaluate the film performance and extract useful properties such as the film resistance and capacitance, each spectrum requires about 10 min to accumulate, precluding a detailed analysis of kinetics on the time scale of several

seconds to a few minutes. To probe the rate of pH-induced response of the copolymer film, a more rapid method to measure film barrier properties is required. One way to achieve a more rapid sampling is to evaluate the pH-response at a fixed frequency. Single frequency measurements can probe the impedance change as a function of time by sampling every few seconds; thus, we can more effectively monitor the rate of film response as the film changes from one state to the other. As shown in Figure 6.1, we have drawn a vertical line connecting the two spectra at a frequency of 100 Hz. At 100 Hz, film capacitance dominates the impedance at pH 4 and interfacial capacitance dominates the impedance at pH 11. By switching solution pH from 4 to 11, the actual value of impedance modulus is altered by more than two orders of magnitude, the largest difference within the studied frequency range. We also expect that the change will be reversible since we have observed repeatable results when we performed EIS over the range from pH 4 to 11 and back.[1]

Figure 6.2 shows the measured impedance upon exposure of a 95 nm, 1% acid film to pH 4 and 11 buffer solutions in a cyclic manner. The system's impedance at 100 Hz changes by a factor of 150 when the pH of the contacting solution is switched from 4 to 11. For each cycle, the measured impedance values increase upon exposure to the pH 4 buffer and decrease upon exposure to the pH 11 buffer solution. Upon cycling pH, the film returns to the initial impedance value, indicating the reversible nature of the pH response. For all the cycles, the steady-state impedance values at pH 4 are within ~5% of each other and those at pH 11 are within ~10% of each other, demonstrating good reversibility. We have previously used EIS to show that the PM-CO2H films exhibit a large response in barrier properties to pH; here, we use fixed frequency impedance

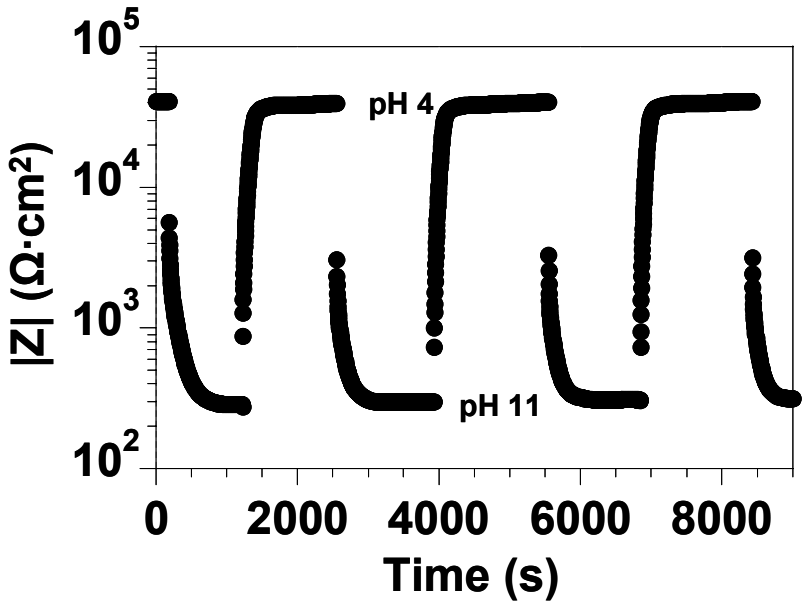

Figure 6.2. Time-dependence of impedance modulus for a 95 nm PM-CO2H film with 1% acid content on gold when the contacting solution pH cycles between pH 4 and pH 11.

measurements to demonstrate that the response is reversible and can be measured in a rapid manner to reveal potential information on response rates.

Effect of Film Composition on the Rate of Film Response

To investigate the effect of film composition on the rate of response, we performed EIS at 100 Hz on PM-CO2H films at 95 nm with 1, 2, and 3% molar acid contents. Since the impedance changes dramatically with pH, we can monitor changes in the real and imagnary components and phase angles with time to obtain an improved understanding of the response process. Figure 6.3 shows the time dependence for |Z|, Z_R, Z_I, and ϕ at 100 Hz for a 1% acid film at 95 nm upon changing pH from 11 to 4 and thereby protonating carboxylates to enhance the hydrophobicity of the film. At pH 11,

Z_R and Z_I are each observed, with Z_I being ~3 times larger. If the polymer/gold interface functions as a pure interfacial capacitor, we would not expect to observe Z_R, and the phase angle should be -90˚. However, the fact that Z_R is observed and the phase angle is

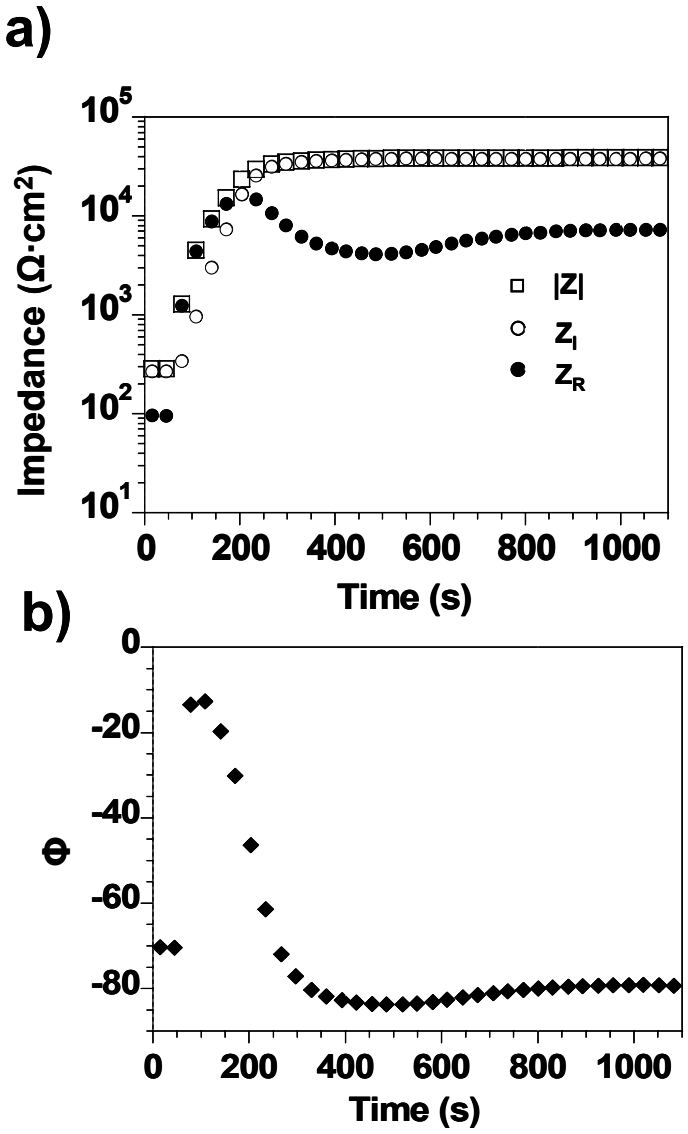

Figure 6.3. The changes of |Z|, Z_R, Z_I, and phase angle as a function of time for a 95 nm PM-CO2H film with 1% acid molar content when pH is changed from 11 to 4.

~-70˚ indicates an easily measurable, albeit minor, contribution to the film impedance due to the resistance of the polymer film against ion transfer with the dominant component being the interfacial capacitance.

When the pH of the contacting solution is changed from 11 to 4, the protonation of the carboxylate side chains within the film increases the film hydrophobicity and leads to an increase of the film impedance. The |Z| changes by 2 orders of magnitude within 160 s after the step change, and gradually approaches a steady value after that. The initial change of |Z| is mainly from the large increase of the film resistance (Z_R) component as it becomes larger than Z_I in the first 120 s, reflecting a reduction in ion conducting pathways due to the increased hydrophobicity of the protonated film. After this time, Z_I becomes dominant as ion conducting pathways are quenched and the film functions as a dielectric to physically separate the conducting solution from the metal electrode.

The change of the phase angle with time also provides very useful information on the response of this system. When the pH is switched from 11 to 4, the phase angle jumps from -70˚ to -20˚ within 3 s and reaches a peak value of -11˚ at 24 s, consistent with the above analysis that the resistance dominates the capacitance during this intermediate state. After 24 s, the phase angle begins to fall gradually although Z_R continues to increase, indicating that Z_I has begun to catch up and will eventually surpass Z_R as the film behaves more as a dielectric. The phase angle reaches its minimum value (-85˚) as Z_R reaches its local minimum at ~500 s, and the phase angle eventually becomes stable at -80˚.

When pH is switched from 4 to 11, the impedance components change even faster, returning (within 10%) to their original values at pH 11 before the cycle was

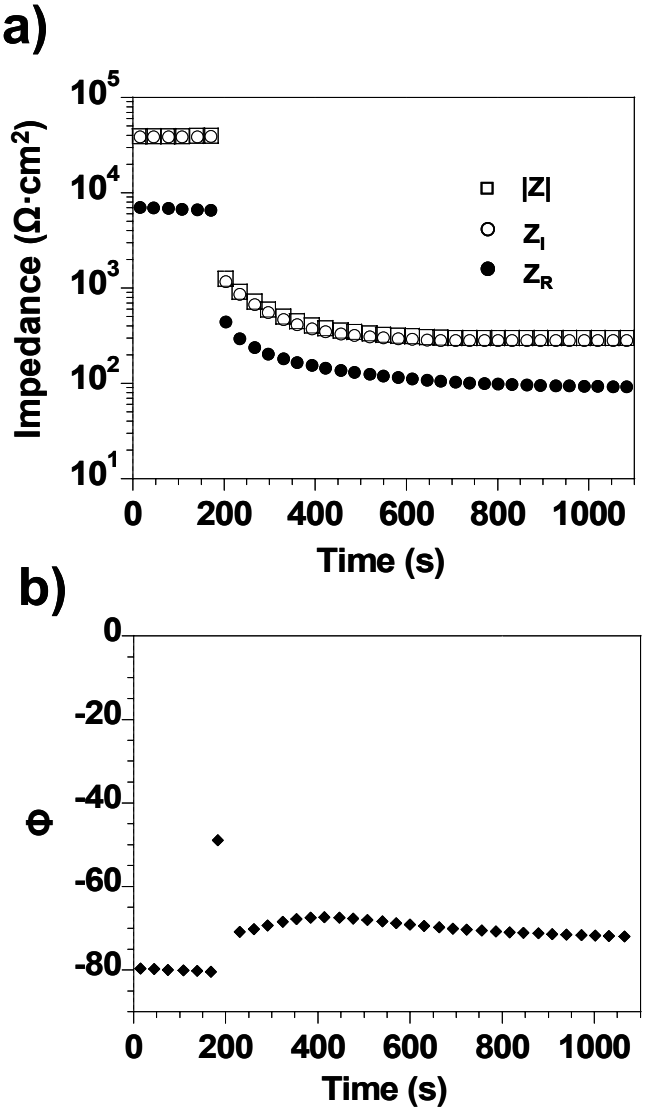

Figure 6.4. The changes of $|Z|$, Z_R, Z_I, and phase angle as a function of time for a 95 nm PM-CO2H film with 1% acid molar content when pH is changed from 4 to 11.

initiated. As shown in Figure 6.4a, $|Z|$ drops from 40000 to 2000 $\Omega \cdot cm^2$ within 10 s. For the entire process, Z_I appears to dominate Z_R. By observing the time dependence of phase angle, we can also obtain some information about the change of film barrier properties. As shown in Figure 6.4b, when pH is switched from 4 to 11, the phase angle increases from -80˚ to a peak value of -49˚ in 3 s corresponding to an increase in relative

contribution by the resistive component as compared to film or interfacial capacitance upon initial deprotonation of the carboxylic acid. As deprotonation continues, the film resistance continues to decrease, and the dominant component is the interfacial capacitance.

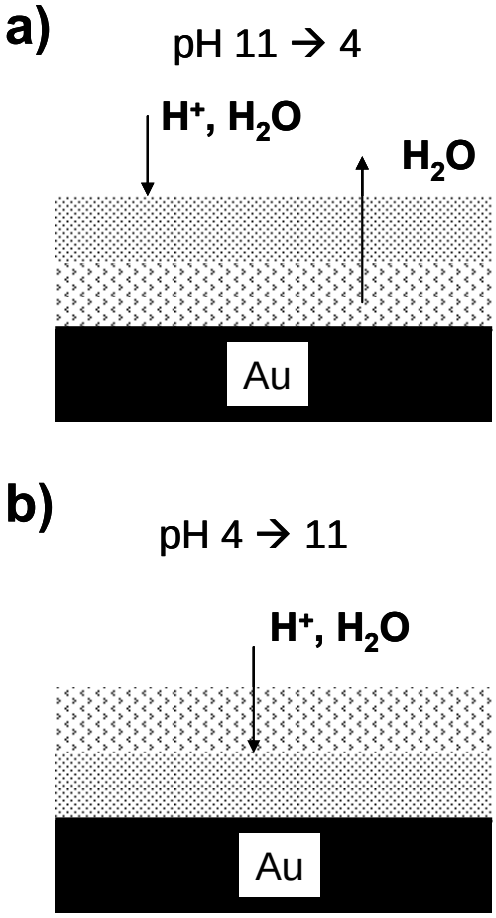

Figure 6.5. Snapshot of an intermediate time scale when pH is changed from a) 11 to 4 and b) 4 to 11.

For all the studied films, the rate of protonation (from pH 11 to 4) is always much slower than that of the deprotonation (pH 4 to 11). To explain this effect, we schematically depict a snapshot of the intermediate time scales for water and ions to

traverse the film in both protonation (Figure 6.5a) and ionization (Figure 6.5b) processes. For protonation, the carboxylate side chains within the film are converted to carboxylic acids. Since the carboxylate group has an octanol-water partition coefficient (Kow) of -5.19 that is over 4 orders of magnitude lower than that of the carboxylic acid (Kow=-1.11),[4] the reacted film becomes dramatically more hydrophobic. At an intermediate time, an outer hydrophobic region of film likely separates the proton-rich aqueous solution from the underlying carboxylate-rich film and impedes the transfer of aqueous protons to further react with the carboxylate groups underneath. In addition, once protonation occurs, water and ions trapped in the film may be slow to diffuse out of the film. In contrast, when the pH changes from 4 to 11, the carboxylic acids at the top part of the film will be ionized to carboxylates, and the film becomes increasingly hydrophilic to facilitate the transfer of water and ions as a moving front through the film.

According to Eq. 3-15 in Chapter III, $Z_I = 1/j\omega C$. Using the Helmholtz model,[5]

$$C = \frac{\varepsilon\varepsilon_0}{d} \tag{6-1}$$

where ε is the dielectric constant of the polymer film, ε_0 is the permittivity of vacuum, and d is the thickness of the film. Therefore, the imaginary impedance becomes

$$Z_I = \frac{d}{\omega\varepsilon\varepsilon_0} \tag{6-2}$$

Since ω and ε_0 are constants and the film thickness only changes slightly from pH 4 to pH 11 due to swelling,[6] Z_I is mostly a function of the ε of the polymer coated on the gold electrode. Water has a much higher dielectric constant (~80) than that of the PM-rich film (~2 to 3),[7] so an increased water content within the film will greatly affect the film capacitance and imaginary impedance. The time dependence of Z_I can be used to examine the extent of the protonation/ionization reaction indirectly through the transport of water and ions into or out of the film. For the ionization, the reaction occurs easily, and the water penetrates into the film very rapidly, observed as a fast drop in Z_I. In the protonation, the reaction is hindered by the increasing hydrophobicity of the film which affects the transport of water out of the film; thus, we observe a slower change in Z_I with time.

To determine if the protonation is diffusion limited or reaction limited, we performed contact angle measurements on a 1% film at 95 nm after switching the pH of the contacting solution from 11 to 4. The contact angle is only sensitive to the top half nanometer of surface composition.[8] If the process is reaction-limited, we expect the measured contact angle to change with the increasing reaction time as the carboxylic acid content changes within the film and on the surface. We immersed the 1% acid content film that was placed in pH 11 solution for at least 60 min into a pH 4 solution for 30, 120, and 600 s and measured the contact angles by using a pH 4 solution as the probe liquid. We observed the same advancing contact angle. Thus, as judged by this result, the protonation reaction at the surface happens very fast, and the reaction is not consistent with a reaction-limited process.

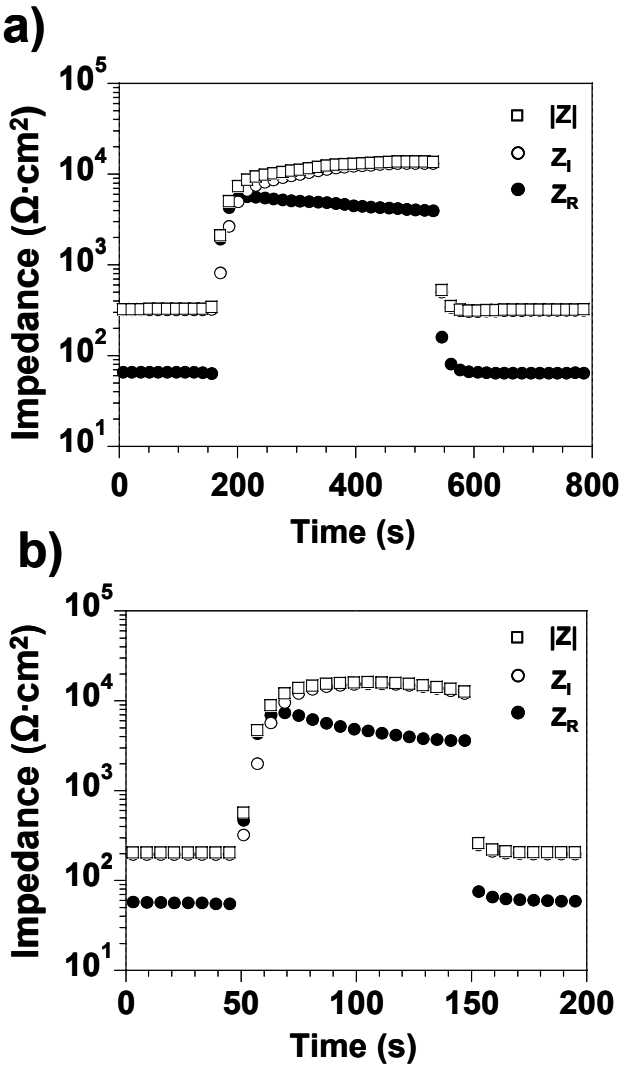

Figure 6.6. The changes of |Z|, Z_R, Z_I, and phase angle as a function of time when the pH changes from 11 to 4 and back to 11 for a 95 nm PM-CO2H film with a) 2% and b) 3% acid molar content.

To investigate the effect of acid content on the rate of film response, we monitored impedance properties at 100 Hz for 95 nm films with 2 (Figure 6.6a) and 3% (Figure 6.6b) molar acid content. These films still yield large responses (~2 orders of magnitude) when pH is switched between 4 and 11, but the 3% film responds

significantly faster, as noted by comparing the time scales on the x-axis. Upon comparison of these results with those shown in Figures 6.3 and 6.4, an increase in the acid content within the film greatly reduces the response time (vide infra), consistent with the decrease of film hydrophobicity (more carboxylate content) with greater acid content.

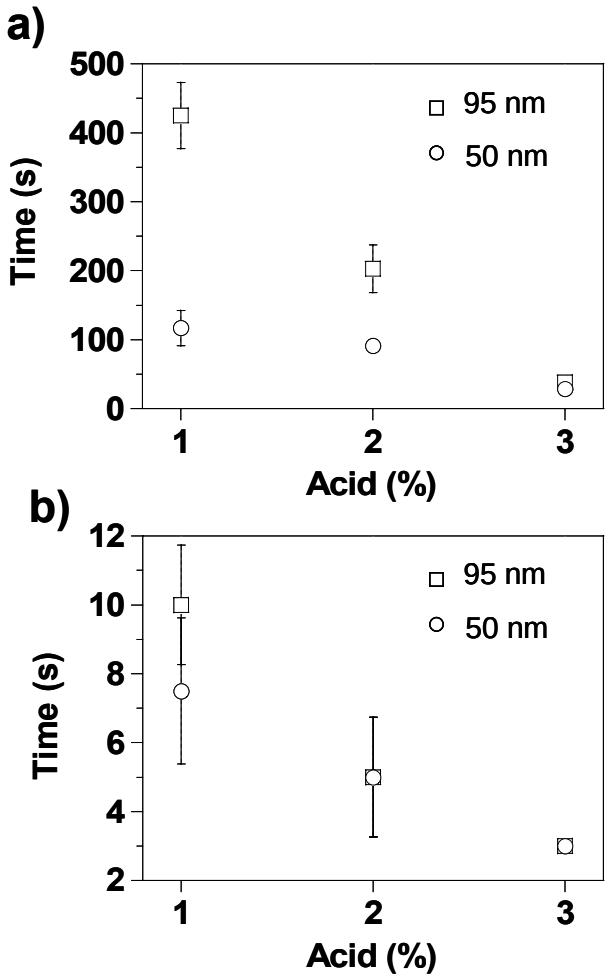

Figure 6.7. Time required for the film with 95 nm and 50 nm thickness to reach 95% of the stable impedance as a function of the acid content when the pH changes from a) 11 to 4 and b) 4 to 11.

To quantify the rate of response, we have determined the time required for a film to reach 95% of the asymptotic impedance (t_{95}) as a function of the acid content within the films (Figure 6.7). This time was chosen because of the widely different transient profiles for the films with different acid contents, which precludes fitting the data with a common model that would enable a simple comparison of rates.

As described previously, there are two stages in the film response, an initial, rapid increase/decrease in film impedance and then a gradual increase/decrease until the impedance reaches a stable value. For a 3% film at 95 nm thickness, the film impedance exhibits a two order of magnitude change within 6 s in both directions. This response is very large and fast as compared to other systems,[9,10] due largely to the thinness and carefully tailored composition of the films. However, at the film thickness of 95 nm, a 1% acid film requires 420 s to reach 95% of the asymptotic value for the protonation process, while the 2 and 3% films require 210 s and 36 s, respectively. By increasing the acid content from 1 to 3%, we can reduce the response time by up to a factor of ~12 but still achieve a large response. The film with 3% acid content is still sufficiently hydrophobic at low pH values (here pH 4) to provide a large film impedance. However, more functional groups are present within the 3% film than in the 1% film to form pathways for water and protons to protonate the unreacted carboxylates so that the response rate is much faster. When pH changes from 4 to 11, the 1, 2 and 3% acid films lose 95% of their impedance in ~10 s, ~5 s and ~3 s, respectively. All films lose more than one order in magnitude in |Z| within 3 s.

Effect of Film Thickness on the Rate of Film Response

We have also investigated the effect of film thickness on the rate of film response by measuring impedance properties at 100 Hz on 50 nm films with 1, 2 and 3% acid contents and comparing t_{95} values with those of the thick 95 nm films in Figure 6.7. Upon decreasing pH from 11 to 4, a 1% acid film at 50 nm requires ~115 s, about a quarter of the time required by the 95 nm film with 1% acid content, to reach 95% of its asymptotic value. For a 1 % film, the protonation is likely a diffusion-limited process since the time required is proportional to the square of the distance (film thickness). However, the diffusion-limited character was not observed for the 2 and 3% acid films. With the increase of acid content in the film, the effect of film thickness on the rate of response is muted. The 2% 50 nm film requires 90 s, which is less than half the time (210 s) required for the 2% 95 nm film, and the 3% 50 nm film requires 27 s, which is only 9 s faster than the 3% 95 nm film. The increased carboxylate content within the film reduces the dependence of the rate of response on film thickness. Similar to the 95 nm films, the 50 nm films respond rapidly when pH is changed from 4 to 11. The t_{95} values for 1, 2, and 3% films are ~7 s, ~5 s, and ~3 s, respectively.

Conclusions

We have investigated the rate of pH-induced response for PM-CO2H films with 1, 2, and 3 % acid content at 50 and 95 nm. For all the studied films, the rate of protonation is slower than that of ionization because for the former case, initial protonation produces regions of hydrophobicity that may impede the transfer of water and ions into and/or out of the film. At the same acid content, the thicker films require a

longer time to reach a new stable state since water and ions must diffuse over a longer distance to reach the electrode. With the increase of acid content within the film, these characteristic times can be shortened for both processes because more water and ion pathways exist within the film, and the effect of film thickness on rate of response becomes weak. By carefully selecting the acid content and film thickness, a fast, large and reversible pH-response can be achieved within the desired pH range.

References

1. Bai, D. S.; Habersberger, B. M.; Jennings, G. K. "pH-Responsive Copolymer Films by Surface-Catalyzed Growth," *Journal of the American Chemical Society* **2005**, *127*, 16486-16493.

2. Yan, D.; Saunders, J. A.; Jennings, G. K. "Kinetics of Formation for *n*-Alkanethiolate Self-Assembled Monolayers onto Gold in Aqueous Micellar Solutions of $C_{12}E_6$ and $C_{12}E_7$," *Langmuir* **2002**, *18*, 10202-10212.

3. Brantley, E. L.; Holmes, T. C.; Jennings, G. K. "Modification of ATRP Surface-Initiated Poly(hydroxyethyl methacrylate) Films with Hydrocarbon Side Chains," *Journal of Physical Chemistry B* **2004**, *108*, 16077-16084.

4. Schwarzenbach, R.; Gschwend, P.; Imboden, D. *Environmental Organic Chemistry*; Wiley: New York, 1993.

5. Bard, A.; Faulkner, L. *Electrochemical Methods Fundamentals and Applications;* John Wiley & Sons: New York, 2000.

6. 20% increase in film thickness was observed for a 50 nm 3% acid film when pH is switched from 4 to 11.

7. Zhu, L.; Chiu, F.; Fu, Q.; Quirk, R.; Cheng, S. Physical Constants of Poly(ethylene). In *Polymer Handbook*; Brandrup, J., Immergut, E. H., Grulke, E. A., Eds.; John Wiley & Sons: New York, 1999.

8. Laibinis, P. E.; Bain, C. D.; Nuzzo, R. G.; Whitesides, G. M. "Structure and Wetting Properties of ω-Alkoxy-*n*-Alkanethiolate Monolayers on Gold and Silver," *Journal of Physical Chemistry* **1995**, *99*, 7663-7676.

9. Cai, Q. Y.; Zeng, K. F.; Ruan, C. M.; Desai, T. A.; Grimes, C. A. "A Wireless, Remote Query Glucose Biosensor Based on a pH-Sensitive Polymer," *Analytical Chemistry* **2004**, *76*, 4038-4043.

10. Richter, A.; Bund, A.; Keller, M.; Arndt, K. F. "Characterization of a Microgravimetric Sensor Based on pH Sensitive Hydrogels," *Sensors and Actuators B-Chemical* **2004**, *99*, 579-585.

CHAPTER VII

pH-RESPONSIVE MEMBRANE SKINS BY SURFACE-CATALYZED POLYMERIZATION

Introduction

Responsive membranes alter their properties when specific stimuli are present in their environment. These stimuli could include temperature,[1-4] pH,[5-8] ions,[9,10] ultrasound,[11] and electric potential.[12] Responsive membranes have important applications in many areas such as controlled drug delivery,[11,13] ion selection,[5-7] molecular separation,[14-16] and regulation of cell adhesion.[10] In this chapter, we report the modification of alumina membranes with ultrathin polymer skins that exhibit unusually large pH-responsive properties.

To date, many methods have been used in the preparation of dense high-performance skins on mechanically strong membranes, including self-assembled monolayers[5-7,11] and polymer films prepared by surface-initiated,[16,17] photo[8,18] and plasma routes,[19] by adsorption of polyelectrolyte multilayers,[20,21] as well as by dip coating[22] and solution casting.[23] Recently, we have reported a new surface-catalyzed polymerization process to grow polymethylene (PM) - rich copolymer films with randomly distributed ester side chains (poly(methylene-*co*-ethyl acetate); PM-CO2Et) from 2-D gold surfaces.[24] This process enables growth of copolymer films with controlled film thickness in the range of a few to several hundred nanometers by controlling polymerization time and/or monomer concentrations.[24] The most important aspect of this PM-CO2Et film is that the ester side chains can be hydrolyzed to carboxylic acids

(denoted as PM-CO2H) to exhibit pH dependent properties.[25] At a 1% - 4% molar acid content, the copolymer film exhibits a five order of magnitude change in its resistance to ion transport over 2 – 3 pH units. In this chapter, we demonstrate that PM-CO2Et films can be grown atop a Au-coated nanoporous alumina support (pore diameter = 20 nm) and hydrolyzed to form a pH-sensitive ultrathin membrane skin. Herein, we use these PM-CO2H skins to examine the effect of solution pH on ion transfer.

Experimental Procedures

Preparation of Gold Coated Silicon Wafers and Membranes

Gold-coated silicon wafers (used for RAIRS and ellipsometry) and alumina membranes were prepared by evaporating chromium (15 Å) and gold (200 Å) in sequence onto silicon (100) wafers and alumina membranes at rates of 1-2 Å s^{-1} in a diffusion-pumped chamber with a base pressure of 4×10^{-6} torr.

Preparation of Membrane Skins

Polymer films were formed by exposure of gold-coated membranes to ether solutions containing 2 mM DM and 160 mM EDA at 0 ^{o}C for 24 h. Upon removal, the samples were rinsed sequentially with ether, ethanol, and DI water, dried with N_2, and stored in the laboratory ambient prior to use.

Hydrolysis

Hydrolysis of the copolymer films was carried out in a solution of 0.1 M KOH in 2-propanol at 0 ^{o}C for 3 h. The hydrolyzed samples were rinsed with ethanol and DI water, and stored in the laboratory ambient to await characterization.

Electrochemical impedance spectroscopy (EIS) was used to investigate the barrier properties of polymer-modified membranes. EIS was performed with a Gamry Instruments CMS300 impedance system interfaced to a personal computer. The permeation cell used is very similar to that shown by Hou et al[7] and is schematically depicted in the inset of Figure 7.4a in the article. The membrane was first mounted between two half U-tubes by using two O-rings to create a water-tight seal. The exposed diameter of the membrane is 20 mm. An Ag/AgCl/saturated KCl reference electrode and a gold substrate counter electrode were placed in one half U-tube and a gold substrate working electrode was placed in the other half U-tube. 50 ml of a pH buffer solution, prepared as described above was poured into each of the half tubes. The measurements were made at the open circuit potential with a 5 mV ac perturbation. All data were collected in the range from 10^{4} to 10^{-1} Hz using 10 points per decade and were fit with an equivalent circuit model to determine resistance and capacitance values. The equivalent circuit model contained the following elements in series: a solution resistance, a parallel combination of capacitance along with resistance and Warburg impedance to each represent the polymer skin of the membrane, and an interfacial capacitance at the gold working electrode. The Warburg impedance is related to diffusion-limited ion transport through the membrane.[26] At each pH value, sufficient time was allowed to make sure that the film reached a stable state as evidenced by the accumulation of repeated spectra

that did not change with time. Reported values and ranges for resistance and capacitance represent the average and standard deviation of values obtained from at least three independent sample preparations.

Results and Discussion

Figure 7.1 shows the strategy we have developed to prepare pH- responsive membrane skins. First, we deposit a thin layer of chromium (1.5 nm) followed by gold (20 nm) onto the feed side of alumina membranes with 20 nm pore sizes. A top-view SEM image (Figure 7.2b) shows that the pores are still open after the gold deposition, as further verified by EIS and UV-Vis. Next, copolymer films are then grown selectively from the gold surface by immersion of the entire membrane in an ether solution at 0 ˚C containing 2 mM diazomethane (DM) and 160 mM ethyl diazoacetate (EDA) for 24 h to yield a film with ester side chains (Figure 7.1). Figure 7.2c shows the PM-CO2Et coated membrane, and Figure 7.2d demonstrates a cross-sectional SEM image of a typical membrane construction. The bright clusters on the membrane surface in Figure 7.2d are gold, which exists at the outer periphery of the pores. From Figure 7.2d, the average thickness of the polymer skin from 10 different sites on the surface is ~100 nm. The PM-CO2Et film only grows from the gold surface as evidenced by the open interiors of the pores. We have placed the bare alumina support into the same solution containing both DM and EDA and found that no polymerization occurred. Alumina is not an appropriate catalytic surface for promoting the polymerization of diazo molecules whereas gold[27] and atomically modified gold[28] surfaces are very effective catalysts.

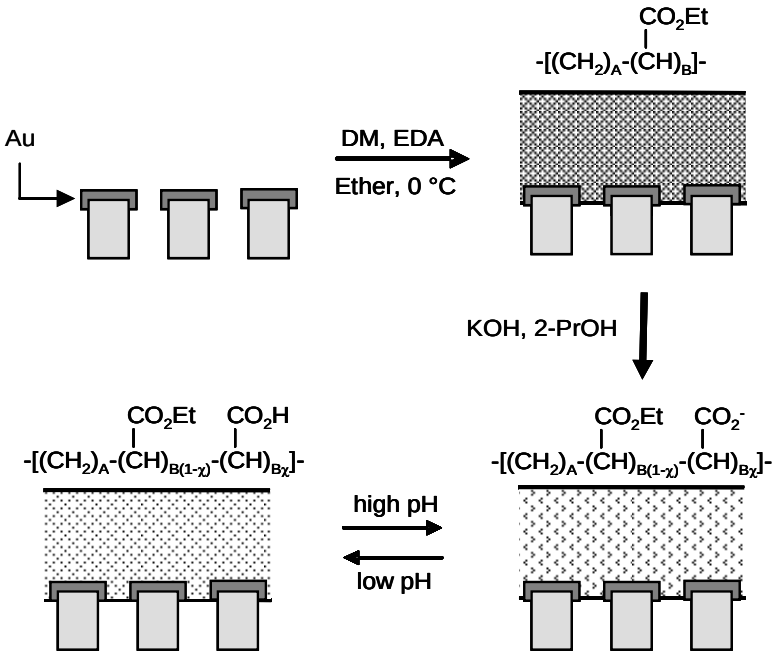

Figure 7.1. The preparation of pH-responsive copolymer films on gold-coated alumina membranes.

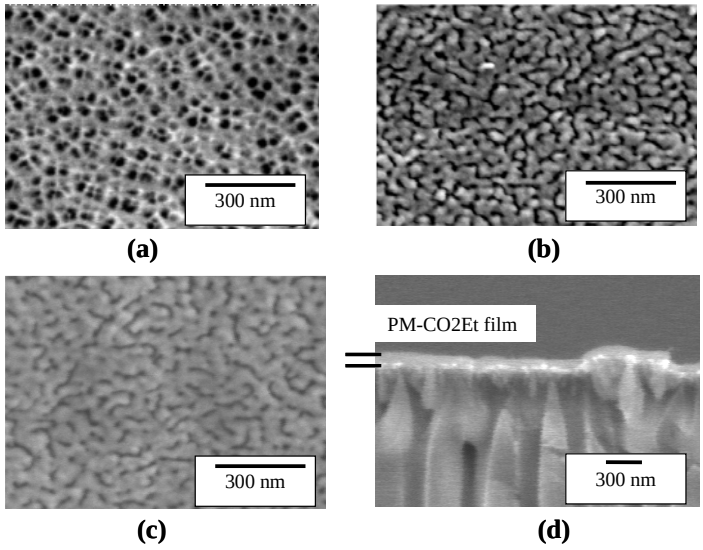

Figure 7.2. SEM images of the feed side of porous alumina (a) before Au deposition (b) after deposition of 20 nm Au and (c) after copolymer growth; (d) shows a cross-sectional image of the membrane from (c).

In the final step of Figure 7.1, the ester side chains within the film are hydrolyzed to carboxylate in a solution of 0.1 M KOH in 2-propanol at 75 ºC for 3 h to prepare a pH-responsive membrane skin. To investigate the ester and carboxylate acid content within the copolymer film after hydrolysis, we performed reflectance-absorption infrared spectroscopy (RAIRS) on a 2D flat silicon surface coated with the same amount of Cr

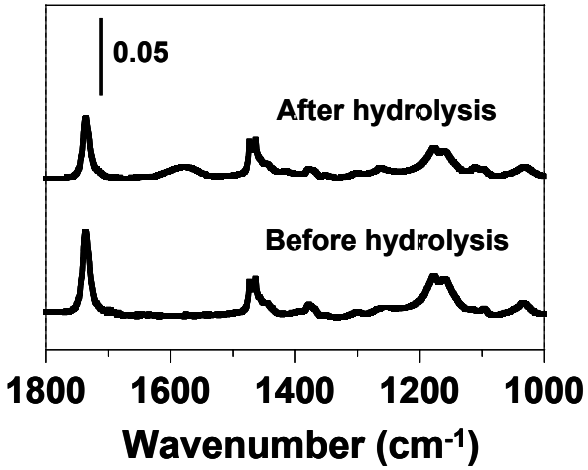

Figure 7.3. Reflectance-absorption IR spectra of copolymer films on 2D surface before and after hydrolysis. The 2D flat silicon wafer was coated with the same amount of Cr and Au and exposed to the same polymerization and hydrolysis conditions as the alumina membranes were.

and Au and exposed to the same conditions of 2 mM DM and 160 mM EDA for 24 h in ether solution at 0 ºC. As shown in Figure 7.3, the ester carbonyl group, represented by a peak at 1735 cm^{-1} in the spectrum for the pre-hydrolysis film, is diminished after hydrolysis, and new peak appears corresponding to the carbonyl stretching vibration in CO_2^- (1560 cm^{-1}). The ester content within the copolymer film is 1.6%, and upon hydrolysis, the conversion (χ) of the ester to carboxylic acid is ~25%. Thus, the final

acid content within the film is ~0.4%. Higher conversion can be obtained by increasing KOH concentration and the hydrolysis time, but these conditions may also damage the

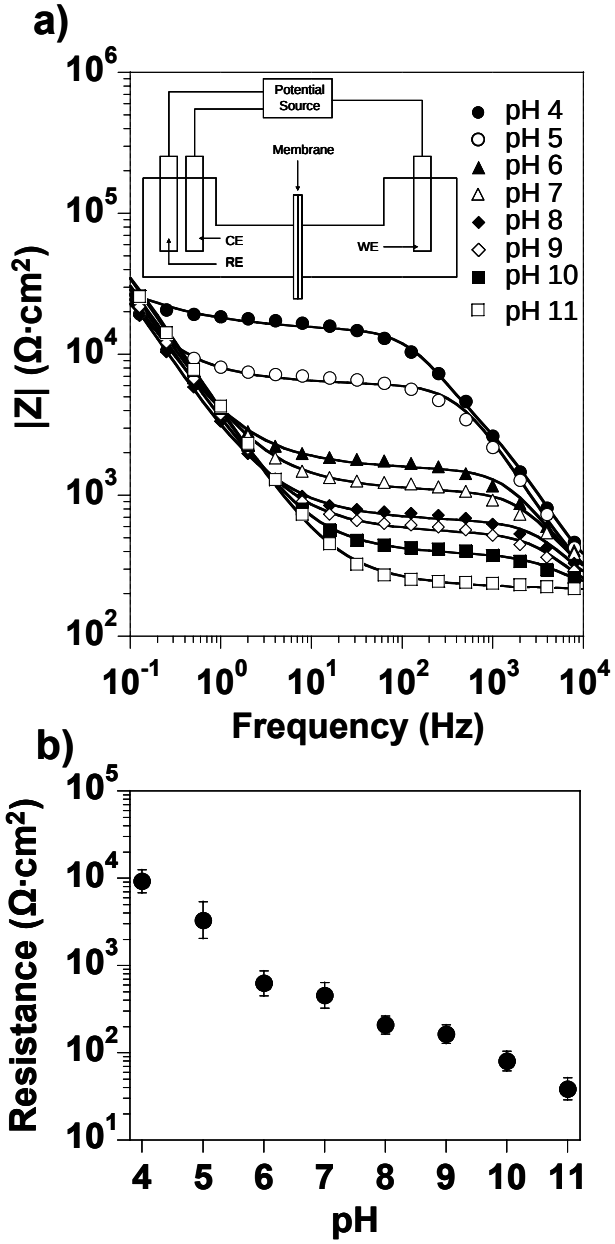

Figure 7.4. a) Electrochemical impedance spectra in the form of Bode plots as a function of pH for membrane skins. The inset shows a schematic of the U-tube test cell with counter electrode (CE), reference electrode (RE), and working electrode (WE). b) Membrane resistance as a function of pH.

alumina membrane. More information on the hydrolysis kinetics and IR spectra of the hydrolyzed copolymers on 2D surfaces can be found in our recent articles.[24,25]

To investigate the response of the polymer skins to pH, we obtained electrochemical impedance spectra (Figure 7.4a) for the PM-CO2H-coated alumina membrane supported between two halves of a U-tube filled with pH buffer solution (see inset of Figure 7.4a). Solid curves in the plot represent best fits of the data with an appropriate equivalent circuit model to provide quantitative information on the effect of pH on membrane properties. Figure 7.4b shows that the average membrane resistance decreases as pH is increased. The membrane resistance decreases from ~10^4 Ω·cm^2 at pH 4 to ~500 Ω·cm^2 at pH 6, and then gradually decreases to ~50 Ω·cm^2 at pH 11, suggesting a small but measurable barrier to ion transfer. This resistance at pH 11 corresponds to an impedance that is only 28% higher than that for a gold-coated membrane without the polymer skin. The film response to pH is reversible as evidenced by obtaining similar membrane resistances (within 10%) upon first decreasing pH incrementally from 11 to 4 and then increasing pH incrementally from 4 back to 11.

The response of the film can be related to its composition, as determined by RAIRS analysis of copolymer films on a 2D surface with 0.4% acid content at each pH increment between 4 and 11; Figure 7.5 shows the CO_2^- to CH_2 (both asymmetric and symmetric) stretching peak ratio within the films as a function of pH. Since the CH_2 stretching peak area does not change, the ratios here reflect the relative concentration of carboxylate within the film. From pH 4 to 6, a slight increase in CO_2^- content corresponds with a dramatic 20-fold reduction in membrane resistance (Figure 7.4b). The initial deprotonation of groups in the film has a profound effect on water and ion

transport, likely leading to some interconnected pathways for ion conduction. As pH is increased from 6 to 11, the CO_2^- content increases in a nearly linear manner and membrane resistance drops by another factor of 10, exhibiting a more gradual decay with pH. These results suggest that a percolation threshold[29] is achieved at lower pH and that further increases in pH enhance the density of ion conducting pathways. Over the entire range of pH (4 to 11), the resistance drops by a factor of 200 but is recovered upon decreasing pH back to 4. The pH response of the membrane skins (factor of 200) is less than that for similar films grown from 2D gold surfaces (factor of 10^5)[25] because of the lower resistance (10^4 vs 10^7 Ω cm^2) of the skins at low pH. We attribute this effect to grain boundaries within the skin (see Figure 7.2c) imparted by surface-initiated growth from the pore-laden surface.

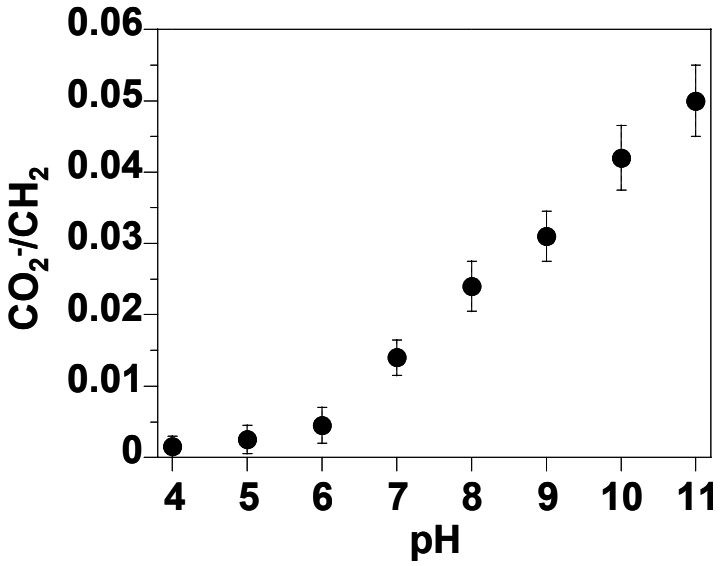

Figure 7.5. The peak area ratio of the carboxylate stretching band at 1560 cm^{-1} to the sum of the asymmetric (2919 cm^{-1}) and symmetric (2851 cm^{-1}) methylene stretching bands as a function of pH for a film with acid content of 0.4 % grown from a 2D gold surface.

Our approach yields a thin polymer skin covering the pores at one end of the membrane but leaves the pores empty to enable further functionalization. In related work, Steinle et al[5] have modified the alumina pores with a carboxyl-terminated silane monolayer that yields a decrease of over 4 orders of magnitude in membrane resistance when the membrane is switched from "off" to "on" with increasing pH. Thus, our approach could be used in conjunction with such strategies for modifying pores to prepare membranes with pH-responsive surface and bulk properties.

Conclusions

In summary, surface-catalyzed polymerization enables selective growth on gold surfaces of any shape, provides a precise control over film thickness,[24] and offers the ability to tune the concentration of the pH-sensitive groups within the film.[25] In this particular application, we have prepared pH-responsive PM-CO2H films atop a porous alumina support by a surface-catalyzed polymerization and subsequent hydrolysis. Film resistances decrease by a factor of 200 between pH 4 and pH 11, demonstrating the effect of pH and charge on film hydrophobicity. The surface-catalyzed growth of the pH-responsive copolymer film on a porous membrane support provides a new way to prepare composite membranes.

References

1. Fu, Q.; Rao, G. V. R.; Ista, L. K.; Wu, Y.; Andrzejewski, B. P.; Sklar, L. A.; Ward, T. L.; Lopez, G. P. "Control of Molecular Transport through Stimuli-Responsive Ordered Mesoporous Materials," *Advanced Materials* **2003**, *15*, 1262-1266.

2. Reber, N.; Kuchel, A.; Spohr, R.; Wolf, A.; Yoshida, M. "Transport Properties of Thermo-Responsive Ion Track Membranes," *Journal of Membrane Science* **2001**, *193*, 49-58.

3. Chu, L. Y.; Zhu, J. H.; Chen, W. M.; Niitsuma, T.; Yamaguchi, T.; Nakao, S. "Effect of Graft Yield on the Thermo-Responsive Permeability through Porous Membranes with Plasma-Grafted Poly (N-Isopropylacrylamide) Gates," *Chinese Journal of Chemical Engineering* **2003**, *11*, 269-275.

4. Lin, S. Y.; Lin, H. L.; Li, M. J. "Adsorption of Binary Liquid Crystals onto Cellulose Membrane for Thermo-Responsive Drug Delivery," *Adsorption* **2002**, *8*, 197-202.

5. Steinle, E. D.; Mitchell, D. T.; Wirtz, M.; Lee, S. B.; Young, V. Y.; Martin, C. R. "Ion Channel Mimetic Micropore and Nanotube Membrane Sensors," *Analytical Chemistry* **2002**, *74*, 2416-2422.

6. Lee, S. B.; Martin, C. R. "pH-Switchable, Ion-Permselective Gold Nanotubule Membrane Based on Chemisorbed Cysteine," *Analytical Chemistry* **2001**, *73*, 768-775.

7. Hou, Z. Z.; Abbott, N. L.; Stroeve, P. "Self-Assembled Monolayers on Electroless Gold Impart pH-Responsive Transport of Ions in Porous Membranes," *Langmuir* **2000**, *16*, 2401-2404.

8. Geismann, C.; Ulbricht, M. "Photoreactive Functionalization of Poly(Ethylene Terephthalate) Track-Etched Pore Surfaces With "Smart" Polymer System's," *Macromolecular Chemistry and Physics* **2005**, *206*, 268-281.

9. Ngila, J. C.; Ddamba, W. A. A. "Studies of Difurylmethane-Maleic Anhydride Copolymer as an Ion-Responsive Membrane for the Determination of Mono-, Di- and Tri-Valent Cations," *Macromolecular Symposia* **2001**, *165*, 73-81.

10. Okajima, S.; Yamaguchi, T.; Sakai, Y.; Nakao, S. "Regulation of Cell Adhesion Using a Signal-Responsive Membrane Substrate," *Biotechnology and Bioengineering* **2005**, *91*, 237-243.

11. Kwok, C. S.; Mourad, P. D.; Crum, L. A.; Ratner, B. D. "Self-Assembled Molecular Structures as Ultrasonically-Responsive Barrier Membranes for

Pulsatile Drug Delivery," *Journal of Biomedical Materials Research* **2001**, *57*, 151-164.

12. Pile, D. L.; Zhang, Y.; Hillier, A. C. "Electrochemically Modulated Permeability of Poly(Aniline) and Composite Poly(Aniline)-Poly(Styrenesulfonate) Membranes," *Langmuir* **2006**, *22*, 5925-5931.

13. Zhang, K.; Wu, X. Y. "Modulated Insulin Permeation across a Glucose-Sensitive Polymeric Composite Membrane," *Journal of Controlled Release* **2002**, *80*, 169-178.

14. Masawaki, T.; Taya, M.; Tone, S. "Evaluation of Molecular Weight Cut-Off Profiles of pH-Responsive Ultrafiltration Membranes Prepared under Various Casting Conditions," *Journal of Chemical Engineering of Japan* **1996**, *29*, 180-183.

15. Masawaki, T.; Sato, H.; Taya, M.; Tone, S. "Molecular-Weight Cutoff Characteristics of pH-Responsive Ultrafiltration Membranes against Macromolecule Solution," *Kagaku Kogaku Ronbunshu* **1993**, *19*, 620-625.

16. Balachandra, A. M.; Baker, G. L.; Bruening, M. L. "Preparation of Composite Membranes by Atom Transfer Radical Polymerization Initiated from a Porous Support," *Journal of Membrane Science* **2003**, *227*, 1-14.

17. Sun, L.; Baker, G. L.; Bruening, M. L. "Polymer Brush Membranes for Pervaporation of Organic Solvents from Water," *Macromolecules* **2005**, *38*, 2307-2314.

18. Liu, C.; Martin, C. R. "Composite Membranes from Photochemical-Synthesis of Ultrathin Polymer-Films," *Nature* **1991**, *352*, 50-52.

19. Hayakawa, Y.; Terasawa, N.; Hayashi, E.; Abe, T. "Plasma Polymerization of Cyclic Perfluoroamines and Composite Membranes for Gas Separation," *Journal of Applied Polymer Science* **1996**, *62*, 951-954.

20. Hammond, P. T. "Form and Function in Multilayer Assembly: New Applications at the Nanoscale," *Advanced Materials* **2004**, *16*, 1271-1293.

21. Malaisamy, R.; Bruening, M. L. "High-Flux Nanofiltration Membranes Prepared by Adsorption of Multilayer Polyelectrolyte Membranes on Polymeric Supports," *Langmuir* **2005**, *21*, 10587-10592.

22. Yanagishita, H.; Kitamoto, D.; Haraya, K.; Nakane, T.; Okada, T.; Matsuda, H.; Idemoto, Y.; Koura, N. "Separation Performance of Polyimide Composite Membrane Prepared by Dip Coating Process," *Journal of Membrane Science* **2001**, *188*, 165-172.

23. Hoshi, M.; Kobayashi, M.; Saitoh, T.; Higuchi, A.; Nakagawa, T. “Separation of Organic Solvent from Dilute Aqueous Solutions and from Organic Solvent Mixtures through Crosslinked Acrylate Copolymer Membranes by Pervaporation,” *Journal of Applied Polymer Science* **1998**, *69*, 1483-1494.

24. Bai, D.; Jennings, G. K. “Surface-Catalyzed Growth of Polymethylene-Rich Copolymer Films on Gold,” *Journal of the American Chemical Society* **2005**, *127*, 3048-3056.

25. Bai, D. S.; Habersberger, B. M.; Jennings, G. K. “pH-Responsive Copolymer Films by Surface-Catalyzed Growth,” *Journal of the American Chemical Society* **2005**, *127*, 16486-16493.

26. Bard, A.; Faulkner, L. *Electrochemical Methods Fundamentals and Applications;* John Wiley & Sons: New York, 2000.

27. Seshadri, K.; Atre, S. V.; Tao, Y. T.; Lee, M. T.; Allara, D. L. “Synthesis of Crystalline, Nanometer-Scale, -(Ch2)(X)- Clusters and Films on Gold Surfaces,” *Journal of the American Chemical Society* **1997**, *119*, 4698-4711.

28. Guo, W. F.; Jennings, G. K. “Use of Underpotentially Deposited Metals on Gold to Affect the Surface-Catalyzed Formation of Polymethylene Films,” *Langmuir* **2002**, *18*, 3123-3126.

29. Mohanty, K. K.; Ottino, J. M.; Davis, H. T. “Reaction and Transport in Disordered Composite Media - Introduction of Percolation Concepts,” *Chemical Engineering Science* **1982**, *37*, 905-924.

CHAPTER VIII

pH-RESPONSIVE RANDOM COPOLYMER FILMS WITH AMINE SIDE CHAINS

Introduction

The two most common types of pH-responsive films are polyacids and polybases. Polyacids such as poly(acrylic acid) (PAAc), are protonated or uncharged at low pH and deprotonated or negatively charged at high pH, while polybases such as poly(N,N'-dimethyl aminoethyl methacrylate) are neutralized at high pH and positively charged at low pH.[1] The appropriate and active pH range should be considered for desired applications.

In Chapter V, we reported the design of a new class of pH-responsive polymer films on gold surfaces by first developing a controlled, surface-catalyzed polymerization in the presence of diazomethane (DM) and ethyl diazoacetate (EDA) to prepare a copolymer film consistent with poly(methylene-*co*-ethyl acetate) and subsequently hydrolyzing the ester side chains to varying extents to yield carboxylic acids (denoted as PM-CO2H) (Scheme 1-Steps 1 and 2).[2,3] These films are predominately hydrophobic but contain a controlled, dilute fraction (1-4%) of carboxylic acid groups to exhibit a huge change in barrier properties when the pH is increased sufficiently to ionize the acid groups. We have shown that at a 1% - 4% molar acid content, the copolymer film exhibits a five order of magnitude change in its resistance to ion transport over 2 – 3 pH units.[3] The onset pH at which this response initiates can be tailored from pH 5 to 10 by decreasing the acid content in the film from 4% to 1%.

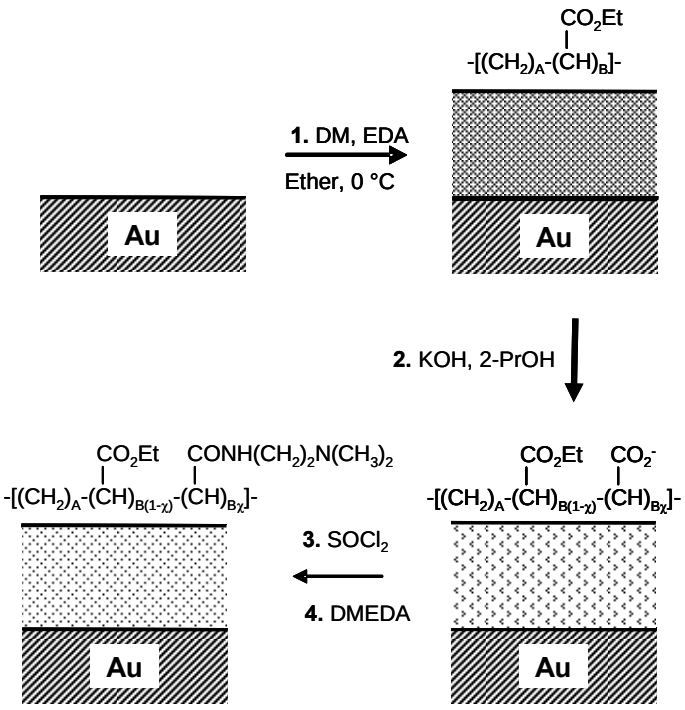

Figure 8.1. Preparation of the PM-rich copolymer films with dilute, randomly distributed amine side chains.

In this chapter, we report the preparation of pH-responsive copolymer films with dimethylamine-terminated side chains PM-CONHR (R represents $–CH_2CH_2N(CH_3)_2$) (Figure 8.1) and compare their pH-responsive behavior with that of PM-CO2H. The PM-CONHR films are prepared by modification of carboxylic acid groups within PM-CO2H films by thionyl chloride to create acid chlorides (PM-COCl; Figure 8.1-Step 3) and further by N,N-dimethylethylenediamine (DMEDA) to generate amide-linked, amine-terminated side groups that are pH active (PM-CONHR; Figure 8.1-Step 4). Both of

these steps proceed with complete conversion, as assessed by reflectance-absorption infrared spectroscopy. Since primary amines react much faster than tertiary amines with acid chloride to form amide,[4] the tertiary amines remain intact after step 4 and function as the pH-responsive moiety as shown in Figure 8.1. Because alkyl amides have very low pKa, for example, acetamide has a pKa of 0.63,[5] the amide groups within the film are uncharged for the whole pH range (pH 4 to pH 11) in this study and do not affect the response of the film.

Since amines have an opposite protonation/deprotonation trend with pH as compared to that of carboxylic acids, the PM-CONHR films prepared here should become increasingly charged, and as a result, more permeable to water and ions as pH is reduced. This reverse response in pH could be useful for targeted, pH-specific swelling and transport, and in combination with PM-CO2H, could provide a broader range of pH sensitivity. In addition, our ability to measure barrier properties of the films with different functional side groups may promote a fundamental understanding of the effect of film composition on response.

Experimental Procedures

Preparation of Polymer Films

Polymer films were prepared by exposure of gold-coated silicon substrates to ether solutions containing 0.3 mM DM and 80 mM EDA at 0 °C for 16 h. Film growth was carried out in capped 20 mL vials, and only one substrate was placed in each vial. Upon removal, the samples were rinsed with ether and ethanol and dried in a stream of

nitrogen. The resulting PM-CO2Et film was 100 nm thick and contained 3.6% (molar) of the ethyl ester group.

Hydrolysis of Polymer Films

Hydrolysis of the copolymer films was carried out in capped 20 mL vials of 0.2 M KOH in 2-propanol at 75 °C for 1 and 4 h to obtain copolymer films with 1% and 3% acid contents, respectively. Only one substrate was placed in each vial. The hydrolyzed samples were rinsed with ethanol and DI water and dried in a N_2 stream.

Preparation of PM-CONHR Films

After hydrolysis, each sample was immersed into 0.5 mM $SOCl_2$ in ether solution for 24 h at room temperature. After the reaction, the samples were rinsed with ether and immediately placed into 50 mM DMEDA, n-butyl amine, or a mixture of both with total concentration of 50 mM in ether or into 50 mM ethylamine in tetrahydrofuran for 24 h at room temperature. Upon removal, the samples were rinsed with ether, ethanol, and DI water and dried in a stream of nitrogen.

Results and Discussion

Preparation of PM-CONHR Films

Upon exposure of gold substrates to 0.3 mM DM and 80 mM EDA in ether at 0 °C for 16 h, PM-CO_2Et films with ester content of 3.6% and film thickness of 100 nm are grown from the surface. RAIR spectra for this film (Figure 8.2) shows C=O stretching at

1735 cm^{-1}, and C-O stretching from 1000-1300 cm^{-1}. After exposure of PM-CO2Et to a 2-propanol solution of 0.2 M KOH at 75 ºC for 4 h, ~80% of the ester groups are hydrolyzed to carboxylates (CO_2^-) as evidenced by the diminution of the ester carbonyl peak at 1735 cm^{-1}, and the appearance of new peaks corresponding to the carbonyl stretching vibration in CO_2^- (1560 and 1420 cm^{-1}) at pH 11. Details on the polymerization and hydrolysis kinetics can be obtained from Chapter IV and V.[2,3]

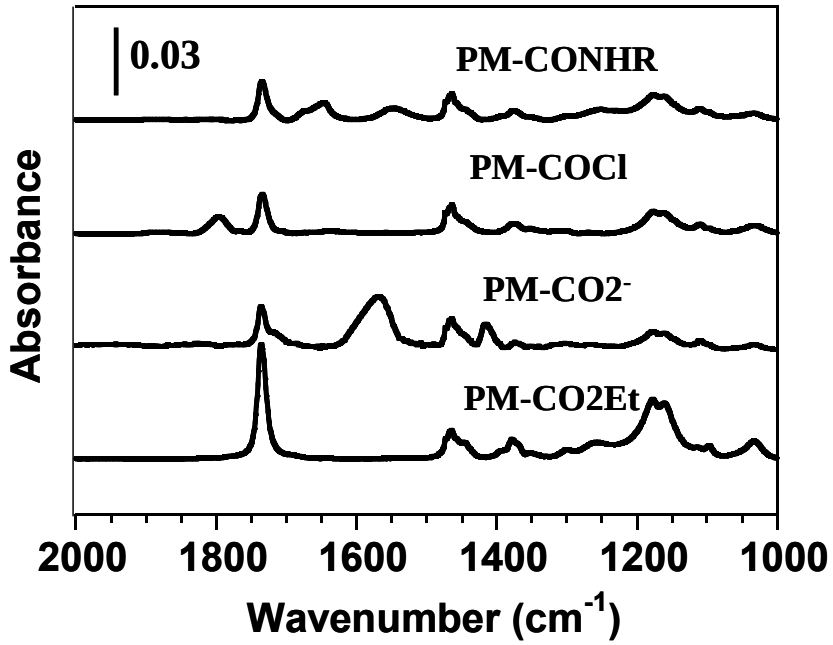

Figure 8.2. RAIR spectra of the PM-rich copolymer films after hydrolysis, treatment with $SOCl_2$, and reaction with DMEDA.

The PM-$CO2^-$ films were treated with 0.5 M thionyl chloride in ether for 24 h to completely convert carboxylates to acid chlorides (PM-COCl), supported by disappearance of the carbonyl stretching vibration in CO_2^- (1560 and 1420 cm^{-1}) and

CO2H (shoulder at 1710 cm^{-1}) and the appearance of a new peak corresponding to C=O stretching within the acid chloride at 1809 cm^{-1}.[6] The PM-COCl films were then immersed into a 50 mM DMEDA solution to convert acid chlorides to amide-linked dimethylamine side chains (PM-CONHR). Complete conversion of PM-COCl to PM-CONHR is indicated by the disappearance of the peak at 1809 cm^{-1} and the appearance of the Amide I peak from amide C=O stretching and the Amide II peak from N-H bending at 1640 and 1540 cm^{-1}, respectively. Others have performed similar experiments to attach amines within polymer films and showed similar peak changes in IR spectra.[7-12] The complete conversion of carboxylates within the film to amides through two steps demonstrates the effectiveness of this synthetic approach for modifying polymer thin films. The hydrolysis and subsequent treatments do not affect the hydrocarbon crystallinity within the film based on the similar peak positions and intensities for asymmetric (2919 cm^{-1}) and symmetric (2851 cm^{-1}) CH_2 stretching (not shown) in all four spectra.

pH-Responsive Barrier Properties

We have used EIS to measure the effect of pH on the barrier properties of PM-CONHR films upon exposure to pH buffer solutions without redox probes. Figure 5.4.a shows a model that is commonly used for polymer-coated metals,[13] which contains two time constants, one due to the polymer film and one due to the polymer-metal interface. The following terms are used to denote various film and solution characteristics: solution resistance, R_s; interfacial capacitance, C_i; interfacial resistance, R_i; film capacitance, C_f; film resistance, R_f; and Warburg impedance, Z_w. Under certain conditions, the model can

be simplified to a one constant model as we have discussed previously.[3] One simplification to the circuit in Figure 5.4.a for the present study is that R_i is effectively infinite since no redox probes are present to transfer charge at the electrode; thus, we do not expect to observe a resistance due to the polymer/metal interface in the spectra.

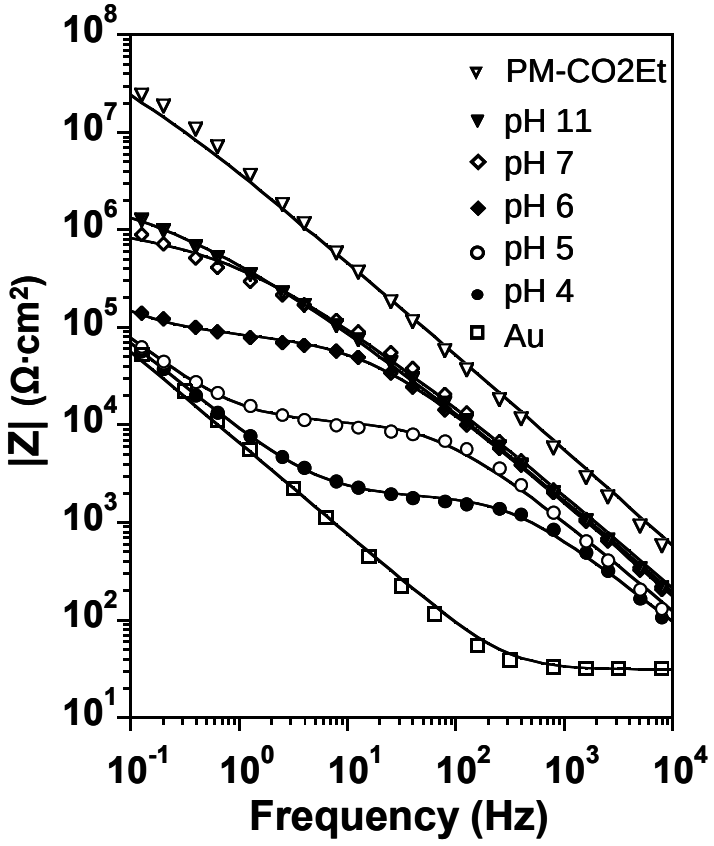

Figure 8.3. Electrochemical impedance spectra in the form of Bode plots as a function of pH for a 100 nm PM-CONHR film with 1% amine content on gold. Spectra for uncoated gold and a PM-CO2Et film are shown for comparison.

To demonstrate the effect of pH on film barrier properties, Figure 8.3 shows impedance spectra in the form of Bode plots for a 100 nm PM-CONHR film on gold with 1% molar amine content. Solid curves in the plot represent best fits of the data using

appropriate equivalent circuit models to provide quantitative information on the effect of pH on film capacitance and resistance. For comparison, the spectrum for bare gold exposed to pH 11 buffer solution is also shown. Since no redox probes are in solution, the spectrum for bare gold is dominated by a double-layer capacitance of ~10^{-5} F/cm^2 from 0.1 – 100 Hz and a solution resistance at high frequencies. Changing solution pH had negligible effect on the spectrum for bare gold. As a second comparison, the spectrum for an unhydrolyzed PM-CO2Et copolymer film on gold at pH 4 is also shown. Changing solution pH from 4 to 11 had negligible effect on the spectrum for PM-CO2Et since no pH-responsive groups are present within the film. The unhydrolyzed polymer film exhibits a straight line of slope -1 with high impedance (>10^7 Ω cm^2) at low frequency, indicating a strong barrier against ion penetration.[14-17]

The impedance spectrum of the PM-CONHR film changes in a pH-dependent manner. From pH 11-7, the film is in the neutral state and provides a moderately strong barrier against ion transfer. However, the impedance of the PM-CONHR film is far below that of a 1% PM-CO2H film that shows very close film impedance to that of the PM-CO2Et film at low pH.[3] The K_{ow} of the tertiary ethyl amine side chain (-CONHR, R=$CH_2CH_2N(CH_3)_2$) is around $10^{-2.28}$ [18] which is an order of magnitude lower than that of -CO2H ($10^{-1.11}$); therefore, even in the uncharged state, more water should be present within the amine film to reduce its barrier properties. From pH 11 to pH 7, the impedance spectra show little change, if any, suggesting that the amines remain in the neutral state at these conditions, but as pH is decreased from 7 to 6, the impedance at low frequency decreases. The increasing charge of the film with decreasing pH results in markedly reduced film resistance such that two time constants appear in the impedance

spectrum. The time constant at lower frequencies is from the interfacial capacitance and the one at higher frequencies is from the polymer film and corresponds to the combined capacitance and resistance of the film.[14,19,20] This latter time constant provides an estimate of the time required for ionic permeation through the film; at pH 6, ~0.1 s. As pH is decreased from 5 to 4, the film resistance decreases further and the time required for ions to reach the interfacial region (~0.005 s) becomes even shorter.

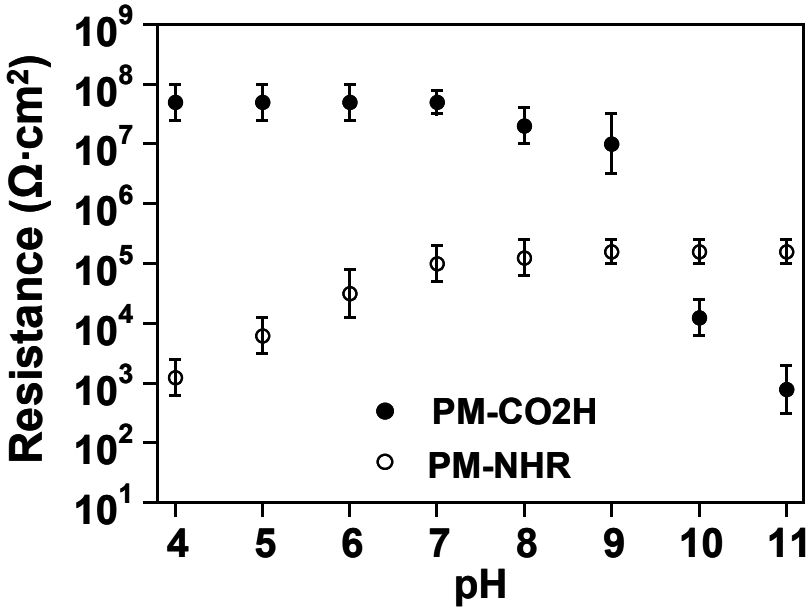

Figure 8.4. pH-Dependent film resistance for a 100 nm film with 1% amine content (PM-NHR) and 75 nm film with 1% acid content (PM-CO2H).

We plot the film resistance of this PM-CONHR film together with that of the PM-CO2H film (75 nm, 1% COOH) from our recent paper in Figure 8.4. As expected, although these two films have similar thickness and concentration of the ionizable group, we observe opposite pH-responsive behavior between the PM-CO2H and PM-CONHR films since they have opposite deprotonation/protonation behavior with the changes in

pH. The PM-CO2H film exhibits high R_f at low pH, and the film resistance decreases with increasing pH from pH 8 to 11. On the other hand, the PM-CONHR film shows moderate R_f at high pH and gradually loses its R_f from pH 7 to pH 4. Although both films show resistance to ion penetration in their less charged state, the R_f of PM-CONHR film (~2×10^5 from pH 11 to 7) is over 2 orders of magnitude lower than that of the PM-CO2H film due to its reduced hydrophobicity as mentioned above. Because of this lower resistance in the neutral state, the overall response of the PM-CONHR film is only 2 orders of magnitude, less than that of 5 orders of magnitude for the PM-CO2H film.

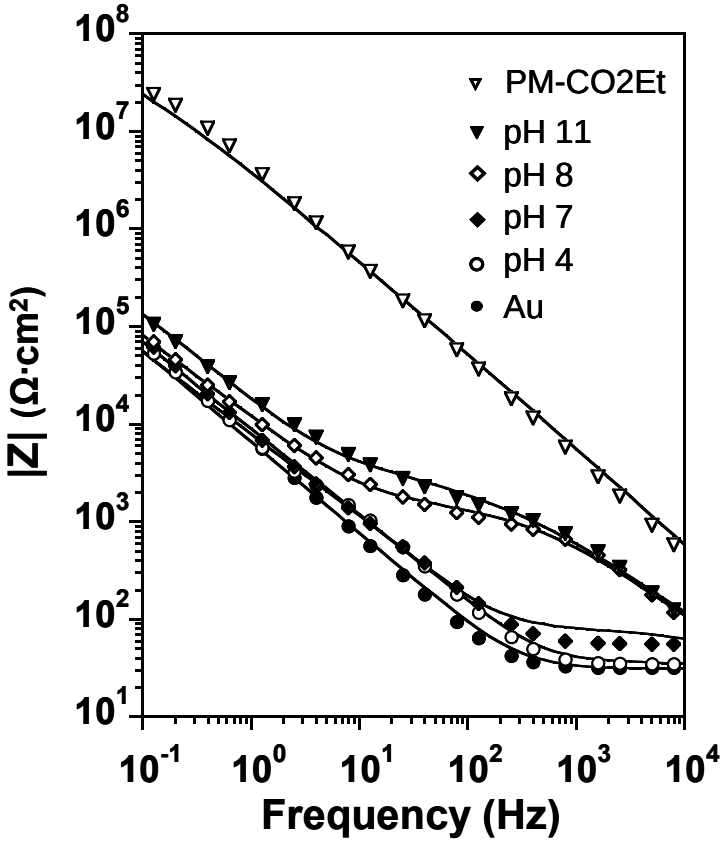

Figure 8.5. Electrochemical impedance spectra in the form of Bode plots as a function of pH for a 100 nm PM-CONHR film with 3% amine content on gold. Spectra for uncoated gold and an unhydrolyzed PM-CO2Et film are shown for comparison.

To investigate the effect of amine concentration on the pH-responsive behavior of PM-CONHR, we also obtained impedance spectra for a 100 nm 3% PM-CONHR film in the form of Bode plots (Figure 8.5). From pH 11 to 8, unlike the more hydrophobic 1% amine film at high pH values, two time constants appear in the spectra. Again, the high frequency time constant is due to the polymer film and the low frequency time constant is due to the capacitance at the polymer/metal interface. At a level of 3% amine, the PM-CONHR film is too hydrophilic and allows rapid transfer of ions, even in the neutral state (pH 8 -11). From pH 6 to pH 4, the film provides no measurable resistance against ion transport, so only R_s was shown in Figure 8.6 below. Spectra at these pH values converge at low to moderate frequencies due to similar C_i, which suggests similar water and ion content near the film/electrode interface.[21]

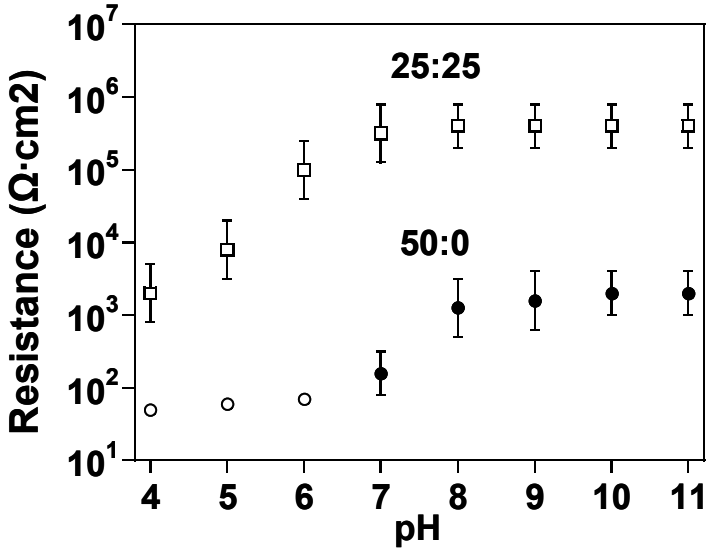

Figure 8.6. pH-Dependent film resistance after exposure of a 100 nm PM-COCl (3%) film to 50 mM DMEDA or 25 mM DMEDA+25 mM n-butyl amine. Open squares represent R_f of the film obtained from 25 mM n-butyl amine and 25 mM DMEDA, and solid and open circles represent R_f and R_s respectively, for the film modified by 50 mM DMEDA.

Another possible way to modulate the hydrophobicity of the PM-CONHR film is by capping the acid chloride side chains of PM-COCl with compounds that will not exhibit a pH response. Here, we used n-butyl amine to form amide linkages upon reaction with the acid chloride group but without the tertiary amine groups on the opposite end. Figure 8.6 shows the effect of pH on the resistance of the PM-CONHR film (3%) and a film prepared through partial pH-inert capping of the PM-COCl by exposure to a solution containing 25 mM n-butyl amine and 25 mM DMEDA. The film prepared by partial capping of n-butyl amine exhibits an enhancement in film resistance from ~10^3 to ~$10^{5.5}$ $\Omega \cdot cm^2$ from pH 4 to pH 7. The resistances of the film partially capped with butyl amine at each pH are slightly higher than that of the 1% PM-CONHR film shown in Figure 8.4. Since a film completely capped with n-butyl amine shows a film resistance very close to that of PM-CO2Et, the increase in film resistance for the partially capped film is due to reduced tertiary amine content within the film; in this case, the tertiary amine content within the film is likely less than 1%, suggesting that n-butyl amine reacted more extensively within the film than did DMEDA. The linear molecular structure of the n-butyl amine likely facilitates its transport through the film to more efficiently cap the acid chloride. The enhanced film hydrophobicity due to hydrophobic capping also requires a more aggressive solution condition (higher H^+ concentration) to trigger the onset of the pH response; as evidence, the pH response begins between pH 6-7, rather than pH 7-8 for the uncapped film.

Capping a 1% film with n-butyl amine also changes the range of the pH response. We first exposed PM-COCl to different concentration ratios of DMEDA to n-butyl amine to vary the hydrophobicity within the film. When we use 50 mM of DMEDA alone

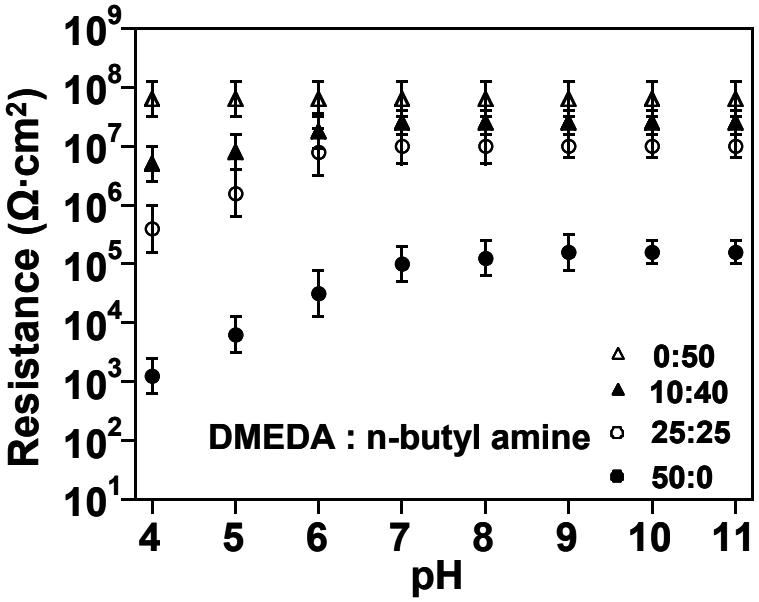

Figure 8.7. pH-Dependent film resistance for a 100 nm film with 1% amine content with/without acid chloride partially capping with n-butyl amine. Total amine concentration is 50 mM.

without n-butyl amine, the pH response begins at pH 7 and the change in film resistance is two orders of magnitude from pH 7 to pH 4. When the concentration ratio is equimolar (25 mM:25 mM) or biased toward butyl amine (10 mM:40 mM), the film resistances for the entire pH range are increased by up to 3.5 orders of magnitude due to the increase of film hydrophobicity, and the pH response begins at pH 6 as pH is reduced from 11 to 4. Consistent with our analysis of the pH-dependence of PM-CO2H films, a more hydrophobic film (less tertiary amine) requires a stronger solution condition (lower pH) to measurably reduce the barrier properties of the film. If we cap the acid chloride side chains completely with n-butyl amine, the film does not exhibit pH-responsive behavior, verifying that the amide groups within the film are uncharged from pH 4 to pH 11 and do not affect the pH-responsive behavior of the film. The film resistance of 6×10^7

$\Omega \cdot cm^2$ is very close to that of the unmodified PM-CO2Et film (8×10^7 $\Omega \cdot cm^2$), indicating that the reactive processing of this film does not degrade its barrier properties.

Effect of Film Hydrophobicity on Resistance

As suggested above, the hydrophilicity of the side chain component seems to greatly influence the resistance of the film against ion transfer. To investigate the effect of film hydrophilicity on film resistance in a more quantitative manner, we have recorded impedance spectra for 1% films with varying hydrophilicity of the side chain, as measured by the octanol-water partition coefficient (K_{ow}).[18] Figure 8.8 shows the measured resistance as a function of relative hydrophilicity (-log K_{ow}) of the functional side chains. In Figure 8.8, the resistances of PM-COO^- and PM-CONHR films were measured at pH 11, and all other resistances were measured at pH 4. The films with -CO2Et, -$CONHCH_2CH_3$ and -$CONH(CH_2)_3CH_3$ side chains are not pH-responsive over this range of pH. For the more hydrophobic side chains (-log K_{ow} < 2), the film resistance is insensitive to side chain hydrophobicity. In these cases, the impedance spectra are capacitive, and these films exhibit resistances that approach maximum values. As the side chain hydrophilicity is increased (-log K_{ow} > 2), the film resistance decreases by three orders of magnitude for the –CONHR side group (in the neutral state) and five orders of magnitude for the charged $–CO_2^-$ and $–CONHR^+$ side groups. These results suggest that a critical side chain hydrophilicity (-log K_{ow} ~ 2) exists for these predominately polymethylene (99%) copolymer films. A sufficiently hydrophilic side chain, even at 1% molar content, allows water and ion penetration, the latter of which is assessed by large changes in the impedance spectrum.

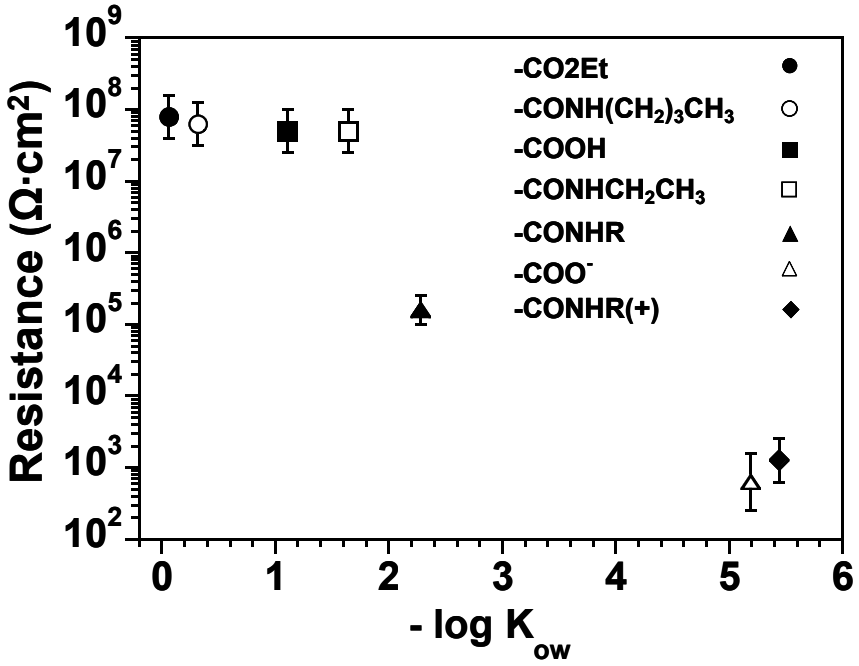

Figure 8.8. Film resistance as a function of the side chain hydrophilicity as measured by the octanol-water partition coefficient.

Conclusions

We have prepared pH-responsive, tertiary amine-containing polymethylene films by a surface-catalyzed polymerization and subsequent modification. The films are uncharged and predominately hydrophobic at high pH but become increasingly charged as pH is reduced to facilitate water and ion transfer. The film hydrophobicity is tunable by adjusting the concentration of active side chains or partially capping the acid chloride groups with pH-inert groups during the modification. This work implies that a critical side chain hydrophilicity exists to observe water and ion transfer. Appropriate molecular

design of the pH-active group within the film allows control over film resistance and the magnitude and range of the response in pH.

References

1. Gil, E. S.; Hudson, S. A. "Stimuli-Reponsive Polymers and Their Bioconjugates," *Progress in Polymer Science* **2004**, *29*, 1173-1222.

2. Bai, D. S.; Jennings, G. K. "Surface-Catalyzed Growth of Polymethylene-Rich Copolymer Films on Gold," *Journal of the American Chemical Society* **2005**, *127*, 3048-3056.

3. Bai, D. S.; Habersberger, B. M.; Jennings, G. K. "pH-Responsive Copolymer Films by Surface-Catalyzed Growth," *Journal of the American Chemical Society* **2005**, *127*, 16486-16493.

4. Morrison, R.T.; Boyd, R. N. *Organic Chemistry;* Ally and Bacon: Boston, 1987.

5. Schwarzenbach, R.; Gschwend, P.; Imboden, D. *Environmental Organic Chemistry*; Wiley: New York, 1993.

6. Silverstein, R. M.; Webster, F. X. *Spectrometric Identification of Organic Compounds*; John Wiley & Sons: New York, 1998.

7. Luo, N.; Husson, S. M.; Hirt, D. E.; Schwark, D. W. "Surface Grafting of Polyacrylamide from Polyethylene-Based Copolymer Film," *Journal of Applied Polymer Science* **2004**, *92*, 1589-1595.

8. Luo, N.; Stewart, M. J.; Hirt, D. E.; Husson, S. M.; Schwark, D. W. "Surface Modification of Ethylene-co-Acrylic Acid Copolymer Films: Addition of Amide Groups by Covalently Bonded Amino Acid Intermediates," *Journal of Applied Polymer Science* **2004**, *92*, 1688-1694.

9. Janorkar, A. V.; Luo, N.; Hirt, D. E. "Surface Modification of an Ethylene-Acrylic Acid Copolymer Film: Grafting Amine-Terminated Linear and Branched Architectures," *Langmuir* **2004**, *20*, 7151-7158.

10. Zhou, Y. F.; Bruening, M. L.; Bergbreiter, D. E.; Crooks, R. M.; Wells, M. "Preparation of Hyperbranched Polymer Films Grafted on Self-Assembled Monolayers," *Journal of the American Chemical Society* **1996**, *118*, 3773-3774.

11. Zhou, Y. F.; Bruening, M. L.; Liu, Y. L.; Crooks, R. M.; Bergbreiter, D. E. "Synthesis of Hyperbranched, Hydrophilic Fluorinated Surface Grafts," *Langmuir* **1996**, *12*, 5519-5521.

12. Bruening, M. L.; Zhou, Y. F.; Aguilar, G.; Agee, R.; Bergbreiter, D. E.; Crooks, R. M. "Synthesis and Characterization of Surface-Grafted, Hyperbranched Polymer Films Containing Fluorescent, Hydrophobic, Ion-Binding, Biocompatible, and Electroactive Groups," *Langmuir* **1997**, *13*, 770-778.

13. Brantley, E. L.; Holmes, T. C.; Jennings, G. K. “Modification of ATRP Surface-Initiated Poly(hydroxyethyl methacrylate) Films with Hydrocarbon Side Chains,” *Journal of Physical Chemistry B* **2004**, *108*, 16077-16084.

14. Loveday, D.; Peterson, P.; Rodgers, B. “Evaluation of Organic Coatings with Electrochemical Impedance Spectroscopy. Part 1: Fundamentals of Electrochemical Impedance Spectroscopy,” *JCT Coatings Technology* August **2004**, 46-52.

15. Park, S. M.; Yoo, J. S. “Electrochemical Impedance Spectroscopy for Better Electrochemical Measurements,” *Analytical Chemistry* **2003**, *75*, 455A-461A.

16. Loveday, D.; Peterson, P.; Rodgers, B. “Evaluation of Organic Coatings with Electrochemical Impedance Spectroscopy. Part 2: Application of EIS to Coatings,” *JCT Coatings Technology* October **2004**, 88-93.

17. Rammelt, U.; Reinhard, G. “Application of Electrochemical Impedance Spectroscopy (EIS) for Characterizing the Corrosion-Protective Performance of Organic Coatings on Metals,” *Progress in Organic Coatings* **1992**, *21*, 205-226.

18. Hansch, C; Leo, A. *Substituent Constants for Correlation Analysis in Chemistry and Biology;* John Wiley & Sons: New York, 1979.

19. Murray, J. N. “Electrochemical Test Methods for Evaluating Organic Coatings on Metals: An Update. Part III: Multiple Test Parameter Measurements,” *Progress in Organic Coatings* **1997**, *31*, 375-391.

20. Bellucci F.; Kloppers M.; Latanision R. M. “Protective Properties of Polyimide (PMDA-ODA) on Aluminum Metallic Substrate,” *Journal of the Electrochemical Society* **1991**, 138, 40-48.

21. Bard, A.; Faulkner, L. *Electrochemical Methods Fundamentals and Applications;* John Wiley & Sons: New York, 2000.

CHAPTER VIIII

CONCLUSIONS AND FUTURE WORK

Conclusions

The overall work presented herein demonstrates a new approach to prepare pH-responsive copolymer films by surface-catalyzed polymerization. The surface-catalyzed preparation of these films enables selective growth on gold surfaces of any shape, provides a precise control over film thickness, and offers the ability to tune the concentration of the pH-sensitive groups within the film. By carefully selecting the acid content and film thickness, a fast, large, and reversible pH-response can be achieved within the desired pH range.

An ester-modified polymethylene film can be prepared on gold surfaces by exposure to a solution containing DM and EDA. This methodology enables a high level of control over film properties. The film thickness can be controlled by time of exposure to the polymerization conditions or by increasing EDA concentration. The molar ester content can be tuned between 0 and 5% by using appropriate solution ratios of EDA to DM, and this content is nearly constant throughout the depths of the film. The results presented in Chapter IV suggest that the films propagate from the metal-polymer interface and that an adsorbed intermediate of EDA functions as a co-catalyst. The most likely mode of propagation is an insertion mechanism, in which adsorbed methylene and/or ethyl ester groups insert into a Au-C bond to push the chain away from the metal surface.

PH-responsive films can be obtained by hydrolyzing the ester side chains within the film to carboxylic acid groups. The hydrolyzed films are uncharged and hydrophobic at low pH but become charged at moderate to high pH to facilitate ion transfer. Film resistances decrease by up to ~5 orders of magnitude over the critical pH range, demonstrating the effect of pH and charge on film hydrophobicity. This critical range can be tuned from pH 5 to 10 by varying the acid content within the film.

The ability to precisely control the acid content within the film and tailor the thickness of these surface-catalyzed polymer films from a few tens to several hundred nm also enables a thorough assessment of film composition and thickness on response rate. For all the studied films, the rate of protonation is slower than that of ionization because in the former case, the water and ions have to penetrate a partially hydrophobic film to react with carboxylates underneath. At the same acid content, the thicker films require longer times to reach a new stable state since water and ions have to diffuse over a longer distance to reach the electrode. With an increase of acid content within the film, these characteristic times can be shortened for both processes because more water and ion pathways exist within the film, and the effect of film thickness on rate of response becomes weak.

The surface-catalyzed growth of the pH-responsive copolymer film on a porous membrane support provides a new way to prepare composite membranes. In this particular application, we have prepared pH-responsive PM-CO2H films atop a porous alumina support by a surface-catalyzed polymerization and subsequent hydrolysis. Film resistances decrease by a factor of 200 between pH 4 and pH 11, demonstrating the effect of pH and charge on film hydrophobicity. Our approach yields a thin polymer skin

covering the pores at one end of the membrane but leaves the pores empty to enable further functionalization. This approach could be used in conjunction with other strategies for modifying pores such as use of a carboxyl-terminated silane monolayer to prepare membranes with pH-responsive surface and bulk properties.

Tertiary amine-containing polymethylene films are also prepared by a surface-catalyzed polymerization and subsequent modification. These films show opposite protonation/deprotonation trends with pH as compared to that of carboxylic acids. This reverse response in pH could be useful for targeted, pH-specific swelling and transport, and in combination with PM-CO2H, could provide a broader range of pH sensitivity. The hydrophobicity of tertiary amine-containing polymethylene films is tunable by adjusting the concentration of active side chains or partially capping the acid chloride groups with pH-inert groups during the modification. This work established that a critical side chain hydrophilicity exists to observe water and ion transfer. Appropriate molecular design of the pH-active group within the film allows control over film resistance and the magnitude and range of the response in pH.

Future Work

Design Dynamic Surfaces

While the responsiveness of film barrier properties is important for separations and chemical sensing, the responsiveness of surface properties can impact adhesion[1] and wettability[2] that often govern the interactions of the films with other materials. Our preliminary results show that the contact angle for PM-CO2H changes by 30° upon adjusting pH from 4 to 11. While this change in wettability is large, a further magnification of the

change could lead to truly remarkable materials with dynamic surfaces. One can further amplify the large response in wettability of film surfaces by carefully engineering film roughness. The observed contact angle θ is related to the true contact angle θ_{true} on a smooth surface by Eq (3-18). Thus, increasing surface roughness (r) enhances contact angles (θ) that are greater than 90° while reducing contact angles that are less than 90°. To manifest the effect of roughness on surface properties, one can direct the polymer growth into discrete squares with well-defined dimensions and spacings. These squares can be prepared by approach that used to prepare the patterned films in Figure 2.1.[3] First, one can microcontact print squares of a hexadecanethiolate SAM, which serves as a template for the upd of a silver monolayer. The SAM features can then be removed by electrochemical reductive desorption[3] to produce gold squares for polymer growth and surrounding regions of Ag-modified gold that are inactive toward polymerization. The size and separation of the squares can be controlled from 1 μm to 50 μm (by changing the master used to fabricate the microlithographic stamps) to alter the surface roughness and influence the response of wettability to pH. From this work, one can define well-controlled microscopic parameters that can amplify pH-dependent wettability and should provide fundamental impact far beyond this project. The idea presented here is supported by Sun et al.,[4] who have recently used micromachining to prepare rough surfaces of a thermally responsive polymer. They observed a remarkably high contact angle difference of 150° on the roughest surface as the temperature was decreased by 15°.

Preparation of PM-Rich Copolymer Films with Perfluoromethyl Side Chains

Innovative new methods to prepare fluorocarbon films could greatly promote their use in advanced materials processing. In addition, controlled methods to prepare diblock

copolymer films with an outer fluorocarbon block could lead to straightforward preparation of polymer films with oleophobic surface properties. One can prepare partially fluorinated thin films via surface-catalyzed decomposition of fluorinated diazo compounds. While difluorodiazomethane (CF_2N_2) is not a viable precursor, 2,2,2-trifluorodiazoethane (TFDE) can be prepared[5] and exhibits chemical behavior similar to DM, including an ability to undergo insertion reactions at metal complexes.[6] Based on our preliminary experimental results, TFDE, like EDA, does not polymerize on gold, silver or copper surface, but it does copolymerize with DM onto gold surfaces. As already discussed, we have evidence for a mechanism of film propagation in which DM and EDA diffuse through the growing film and insert between the gold surface and the polymer chain. Here, one can exploit this film growth mechanism to prepare diblock copolymer films. One can first grow a thin fluorinated film from DM and TFDE and then expose to DM and EDA so that its insertion into the active chains would push up the fluorinated film. If successful, this method would produce a layered, diblock copolymer film in which poly(methylene-*co*-ethyl acetate) comprises an inexpensive and inert foundation whereas the outer surface is rich in fluorocarbon for oleophobic or lubricating surfaces. These diblock copolymer films consisting of predominately PM (or functionalized PM) would be extremely useful for applications that are governed by specialized surface properties (adsorption, wetting, friction) and not by the bulk film.

Growing Multilayer Copolymer Films with Different Compositions

Since the surface-catalyzed polymerization process is a "living" process, we can prepare multilayers of copolymer films with different composition in each layer by

switching the gold substrate from one EDA to DM ratio to the other. One can then hydrolyze the ester side chains to carboxylic acid and study the film pH-dependent barrier properties by EIS. Since the acid content varies in the different layers, we would expect to observe different time constants in Bode plots with each time constant corresponding to a polymer layer with discrete acid concentration. Through this method, we can verify the hypothesis of the insertion mechanism in Chapter V and also prepare a polymer film with an acid–rich surface composition and a good barrier layer underneath.

Expand to Bioapplications

Since there are carboxylic acid groups within the PM-CO2H films, one can couple appropriate biological molecules to the surface of the film to make pH-sensitive films for in-situ measurement of the concentration of analytes that are acted upon by the attached biomolecules to release H^+ or OH^-. For example, one can prepare a glucose sensor by coupling glucose oxidase onto the film surface as shown by Cai et al.[7] The enzymatic oxidation of glucose will produce gluconic acid when glucose is introduced into the system and change the environmental pH. One can then monitor the change of film impedance with pH and correlate these changes to the H^+ concentration within the solution to assess the glucose concentration.

References

1. Zhu, X.; De Graaf, J.; Winnik, F. M.; Leckband, D. "Tuning the Interfacial Properties of Grafted Chains with a pH Switch," *Langmuir* **2004**, *20*, 1459.

2. Abbott, N. L.; Whitesides, G. M. "Potential-Dependent Wetting of Aqueous-Solutions on Self-Assembled Monolayers Formed from 15-(Ferrocenylcarbonyl)Pentadecanethiol on Gold," *Langmuir* **1994**, *10*, 1493-1497.

3. Guo, W. F.; Jennings, G. K. "Directed Growth of Polymethylene Films on Atomically Modified Gold Surfaces," *Advanced Materials* **2003**, *15*, 588-591.

4. Sun, T. L.; Wang, G. J.; Feng, L.; Liu, B. Q.; Ma, Y. M.; Jiang, L.; Zhu, D. B. "Reversible Switching between Superhydrophilicity and Superhydrophobicity," *Angewandte Chemie-International Edition* **2004**, *43*, 357-360.

5. Ogara, J. E.; Dailey, W. P. "Matrix-Isolation and ab-initio Molecular-Orbital Study of 2,2,2-Trifluoroethylidene," *Journal of the American Chemical Society* **1994**, *116*, 12016-12021.

6. Herrmann, W. A.; Huggins, J. M.; Reiter, B.; Bauer, C.; "Transition Metal-Methylene Complexes. Xxiv. Carbene Addition to a Cobalt-Cobalt Double Bond," *Journal of Organometallic Chemistry* **1981**, 214, C19-C24.

7. Cai, Q. Y.; Zeng, K. F.; Ruan, C. M.; Desai, T. A.; Grimes, C. A. "A Wireless, Remote Query Glucose Biosensor Based on a pH-Sensitive Polymer," *Analytical Chemistry* **2004**, *76*, 4038-4043.